

THE DESIGN AND SYNTHESIS OF ELECTROACTIVE AND
MAGNETIC POLYMERS

Thesis by

Michael M. Rock, Jr.

In Partial Fulfillment of the Requirements
for the Degree of
Doctor of Philosophy

California Institute of Technology
Pasadena, California

1993

(Submitted November 9, 1992)

*To my family: Mom, Dad, Jillayne,
Jennifer, and Joseph*

Acknowledgements

Upon reflection, the last five years have been incredibly enjoyable. I am fortunate to have been a part of an atmosphere of unrivaled academic freedom and strong divisional fellowship.

My greatest thanks are reserved for my advisor, Bob Grubbs. An extremely humorous, down-to-earth, and talented gentleman, Bob has provided not only financial, technical, and moral support during the course of this research, but has also, more importantly, become a good friend. He is one of a kind.

There is little doubt that Jack Halpern was responsible for my admission to Caltech. A man of few words and imposing intellect, Professor Halpern allowed me to work in his research lab as a University of Chicago undergraduate, something rarely done, as I later understood. Though my time in his lab was, in my mind, not particularly productive, I learned a great deal about the often elusive pursuit of science and the value of a supportive research advisor.

My interest in experimental science is a direct consequence of my interaction with Ms. Carol Kolodziej. Her enthusiasm for science was contagious and provided the spark for my scientific career. There is no question that her influence has strengthened this tome and its author.

Research is not a solo flight, and many people have contributed to the technical work included within these pages. Collaboration with Dennis Dougherty, and his group members Josh Jacobs and Dave Shultz, has strengthened our work with organic ferromagnets. Randy Lee and P. T. (Joe) Ho must also be recognized for their substantial contributions to the

ferromagnet work. Tom Jozefiak has unselfishly performed most of the electrochemical experiments involved with the imine and quinone projects and has provided insights into the electrochemical behavior of many of my materials. Lynda Johnson has been extremely generous with donations of copious quantities of her tungsten alkylidene catalysts. Her generosity and synthetic ability are unsurpassed. The generosity of Vince Conticello must be recognized, for without his donation of molybdenum catalyst derivatives, the 3,4-substituted cyclobutene project would still be struggling.

Thanks must be extended to those of the secretarial, shop, physical plant, and transportation staffs, for without whose assistance, Institute research would cease. The work of Linda Clark, Chris Smith, Fran Bennett, Tom Dunn, Louie Borbon, Steve Gould, Dan Fralin, Gabor Faludi, John Pirolo, and a host of others often goes unheralded. I sincerely appreciate their help and assistance these past years.

Friends and colleagues make life richer and more enjoyable. I am fortunate to have met a great number of people and to have formed several strong friendships during my stay in California. I owe a great deal to Tim Swager and Dave Wheeler for my introduction to the world of graduate research and Bob's "ROMPer Room." Dom McGrath, Rick Fisher, Chris Gorman, and Marc Hillmyer have also added to the joy of chemistry.

The exploits of Hum Baby Scum and The Chicken have provided great joy and numerous diversions from the rigors of academic research. For many incidents and adventures outside of lab, I remain grateful to Steve and Laura Buratto, Dan Jones, Rick and Mary Fisher, Marc Hillmyer, Gary and Dawn Guthart, and Todd and Melissa Richmond.

Abstract

Ring-opening metathesis polymerization (ROMP) remains a valuable tool in polymer synthesis because it affords structurally well-defined, functionalized materials with highly unsaturated polymer backbones. The power and flexibility of organic and polymer chemistry are used here to create fully conjugated, electroactive organic polymers.

A series of electroactive poly(norbornadienebenzoquinone-imine) and poly(norbornadienebenzoquinone) polymers have been synthesized by the ring-opening metathesis polymerization (ROMP) of functionalized bicyclo[2.2.1]hepta-2,5-dienes using alkylidene metathesis catalysts. Incorporation of these quinone and imine redox units into organic norbornadiene polymers generates highly reactive and conductive materials capable of charge storage and electrochromism.

In a second effort, we describe an improved precursor polymer route to polyparaphenylene (PPP) based upon the ring-opening metathesis polymerization (ROMP) chemistry of cis-di(3,4-dihydroxymethyl)cyclobutene dicarbonate. These precursor polybutenamers undergo a final conversion, under mild reaction conditions, to insoluble polyparaphenylene (PPP) without destroying or disturbing the existing polymer structure. These polybutenamers, in addition to their success in PPP conversion, are of great interest because they incorporate high degrees of acid, oxygen, and heteroatom functionality into a soluble 1,4-poly(butadiene) structure.

Finally, organic magnets offer new insights into the nature of magnetism and lead to the development of materials with unique optical, electrical, and magnetic properties. To test the claims and postulates of the Topological Coupling Model, an organic-based ferromagnetic polymer was designed around the ring-opening metathesis polymerization (ROMP) of 3-diphenylmethylenecyclobutene. Doping, the generation of charged species along the polymer, generates a radical spin ($1/2$) on every monomer unit in the polymer chain, resulting in a fully conjugated polybutenamer polymer with active spin centers every five (5) carbons apart. Oxidative doping of this material evokes ferromagnetic couplings among unpaired spins in the material.

Table of Contents

ACKNOWLEDGEMENTS.....	iii
ABSTRACT.....	v
TABLE OF FIGURES.....	ix
INTRODUCTION.....	1
References.....	8
CHAPTER ONE. Polymerization of Functionalized Quinones.....	10
Introduction.....	11
Synthesis.....	13
Polymerization.....	20
Reaction Chemistry.....	34
Conclusions and Future Prospects.....	49
Experimentals.....	50
References.....	66
CHAPTER TWO. Precursors to Polyparaphenylene.....	71
Introduction.....	72
Synthesis.....	80
Polymerization.....	92
Conclusions and Future Prospects.....	109
Experimentals.....	112
References.....	121
CHAPTER THREE: Preparations to Organic Ferromagnets.....	124

Introduction.....	125
Synthesis and Polymerization.....	134
Doping Efforts.....	145
Conclusions and Future Prospects.....	158
Experimentals.....	159
References.....	170

Table of Figures

CHAPTER ONE. Polymerization of Functionalized Quinones.

Figure 1: Electroactive polymers.....	12
Figure 2: Direct polymerization of naked quinones.....	14
Figure 3: Synthesis of benzoquinone-bis ketal monomer [3].....	15
Figure 4: Synthesis of benzoquinone bis silyl ether monomer [5].....	16
Figure 5: Synthesis of benzoquinone-imine/amine monomers [9] and [10].....	17
Figure 6: Attempts at heteroatom substitution.....	19
Figure 7: Attempts at heteroatom substitution.....	19
Figure 8: Attempts at heteroatom substitution.....	20
Figure 9: Non-Lewis acidic ROMP metathesis catalysts.....	21
Figure 10: Polymerization of bis ketal monomer.....	22
Figure 11: GPC results for bis ketal polymerizations.....	22
Figure 12: Polymerization of bis silyl monomer.....	24
Figure 13: Representative bis silyl ether polymerizations.....	24
Figure 14: ^1H and ^{13}C NMR spectra of PBS.....	25
Figure 15: ^1H and ^{13}C NMR spectra of PNS.....	26
Figure 16: Polymer diads.....	27
Figure 17: Thermal analysis (TGA) of PBS and PNS.....	29
Figure 18: Polymerization of imine monomer [9].....	30
Figure 19: ^{13}C NMR spectra of benzoquinone-imine [9] (top) and PAN (bottom).....	31
Figure 20: Attempts at aqueous ruthenium polymerization.....	33
Figure 21: Aqueous polymerization of dimethoxy- benzoquinone [2].....	33

Figure 22: Proposed doping to highly conductive structures.....	36
Figure 23: Hydrolysis and Oxidation of polybenzoquinone bis ketal.....	37
Figure 24: Polymer hydrolysis.....	38
Figure 25: Incomplete polymer elimination.....	38
Figure 26: Thermal elimination of methanol.....	39
Figure 27: Catalyzed methanol elimination.....	40
Figure 28: Electrochemical generation of quinone dianion.....	41
Figure 29: Treatment of bis silyl ethers with fluoride ion.....	42
Figure 30: Incomplete tautomerization to polyhydroquinone.....	44
Figure 31: DPPD imine and amine electrochemistry.....	45
Figure 32: Electrochemistry of protonated polyimine.....	45
Figure 33: Electrochemistry of DPPD under Et_4NClO_4 in CH_3CN conditions.....	46
Figure 34: Electrochemistry of PAN under conditions of TBAP, HClO_4 , and CH_3CN on glassy carbon electrode, 50 mv/sec.....	46
Figure 35: Electroactivity of (PAN) under conditions of TBAP, HClO_4 , and CH_3CN on glassy carbon electrode, 50 mv/sec.....	47
Figure 36: Disproportionation of DPPI and DPPD.....	48

CHAPTER TWO. Precursors to Polyparaphenylene.

Figure 1: Kovacic's PPP preparation.....	72
Figure 2: PPP carbonate precursor route.....	73
Figure 3: Proposed PPP precursor pathway.....	74
Figure 4: Polymerization of dimethylene cyclobutene (DMCB).....	75
Figure 5: (E,Z) isomer formation upon thermolysis.....	76
Figure 6: Cyclobutene precursor to methylenomycin A.....	77

Figure 7: Pyrolysis of 1,5 hexadiyne.....	78
Figure 8: Photogeneration of cis-3,4-cyclobutenedicarboxylic acid anhydride.....	81
Figure 9: Dimethyl oxetane side reaction.....	81
Figure 10: Photolysis (acetylene deficient) side reactions.....	82
Figure 11: Photogeneration of cis-3,4-cyclobutene dicarboxylic acid anhydride.....	84
Figure 12: Photoproducts with substituted acetylenes.....	85
Figure 13: Unsuccessful photoadducts.....	85
Figure 14: Protein conjugate monomer synthesis.....	86
Figure 15: Unsuitable monomers for polymerization.....	87
Figure 16: Reduction of cis-3,4-cyclobutenedicarboxylic acid anhydride [3].....	87
Figure 17: Synthesis of cis-3,4-di(hydroxymethyl) cyclobutene diacetate [4].....	88
Figure 18: Synthesis of cis-3,4-di(hydroxymethyl) cyclobutene dicarbonate [6].....	89
Figure 19: Synthesis of cis-3,4-di(hydroxymethyl) cyclobutene dimesylate [5].....	90
Figure 20: Generation of DMCB from [6].....	91
Figure 21: Non-Lewis acidic ROMP metathesis catalysts.....	92
Figure 22: Unsuccessful polymerization of anhydride [1].....	93
Figure 23: Attempted aqueous ruthenium polymerizations.....	93
Figure 24: Unsuccessful polymerization of cis-3,4- di(hydroxymethyl)cyclobutene diacetate.....	94
Figure 25: Polymerization of cis-3,4-di(hydroxymethyl) cyclobutene dimesylate.....	96
Figure 26: Aqueous and organic polymerizations of [6].....	97
Figure 27: ^1H and ^{13}C NMR spectra of poly(3,4-dihydroxymethyl) cyclobutene dicarbonate.....	100

Figure 28: Proposed diad structures.....	101
Figure 29: Thermal analysis (TGA) of dimesylate [5] and dicarbonate [6].....	102
Figure 30: Unidentified polymerization behavior.....	103
Figure 31: Full carbonate elimination toward PPP.....	105
Figure 32: Catalyzed elimination of polymerized [6] with amine...	106
Figure 33: Incomplete polymer elimination.....	107
Figure 34: IR and ^{13}C -CPMAS NMR of carbonate elimination products.....	108
Figure 35: Protein conjugate polymaleimide.....	109
Figure 36: Carbohydrate-protein conjugates.....	110

CHAPTER THREE: Preparations to Organic Ferromagnets.

Figure 1: Paramagnetic spins: zero overall magnetic moment.....	125
Figure 2: Ferromagnetic spins: non-zero overall magnetic moment.....	126
Figure 3: High spin polycarbene and galvinoxyl materials.....	128
Figure 4: Miller's charge transfer materials.....	129
Figure 5: Polaronic ferromagnetism model.....	129
Figure 6: Polaronic coupling and polymer systems.....	130
Figure 7: Ferromagnetically active 1,3,5-triaminobenzene.....	131
Figure 8: Ovchinikov's device for high spin molecules.....	132
Figure 9: Proposed route into ferromagnetic materials.....	134
Figure 10: Synthesis of 3-diphenylmethylene-1-chlorocyclobutane.....	135
Figure 11: Modified synthesis of phenylcyclobutanes.....	136
Figure 12: Substituted phenyl cyclobutane monomers.....	137
Figure 13: Elimination to yield ROMP-able cyclobutene.....	138

Figure 14: Titanium ROMP polymerization.....	138
Figure 15: Early tungsten alkylidene polymerizations.....	139
Figure 16: "One pot" elimination and polymerization.....	140
Figure 17: ^1H NMR and IR spectra of poly(3- diphenylmethylene cyclobutene).....	142
Figure 18: Successful "one pot" polymerizations.....	141
Figure 19: Thermal analysis (TGA and DSC) of poly(3- diphenylmethylenecyclobutene).....	144
Figure 20: Unsuccessful polymerizations (amorphous NMR spectra).....	143
Figure 21: Amorphous, non-descript ^1H NMR of poly(3- diphenylmethylenecyclobutene).....	145
Figure 22: Ferromagnetic organic polymer design.....	146
Figure 23: General doping approach to magnetic materials.....	147
Figure 24: Oxidative doping of polymer.....	149
Figure 25: Rajca-type attempt at neutral radical generation.....	150
Figure 26: Allylic deprotonation and radical generation.....	150
Figure 27: Hydrogen abstraction.....	151
Figure 28: Radical generation by UV irradiation.....	153
Figure 29: SQUID measurements for a photolyzed polymer sample.....	155
Figure 30: Raw data fit to magnetic data of iodine doped polymer.....	156
Figure 31: Curie plot of doped iodine sample.....	157
Figure 32: Electrochemical attempts at radical generation.....	157

Introduction to Ring-Opening Metathesis Polymerization

Introduction to Ring-Opening Metathesis Polymerization (ROMP)

Ring-opening metathesis polymerization (ROMP) remains a valuable tool in polymer synthesis because it affords structurally well-defined, functionalized materials with highly unsaturated polymer backbones. Such polymer backbones are especially well suited for the preparation of materials with interesting electronic and optical properties.¹ The development of tolerant catalysts has widened the versatility of ROMP, having allowed the polymerization of highly functionalized materials, including end capped polyalkenamers, conductive and magnetic polymers, ion chelating polyethers, polysulfone membranes, and catalytic (polymer) antibodies.

The projects described within this thesis have the use of ring-opening metathesis polymerization (ROMP) in common and focus upon the design, synthesis, and polymerization of materials which exhibit unique conductive, magnetic, and optical properties.

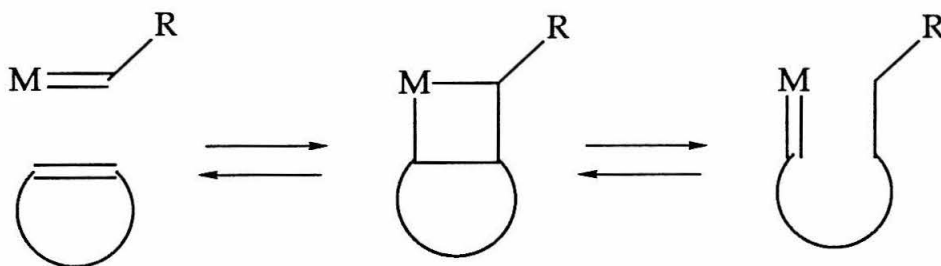
Chapter One describes efforts in the synthesis of electroactive and intrinsically conductive materials based upon the ring-opening metathesis polymerization of quinone- and imine-functionalized bicyclo[2.2.1]hepta-2,5-dienes. Originally envisioned as intrinsically conductive materials, these quinones have shown electrical conductivity in the semiconductor region.

Chapter Two describes the ring-opening metathesis polymerization of 3,4-substituted cyclobutenes for use as polymer precursors to polyparaphenylene (PPP). These highly functionalized precursors

demonstrate the usefulness of precursor methods in the synthesis of insoluble, rigid rod polymers.

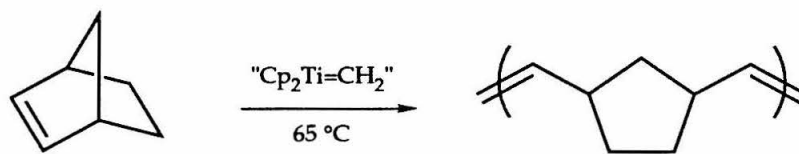
Chapter Three describes the design and synthesis of organic-based magnetic materials. The ring-opening metathesis polymerization of 3-diphenylmethylenecyclobutene affords high molecular weight materials that show ferromagnetic activity when oxidatively doped.

ROMP as described below, involves the [2 + 2] cycloaddition of an alkene and metal alkylidene to form a reactive metallacyclobutane intermediate, which upon productive cleavage, generates a polymerization-active propagating carbene along with an endcapped polymer chain. Additional equivalents of olefin add to generate a highly unsaturated polymer structure. Strained cyclic olefins are excellent substrates for ROMP because the ring strain in the cyclic monomers provides a strong thermodynamic driving force toward polymerization.



ROMP is unique in that monomer unsaturation is preserved within the polymer structure, making it attractive for the preparation of highly unsaturated, fully conjugated conductive polymers.

In 1986, Gilliom and Grubbs reported the first living ring-opening polymerization of a cyclic olefins.²



Gilliom, 1986

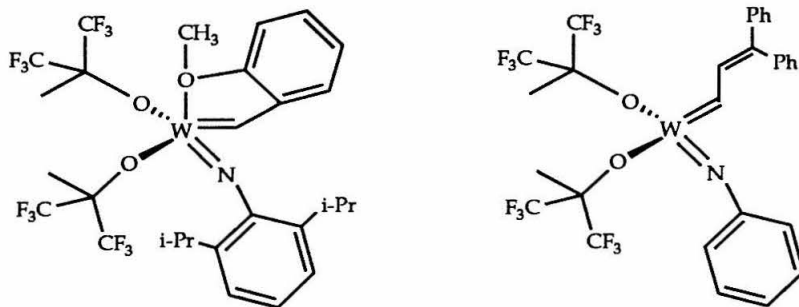
A series of titanacyclobutanes catalyzed the polymerization of norbornene and produced a polymer with a narrow and controllable molecular weight distribution. The titanium system afforded a living polymerization, a special case of chain growth polymerization in which chain transfer and chain termination processes are very slow compared to chain initiation and chain propagation.³

This catalyst system improved upon early classical ROMP systems because it afforded total and absolute control over the polymerization reaction. While the polymerization of cyclic olefins with these early Lewis acidic species, including $\text{WCl}_6/\text{EtAlCl}_2/\text{EtOH}$, was often accompanied by cyclopropanation, back-biting, and cyclic oligomer side reactions, these new titanacyclobutanes polymerized strained cyclic olefins with Lewis acid sensitive functionalities under mild conditions. This development held obvious advantages and applications for ROMP polymers of functionalized monomers with reactive heteroatoms.

This new living catalyst system led directly to the synthesis of polymers with controlled structures. The living nature of the titanacyclobutanes allow for specific endcapping of the polymer chain and the preparation of well-defined block co-polymers of norbornene with other strained cyclic olefins. Chain propagating polymer intermediates (carbenes)

are well characterized species and lead to the controlled synthesis of phase separated and uniform block copolymers with monodisperse segments.⁴

To complement the series of ROMP-active titanocyclobutanes, a series of highly active tungsten alkylidene catalysts have been synthesized and shown to be active ring-opening metathesis polymerization catalysts.⁵



Modelled after compounds developed by Schrock and Osborn, these living catalysts efficiently polymerize both strained and unstrained cyclic olefins, yielding polymers with diverse and interesting properties.⁶

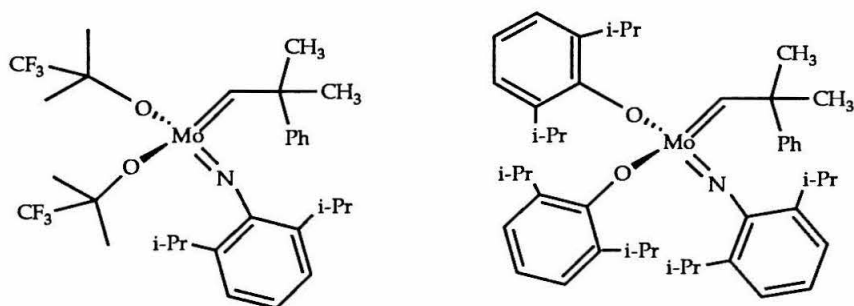
The living nature of the tungsten alkylidene catalyst is attributed, in part, to its inactivity towards unactivated double bonds (i.e., internal olefins present in the polymer backbone). However, the success of the well-defined titanium and tungsten catalysts is often limited by their significant reactivity toward alcohols, ketone, esters, and aldehydes. While, late transition metal catalysts have been more tolerant than their early transition metal counterparts, their polymerizations are inefficient and low yield reactions.

The incorporation of functional groups within a polymer structure can have dramatic influences on the material's mechanical, electrical, and thermal properties. However, the sensitivity of these organometallic catalysts to

oxygen, water, and heteroatom functionality has hampered the search for a functional group-tolerant, polymerization catalyst.

The extension of ROMP methods to monomers other than hydrocarbons has been more challenging. Metathesis polymerizations of monomers containing pendant functionalities have met with only limited success, and polymerizations of strained heterocyclic monomers are more rare. These limitations are primarily the result of side reactions between the monomer heteroatoms and the oxophilic alkylidene ROMP catalysts.

Synthetic utility, however, is introduced into these reactive alkylidene complexes by changing the metal. Molybdenum is less oxophilic than tungsten and will tolerate monomers containing mildly reactive functionalities as esters, and nitriles without large scale catalyst deactivation. Recent ruthenium catalysts show higher reactivity toward olefins than aldehydes and promise to be even more functional-group tolerant.



With this ability to polymerize functionality-containing monomers, comes the ability to generate well-defined polymer structures while incorporating high degrees of unsaturation and functionality within the polymer structure. It is this ability we draw upon in the preparation of electroactive and magnetic polymers. Research efforts in organometallic chemistry are providing

catalysts for a wide range of polymeric structures not accessible with other techniques.

Ring-Opening Metathesis Polymerization (ROMP) References:

General references for this introduction include:

- 1) Grubbs, R. H.; Tumas, W. *Science*. **1989**, 243, 907. Schrock, R. R. *Acc. Chem. Res.* **1990**, 23, 158.
- 2) Gilliom, L. R.; Grubbs, R. H. *J. Am. Chem. Soc.* **1986**, 108, 733.
- 3) Strauss, D. A.; Grubbs, R. H. *J. Mol. Cat.* **1985**, 28. Gilliom, L. R.; Grubbs, R. H. *Organometallics*. **1986**, 5, 721
- 4) Noshay, A.; McGrath, J. E. Block Copolymers. Academic. New York. 1977. Risse, W.; Grubbs, R. H. *Macromolecules*. **1989**, 22, 4462. Risse, W.; Grubbs, R. H. *Macromolecules*. **1989**, 22, 1558. Feast, W. J.; Winter, J. N. *J. Chem. Soc. Chem. Commun.* **1985**, 202 and references within. Krouse, S. A.; Schrock, R. R. *Macromolecules*. **1988**, 21, 1885.
- 5) Schaverien, C. J.; Dewan, J. C.; Schrock, R. R. *J. Am. Chem. Soc.* **1986**, 108, 2771. Schrock, R. R.; Depue, R. T.; Feldman, J.; Schaverien, C. J.; Dewan, J. C., Liu, A. H. *J. Am. Chem. Soc.* **1988**, 110, 1423. Kress, J.; Osborn, J. A. *J. Am. Chem. Soc.* **1983**, 105, 6346. Quignard, F.; Leconte, M.; Basset, J. M. *J. Chem Soc. Chem. Commun.* **1985**, 1816. Schaverien, C. J.; Dewan, J. C.; Schrock, R. R. *J. Am. Chem. Soc.* **1986**, 108, 2771. Schrock, R. R.; Depue, R. T.; Feldman, J.; Schaverien, C. J.; Dewan, J. C., Liu, A. H. *J. Am. Chem. Soc.* **1988**, 110, 1423. Johnson, L. K.; Virgil, S. C.; Grubbs, R. H. *J. Am. Chem. Soc.* **1990**, 112, 5384.
- 6) Ginsburg, E.J.; Gorman, C. B.; Marder, S. M.; Grubbs, R. H. *J. Am. Chem. Soc.* **1989**, 111, 7621. Gorman, C. B.; Ginsburg, E.J.; Marder, S. M.; Grubbs, R. H. *Angew. Chem.* **1989**, 101, 1603.

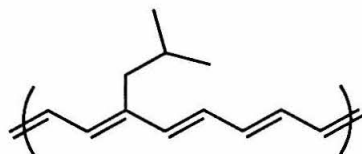
Sailor, M. J.; Ginsburg, E.J.; Gorman, C. B.; Kumar, A.; Grubbs, R. H.; Lewis, N. S. *Science*. **1990**, *249*, 1149. Ginsburg, E.J.; Gorman, C. B.; Grubbs, R. H.; Klavetter, F. L.; Lewis, N. S.; Marder, S. M.; Perry, J. W.; Sailor, M. J. in *Conjugated Polymeric Materials: Opportunities in Electronics, Optoelectronics, and Molecular Electronics*. Kluwer. Netherlands. 1990. Swager, T. M.; Grubbs, R. H. *J. Am. Chem. Soc.* **1989**, *111*, 4413. Swager, T. M.; Dougherty, D. A.; Grubbs, R. H. *J. Am. Chem. Soc.* **1988**, *110*, 2973. Swager, T. M.; Grubbs, R. H. *J. Am. Chem. Soc.* **1987**, *109*, 894.

Chapter One. Polymerization of Functionalized
Quinones

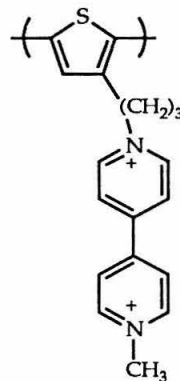
Introduction

Polymers with the capacity to store charge, or switch electrochemically are a topic of continued interest in the material science community.¹ The power and flexibility of organic and polymer chemistry are used here to create fully conjugated, electroactive organic polymers.

Electroactive polymer synthesis is often rife with problems of insolubility and intractability because of extensive unsaturation in the polymer backbones of these materials. Solubilizing groups have been used successfully to combat problems of polymer solubility in a series of polyacetylenes and polyalkylthiophenes.² We have chosen, instead, to use soluble precursor routes to these electroactive materials.



sec butyl Polyacetylene



Poly(alkyl)thiophene

The synthesis of these polymers via soluble precursor routes generates high molecular weight, highly reactive, structurally-defined electroactive materials and have, most recently, been used in the synthesis of polyparaphenylene and polyparaphenylene vinylene.³ Precursor

materials do not suffer from the problems associated with highly conjugated polymers, namely insolubility, chemical instability, and decomposition below a melting point.

A series of electroactive poly(norbornadienebenzoquinone-imine) (**PAN**) and poly(norbornadienebenzoquinone) (**PBQ**) polymers have been synthesized by the ring-opening metathesis polymerization (ROMP) of functionalized bicyclo[2.2.1]hepta-2,5-dienes (Figure 1). The proposed norbornadienequinone monomers are strained [2.2.1] cyclic olefins, synthetically accessible through Diels-Alder and standard protection-group chemistry. Their ring-opening metathesis polymerization (ROMP) preserves all monomer double bonds during polymerization and generates materials with unusual and highly unsaturated polymer backbones.

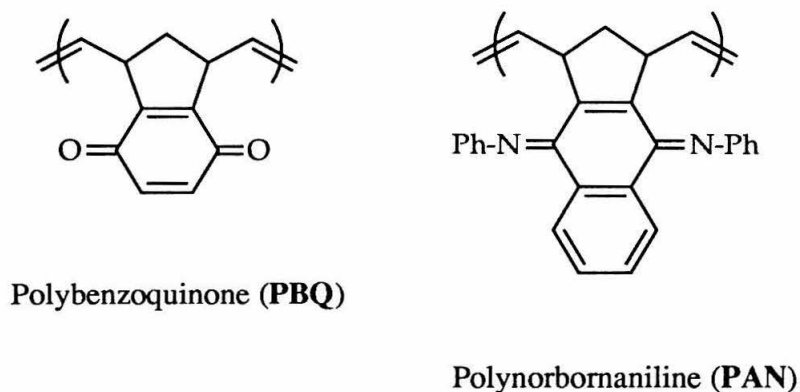


Figure 1: Electroactive polymers.

The pendant quinones⁴ and anilines⁵ are versatile redox units with established electrochemical behaviors. They form charge transfer complexes with hydroquinones and other electron rich molecules, and the

formation of these semiquinones along the polymer chain provides a mechanism for facile intra- and interchain electrical conduction. Additionally, the reversible quinone redox potential has commercial applications in lightweight rechargeable battery material, while the variable conductivity (with doping) of quinones provides a basis for electrochemical switches and sensors.

Incorporation of these redox units into organic norbornadiene polymers generates highly reactive and conductive materials. These electroactive quinone- and imine-functionalized polynorbornadienes exhibit significant dc electrical conductivity and are capable of charge storage and electrochromism. The polyquinones, envisioned as intrinsically conducting materials, do not, however, have metallic conductivities, they remain semiconductors upon oxidative doping. The polyimines, being polyaniline oligomers, mimic many electrochromic and conductive behaviors of the parent polyaniline and may act as polymeric Schiff bases.

Synthesis

Initial attempts at the direct synthesis of **PBQ** by polymerization of the norbornadiene-quinone monomers [1]⁶ were unsuccessful because of catalyst decomposition and Wittig-type side reactions (Figure 2). Polymerization of the naked quinone remains doubtful with the available early and late transition metal titanium, tungsten, molybdenum, ruthenium, rhenium, and iridium ROMP catalysts.

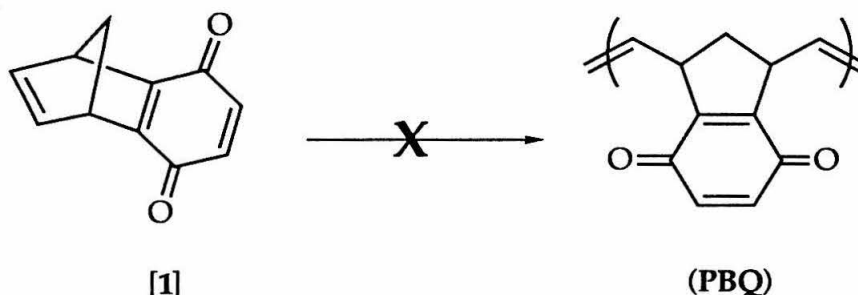
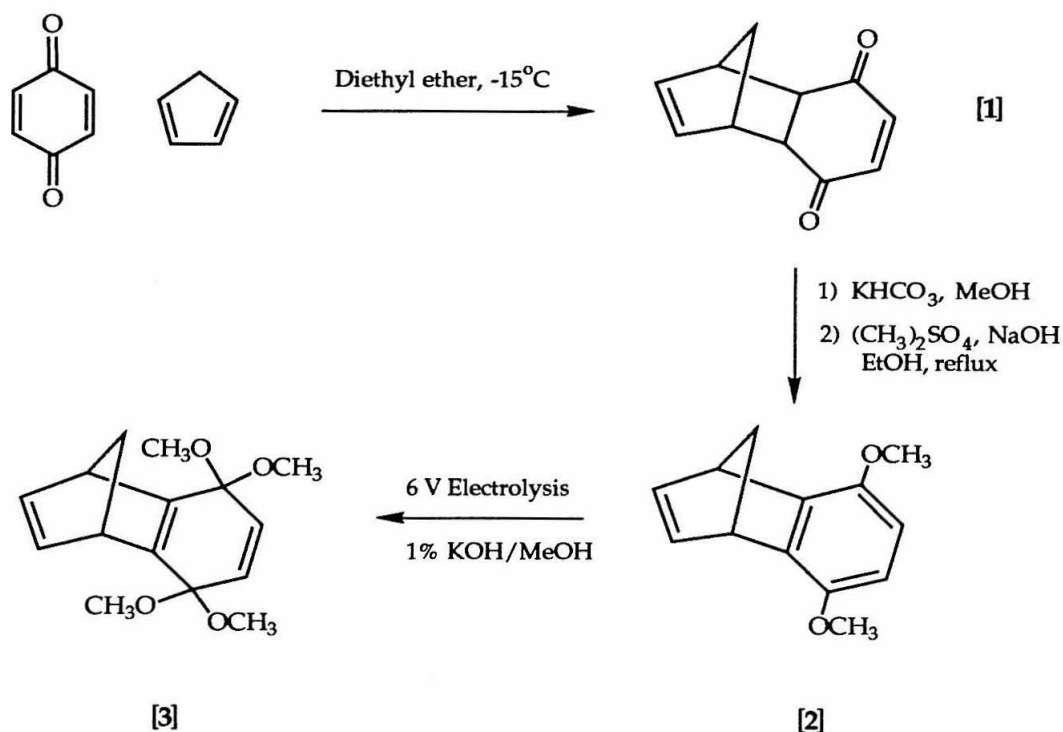


Figure 2: Direct polymerization of naked quinones.

In response to the incompatibility of quinone groups with ROMP catalysts, all quinones were protected as bis ketals, bis silyl ethers, or bis imines, which are all compatible with ROMP conditions. Monomer synthesis of each electroactive [2.2.1] norbornadienebenzoquinone begins with the Diels Alder preparation of cyclopentadiene and benzoquinone and ends with protection of the chemically active quinone groups.

The synthesis of norbornadienebenzoquinone-bis ketals [3] and [4] requires a five day, 6 V electrochemical oxidation of the dimethoxy-norbornadienebenzoquinone [2] in a 0.1 M methanolic potassium hydroxide solution (Figure 3).



Soluble Monomer, sublimed
to white crystalline solid

Figure 3: Synthesis of benzoquinone-bis ketal monomer [3].

This electrochemical transformation cleanly produces the air sensitive benzoquinone-bis ketal monomer [3] in 70 % yield.⁷ The benzo- and naphthoquinone-bis ketals sublime at 70 - 85 °C and 110 - 115 °C, respectively, to yield pristine, white, highly crystalline solids. Structures of compounds [3] and [4] are consistent with NMR spectra and elemental analyses. The presence of characteristic ^{13}C ketal resonances at 95 - 99 ppm and ^1H resonances of a [2.2.1] ring system with the bridgehead protons (~ 4 ppm) coupled to the disubstituted olefin confirm all structural assignments.

A series of substituted alkyl and aryl substituted benzo- and naphthoquinone monomers were synthesized to probe the effects of ring

substituents upon ROMP. The phenyl- and methylbenzoquinone bis ketal monomers will neither recrystallize nor sublime, but instead remain dark oils. They decompose slowly when exposed to ambient conditions, and when partially decomposed, are virtually impossible to re-purify.

The synthesis of norbornadienebenzoquinone-bis(*t*butyldimethyl)silyl ethers [5] and [6] requires the addition of *tert*butyldimethylsilyl chloride (TBSCl) to a solution of Diels Alder norbornenebenzoquinone [1], triethylamine, and 4-dimethylaminopyridine (DMAP) at room temperature (Figure 4).⁸

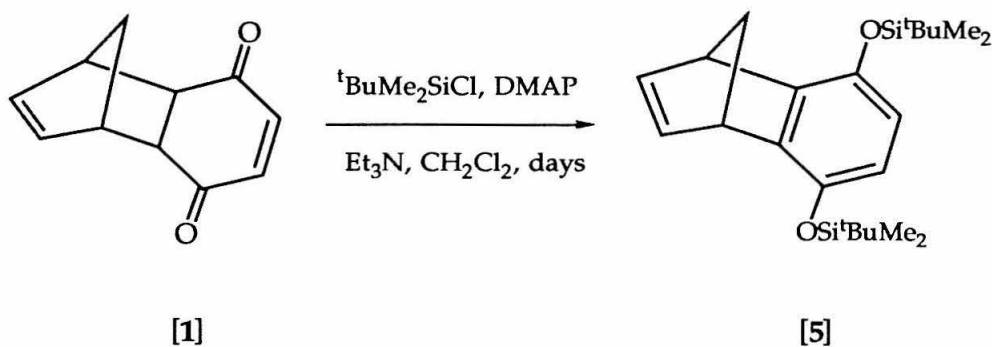


Figure 4: Synthesis of benzoquinone bis silyl ether monomer[5].

Reaction for several days under argon yields, upon chromatography, a white, crystalline, air stable compound. Sublimation of the crystalline solids insures rigorous monomer purity for polymerization. NMR data confirm all the structural assignments of these [2.2.1] cyclic olefins, [5] and [6]. The ¹H and ¹³C resonances of the silyl protecting groups, along with the high field ¹³C ether resonances at 144.08 and 141.46 ppm ([5] and [6], respectively), are consistent with the proposed structures.

Because these silyl ethers are neither dependent upon a 6 V electrochemical oxidation, nor are air sensitive compounds, their easy preparation encourages large scale (20 g) synthesis. As a direct

consequence, reaction yields for both the benzo- and naphthoquinone bis silyl ethers are much improved (70 %) over the earlier bis ketal syntheses. The norbornadienebenzoquinone-bis(trimethylsilyl) ether (TMS) was discarded for the more stable tertbutyldimethylsilyl (TBS) ether because the TMS compound proved "touchier" and easily hydrolyzed.

We also report the synthesis of an electroactive norbornadienenaphthoquinone monomer [9] functionalized with N-phenyl imine moieties. Also a [2.2.1] strained cyclic olefin, imine monomer synthesis includes the argenic oxide (AgO) or ceric ammonium nitrate $[(\text{NH}_4)_2\text{Ce}(\text{NO}_3)_6]$ oxidation of the dimethoxynorbornadiene naphthoquinone adduct [7], itself the Diels Alder product of cyclopentadiene and naphthoquinone [1] (Figure 5).

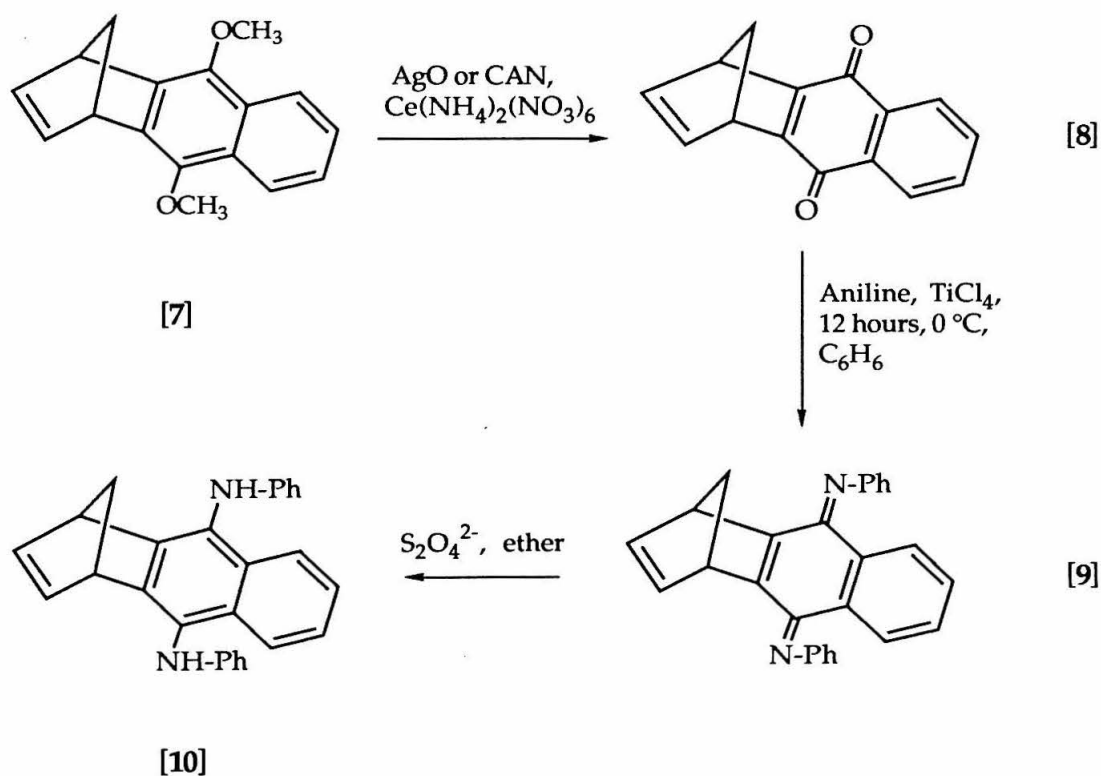


Figure 5: Synthesis of benzoquinone-imine/amine monomers [9] and [10].

Carbonyl condensation of this naphthoquinone with aniline and TiCl_4 for 12 hours at 0 °C yields a red, crystalline solid in 60 % yield, after chromatography.⁹ Sodium hydrosulfite reduction of the ruby red imine generates the expected amine compound [10] as a pale purple (fuschia) solid in quantitative yield and provides another polymerization substrate. Structures of these compounds are consistent with the NMR data and elemental analyses. Characteristic resonances as the ^{13}C imine carbon (153.95 ppm in [9]) and ^1H amine proton (4.03 ppm in [10]) remain consistent with the proposed structures.

Several acids, including TsOH , AlCl_3 , and $\text{BF}_3 \cdot \text{Et}_2\text{O}$, successfully catalyzed the carbonyl condensation with aniline, though TiCl_4 proved the most selective reagent. Condensation was also attempted with the aniline dimer in an effort to extend the electroactivity of the side group. When combined with the naphthoquinone, the dimer turned a wicked shade of violet, became heterogeneous with the reaction solution, and left the naphthoquinone untouched. The condensation reactions are only successful with naphthoquinone derivatives, however. The presence of labile benzoquinone protons makes benzoquinones unsuitable substrates for this carbonyl condensation reaction. Efforts toward the synthesis of benzoquinone-imines, via alkylation and halogenation of the benzoquinone protons, are underway.

Additionally, heteroatoms along the backbone were envisioned as a way to increase the electrical conductivity of these materials. Building upon the work of Cannizzo and Gilliom, showing that 7-aza and 7-oxabenzonorbornadienes successfully ROMP,¹⁰ we ventured to put an

oxygen heteroatom at the bridge, hoping that the increased electron density of oxygen would aid conjugation, carrier mobility, and conductivity (Figure 6).

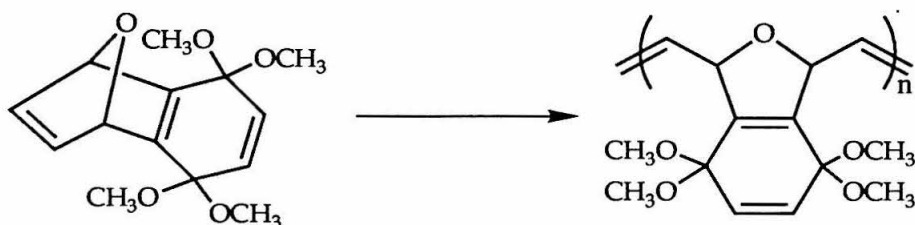


Figure 6: Attempts at heteroatom substitution.

The synthetic route to these furan monomers involves the reaction of 1-bromo-2,5-dimethoxybenzene with freshly distilled furan to form adduct 1,4 dihydro-5,8-dimethoxy-1,4-epoxynaphthalene [11] through a benzyne intermediate (Figures 7, 8).

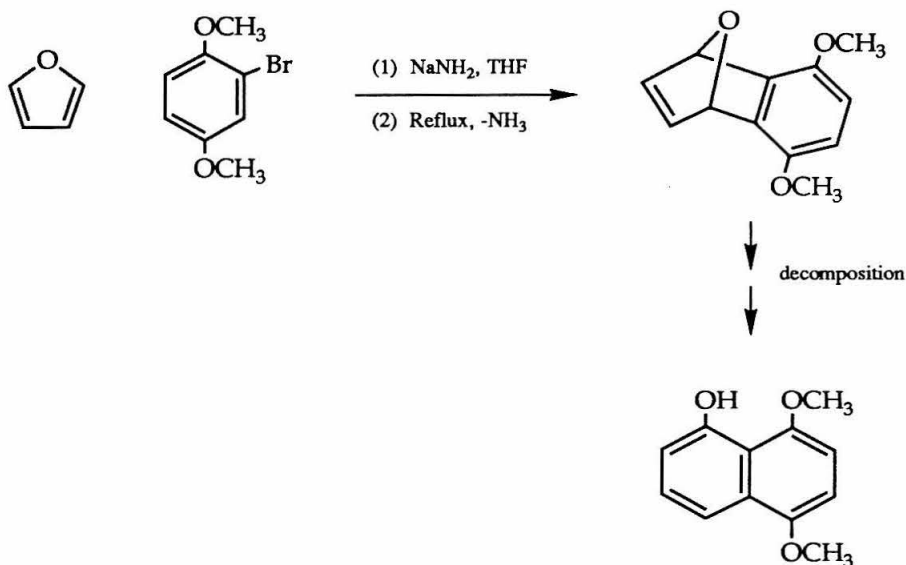


Figure 7: Attempts at heteroatom substitution.

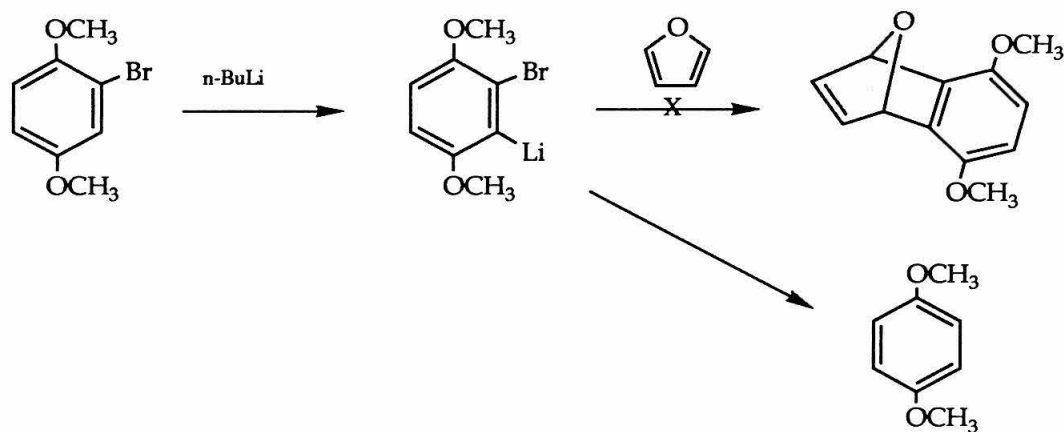


Figure 8: Attempts at heteroatom substitution.

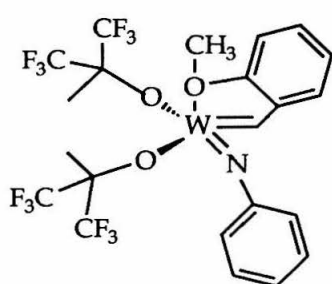
Though several literature sources cite respectable reaction yields (77%),¹¹ these synthetic efforts have been stifled. There has been no evidence to suggest synthesis of the Diels Alder product with the unsubstituted furan. Instead, only large amounts of ring opened α -naphthol derivatives have been isolated, indicating an acid-catalyzed opening of the bridging epoxide. While such reactions are important in the preparation of benzoxepines¹² and other synthetic targets, they do not advance the synthesis of a heteroatom-substituted norbornadienequinone. Synthetic routes into substituted benzyne (anthranilic acid, triaza amines, etc.) have not facilitated the synthesis of an isolated bisketal furan monomer.

Polymerization

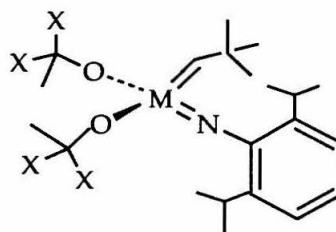
The polymerization of functionalized monomers enables the direct incorporation of functionality into the polymer structure. Such inclusion of chemically active pendant groups within the polymer circumvents the

difficulty of chemically modifying an existing polymer structure. An overwhelming problem with most early transition metal catalysts, however, is their high reactivity with polar functionalities present in organic monomers. The non-Lewis acidic, tungsten and molybdenum catalysts, used in the ring-opening metathesis polymerization (ROMP) of these norbornadienequinone derivatives, are multi-coordinate tungsten and molybdenum alkylidenes. These complexes readily form stable metallacycles upon olefin addition without ligand dissociation¹³ and polymerize cyclic olefins with Lewis acid sensitive functionalities.¹⁴ Because ROMP preserves all monomer double bonds during polymerization, it generates unusual and highly unsaturated polymer backbones.

In particular, $[(OC(CF_3)_2CH_3)_2W(ChPh(OCH_3))(NPh)]$ [I], polymerizes the quinone-bisketals ([3], [4]) and the quinone-bis silyl ethers ([5], [6]) in quantitative yields (Figure 9).



[I]



X = CH₃, CF₃

M = W, Mo

[II]

Figure 9: Non-Lewis acidic ROMP metathesis catalysts.

The bis ketal and bis silyl ether monomers polymerize similarly under room temperature conditions. The bis ketal monomers polymerize over 3 - 6 hours to give atactic, trans olefin polymer without appreciable backbiting, chain transfer, or decomposition of the backbone chain (Figure 10).

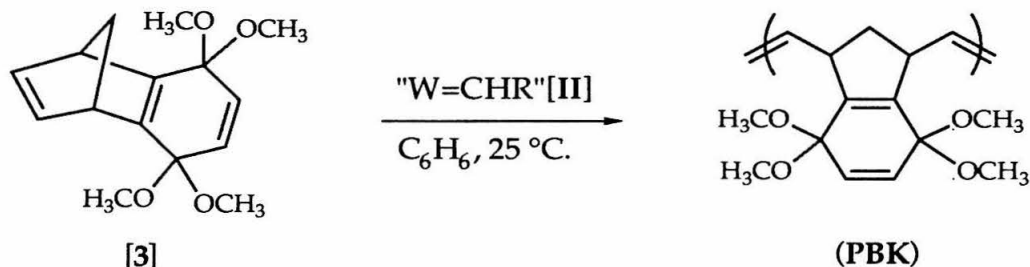


Figure 10: Polymerization of bis ketal monomer.

The t-butoxy tungsten catalyst $[(^t\text{BuO})_2\text{W}(\text{CHC}(\text{CH}_3)_3)(\text{NPh}(2,6\text{-isoprop})_2)]$ [II] reacts slowly and selectively with the cyclic olefin of the bis ketal system, minimizes polymer cross linking upon standing, and gives physically manageable polymers (Figure 11).

MMR-I-043	$M_n = 27,600$	MMR-I-123	$M_n = 23,000$
	$M_w = 36,500$		$M_w = 30,000$
	PDI = 1.35		PDI = 1.28
MMR-I-073	$M_n = 51,000$	MMR-I-161	$M_n = 14,000$
	$M_w = 85,000$		$M_w = 18,000$
	PDI = 1.66		PDI = 1.24

Figure 11: GPC results for bis ketal polymerizations.

Spectral shifts (^1H and ^{13}C NMR) of the polymer closely resemble those of the corresponding monomer, with the exception of the strained cyclic olefin and methylene bridges. These resonances significantly change

chemical shifts upon polymerization: 6.3 to 5.5 ppm and 4.1 to 2.1 ppm, respectively for the case of the quinone-bis ketal. Attached Proton Test (APT) NMR experiments verify all proton and carbon resonance assignments and these results are consistent with the proposed ROMP of the norbornadienequinone-bis ketals.

Differential scanning calorimetry of polybenzoquinone-bis ketal (PBK) show two exotherms at 150° and 230°C believed to be the stepwise loss of methanol. Polynaphthoquinone bis ketal plots indicate a single, broad DSC exotherm from 210° to 280°C. Thermogravimetric analyses of PBK and PNK display stepwise weight losses of 20% and 25%, respectively, at 250 °C, in keeping with the expected loss of two equivalents of methanol from the polymer.

The hexafluoro tungsten derivative, $[(OC(CF_3)_2CH_3)_2W(ChC(CH_3)_3)(NPh)]$ [II], used successfully in the polymerization of cyclooctatetraene¹⁵ is too reactive for the quinone-bis ketal system and backbites adjacent olefins, resulting in low yield, low molecular weight, sparingly soluble polymer.¹⁶ Methyl and phenyl substituted norbornadienequinone-bis ketals [5] also do not polymerize at elevated temperatures with less sterically-demanding catalysts.

The benzo- and naphthoquinone-bis silyl ethers [5], [6] polymerize quantitatively with several tungsten catalysts at room temperature in either benzene or THF (Figure 12). The best and most reproducible polymerization results are achieved using the fluorinated $[(OC(CF_3)_2CH_3)_2W(ChPh(OCH_3))(NPh)]$ [I]¹⁷, in THF, though complete polymerization takes days.

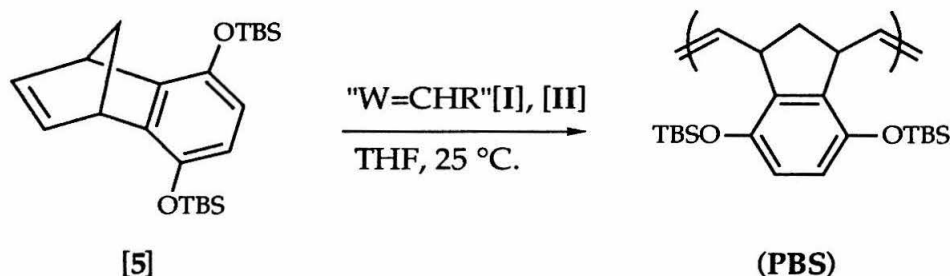


Figure 12: Polymerization of bis silyl monomer.

Materials with molecular weights (M_w) of 28,000, PDI of 1.07 have been polymerized with $[(^t\text{BuO})_2\text{W}(\text{CHC}(\text{CH}_3)_3)(\text{NPh}(2,6\text{-isoprop})_2)]$ [II], while samples of molecular weight 67,000 and 61,500. PDI 1.17 and 1.62, respectively, are reported using $[(\text{OC}(\text{CF}_3)_2\text{CH}_3)_2\text{W}(\text{CHPh}(\text{OCH}_3))(\text{NPh})]$ [I]. Silyl polymers often show higher molecular weights (M_w of 80,000) and narrower polydispersities (1.10 - 1.25) than batches of bis ketal polymer at similar monomer to catalyst ratios (Figure 13).

MMR-V-010	$M_n = 40,000$ $M_w = 143,000$ PDI = 3.58	MMR-II-145	$M_n = 57,000$ $M_w = 67,000$ PDI = 1.18
MMR-I-017	$M_n = 38,000$ $M_w = 61,500$ PDI = 1.62	MMR-K-185	$M_n = 26,000$ $M_w = 27,900$ PDI = 1.07
MMR-K-188	$M_n = 23,100$ $M_w = 97,400$ PDI = 4.22		

Figure 13: Representative bis silyl ether polymerizations.

NMR data remains consistent with the proposed ROMP of the cyclic olefin monomers (Figures 14, 15). Polymerization is accompanied by broadening and noticeable shifts in the resonances of the metathesized

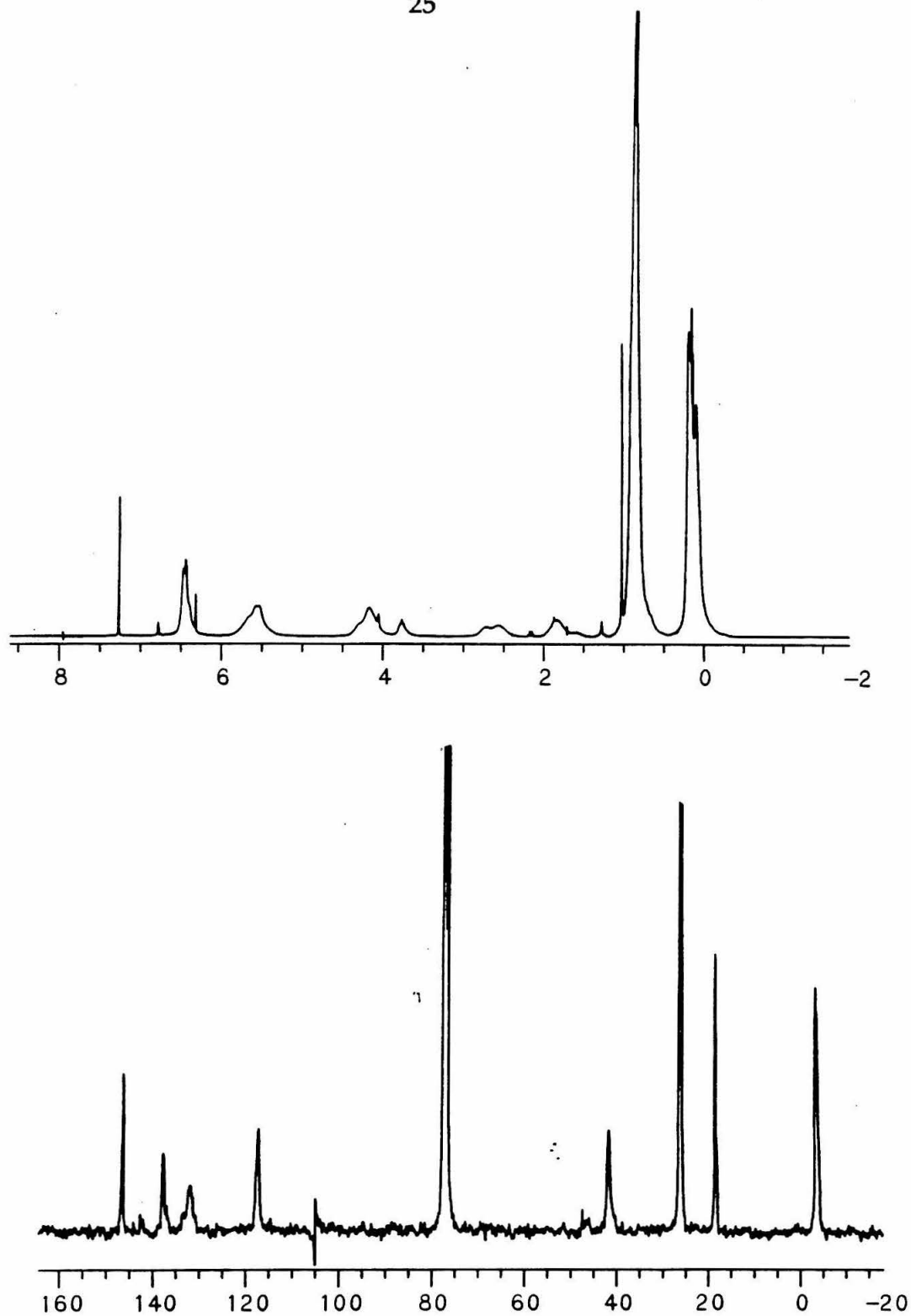


Figure 14: ^1H and ^{13}C NMR spectra of PBS.

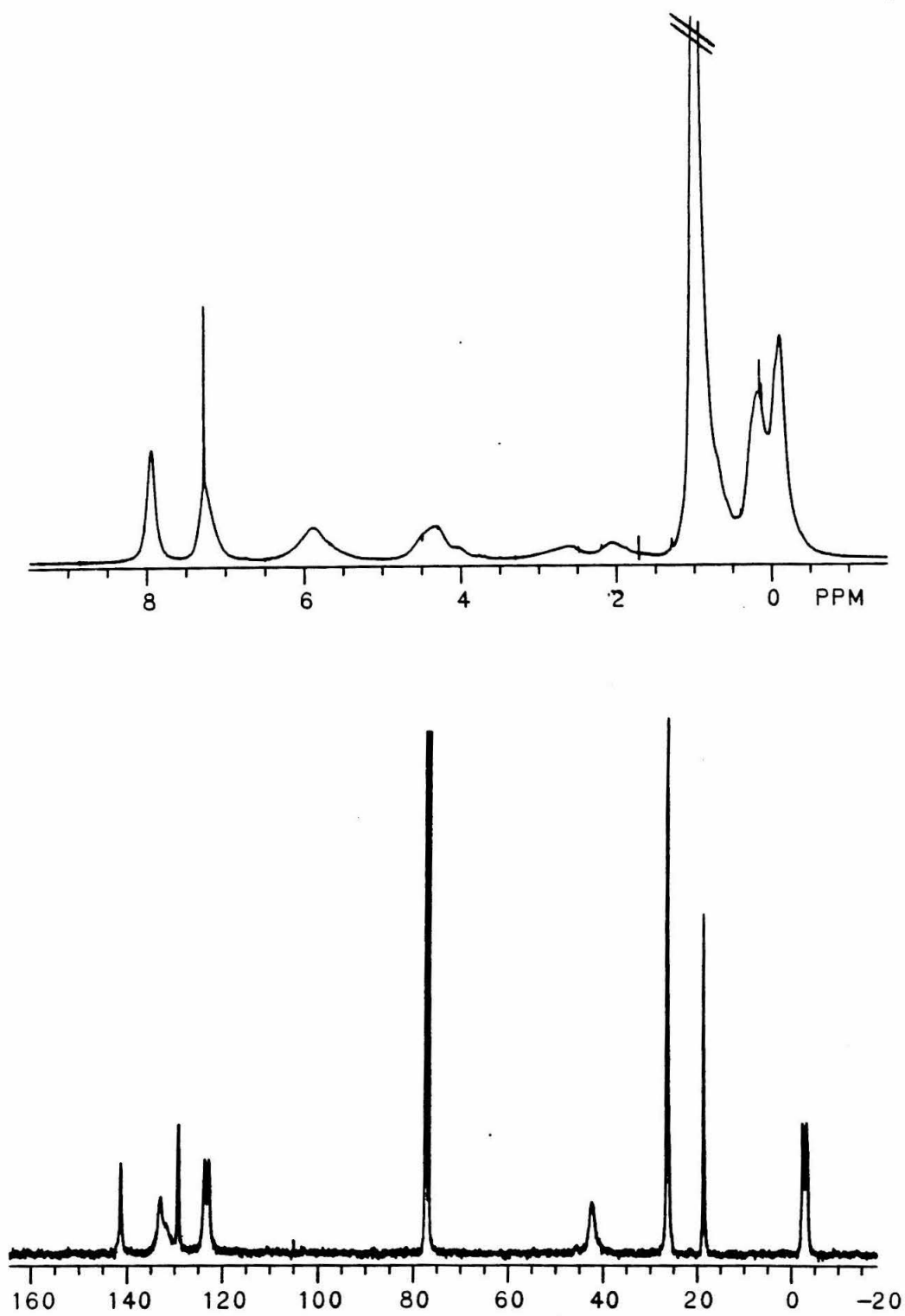


Figure 15: ^1H and ^{13}C NMR spectra of PNS.

olefin (6.28 to 5.8 ppm) and the bridgehead protons (4.03 to 2.0 ppm). Additionally, the upfield resonances of the silyl ethers confirm the incorporation of the silyl groups within the polymer structure.

Diad tacticity is also apparent within these polymers, resonances at 1.8 and 2.4 ppm and 40.5 and 46.0 ppm correspond to the tacticity-sensitive methylenes in the benzoquinone-bis silyl ether polymer (**PBS**) (Figure 16). Since the bis ketal monomers, like the other norbornadienequinones, have a plane of symmetry, there are no issues of head and tail polymer tacticity, only issues of m and r polymer diads. Tungsten polymerizations of these norbornadienequinones at room temperature appear to give nearly equal amounts of m and r diads.

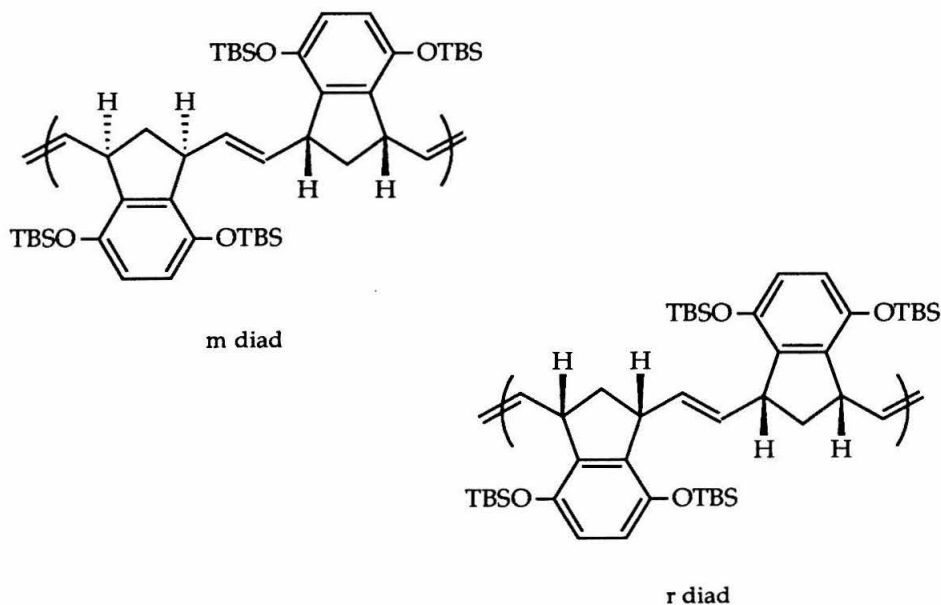


Figure 16: Polymer diads.

With glass transition temperatures of 203 °C and 230 °C, the benzo- and naphthoquinone-silyl ether polymers show great thermal stability

approaching 300 °C (Figure 17). Above that temperature, the benzoquinone- bis silyl polymer decomposes in a single step, while the naphtho polymer only drops 66 % of its weight by 450 °C. Weight loss closely corresponds to the loss of two equivalents of silanol (60 %). DSC shows several unidentified thermal transitions, believed crosslinking reactions, for these polymers.

Allowing the golden yellow quinone-bis ketal polymerization solutions (or dark orange quinone-bis silyl ether polymerization solutions) to sit more than 18 hours does not adversely affect the yield of polymer upon precipitation, but encourages longer chain lengths and wider polydispersities. Polyquinone-bis ketals (**PBK**, **PNK**), and polyquinone-bis silyl ethers (**PBS**, **PNS**) are all highly soluble in polar and halogenated solvents, and may be cast into golden, free standing films or quantitatively precipitated into hexane or methanol as white powders. Their solubility allows multiple precipitation as a means of further purification. Polyquinone bisketal polymers yellow, while bis silyl materials, especially the polynaphthoquinone-bis silyl, darken after 2-3 weeks of exposure to ambient conditions. Aged samples are restored to their original pristine conditions upon chromatography, though the NMR spectra of yellowed samples remain unchanged with aging.

The imine was successfully polymerized at room temperature using the $[(tBuO)_2W(CHC(CH_3)_3)(NPh(2,6-isoprop)_2)]$ **[I]** and $[(OC(CF_3)_2CH_3)_2W(CHPh(OCH_3))(NPh)]$ **[II]** catalysts. After 2 hours at room temperature, the polymerization mixture (of **[9]** and **[I]**) contains >95 % polymer by NMR (Figure 18). Polymerizations at elevated temperatures do not improve polymer yields or the cis and trans polymer content.

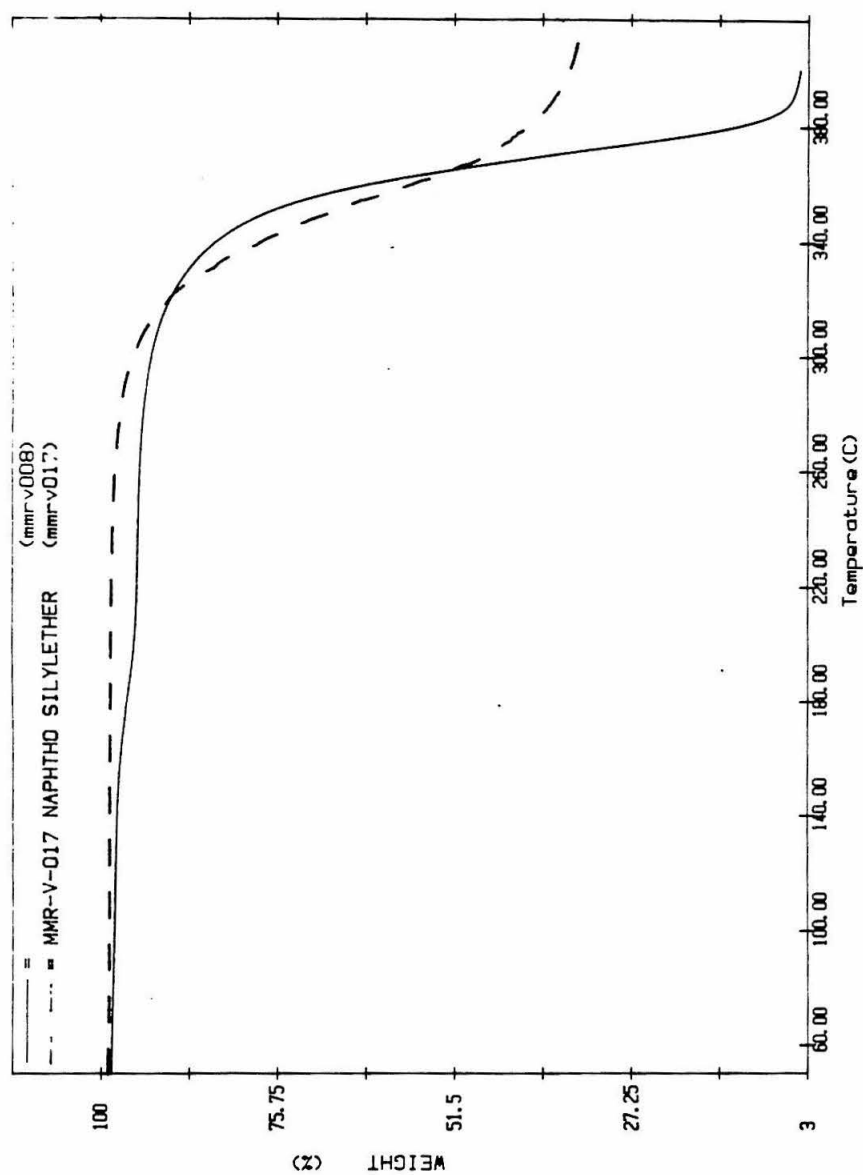


Figure 17: Thermal analysis (TGA) of PBS and PNS.

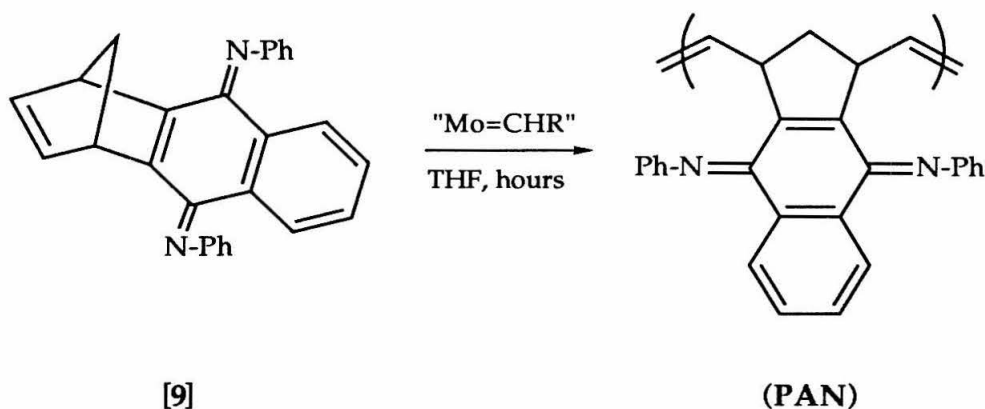


Figure 18: Polymerization of imine monomer [9].

Molybdenum polymerizations $[(OC(CH_3)_2CF_3)_2Mo(ChC(Me_2Ph)(NPh))]$ are more reliable, though much slower reactions, often taking 12 hours for complete polymerization. Precipitation of the orange solutions into petroleum ether yields a soluble, flocculent orange solid with molecular weights (M_w) of 53,500 (vs. polystyrene standards) with PDI 1.81. The proposed structure is consistent with ^{13}C NMR spectra and confirm the incorporation of the imine functionality within the polymer structure (Figure 19). The imine polymer (PAN), like their bis ketal and bis silyl ether counterparts, are fully soluble in organic solvents, including CH_2Cl_2 , THF, and C_6H_6 , but give brightly colored orange and scarlet hues in solution.

Films cast of imine polymers (PAN) are not free-standing and generally flaky in texture. Tungsten polymerizations yield orange films, while molybdenum polymerizations give brittle, red materials when cast onto glass or electrode substrates. Though polymers are reprecipitated to insure purity, discolorations result from residual catalyst amongst the polymer.

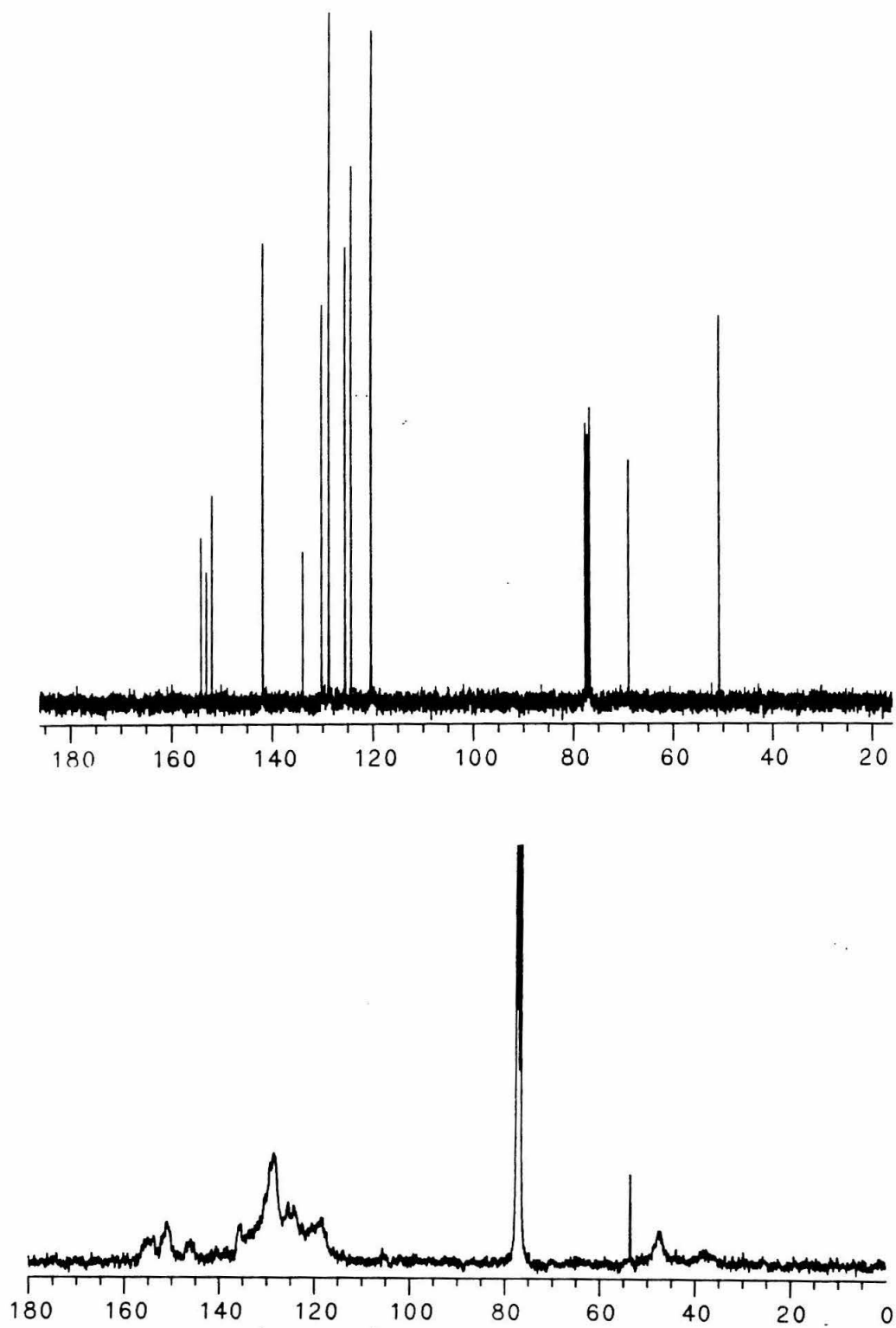


Figure 19: ^{13}C NMR spectra of benzoquinone-imine [9] (top) and PAN (bottom).

The imine polymer (**PAN**) displays a broad DSC exotherm at 200 - 240 °C with the onset of polymer decomposition at 210 °C. A 50 % weight loss at 560 °C indicates great thermal resistance and may correspond to the loss of two equivalents of aniline (52 %) from the polymer.

Though the imine monomer polymerizes, the amine will not. After one day's reaction at room temperature with a molybdenum alkylidene, monomer remains suspended in a milky white suspension, indicating a solubility problem with the amine monomer.

Late Transition Metal Catalysis Attempts

Late transition metal catalysts (Os, Ru, Ir) have greater tolerance for functional groups than their early metal counterparts (Ti, W, Mo) and though they exhibit metathesis activity,¹⁸ aqueous polymerizations often resulted in poor yields and poorer quality materials. Functionalized 7-oxanorbornadienes have now been polymerized in an entirely aqueous environment and water has been shown to decrease the initiation time of polymerization, as compared to polymerization in organics.

$\text{Ru}(\text{H}_2\text{O})_6^{+2}$ has proven to be the most active aqueous catalyst, successfully polymerizing hydroxyl, carboxy, and alkoxy substituted 7-oxanorbornadienes. The success of aqueous ROMP using ruthenium catalysts²⁸ prompted polymerization attempts of the [2.2.1] norbornadienebenzoquinone compounds. Though it would be convenient to directly polymerize the naked quinone, the insolubility of

polymeric quinones and hydroquinones in organic solvents remains disconcerting.

Combination of the quinone-bis ketal [3, 4] and quinone-bis silyl ether monomers [5, 6] with catalyst in water, or a water/ethanol solution, often turns the solution yellow immediately -- consistent with formation of an active $[\text{Ru}^{2+}\text{-olefin}]$ complex. Most of these yellow solutions, however, quickly turn dark brown or green upon catalyst decomposition. RuCl_3 and $\text{Ru}(\text{H}_2\text{O})_6^{+2}$ do not show any polymerization activity toward the quinone-bis silyl ethers, though $\text{Ru}(\text{H}_2\text{O})_6^{+2}$ does turn the polymerization solution yellow, a possible indication of an olefin complex, though there is loose spectroscopic evidence for such a complex (Figure 20).

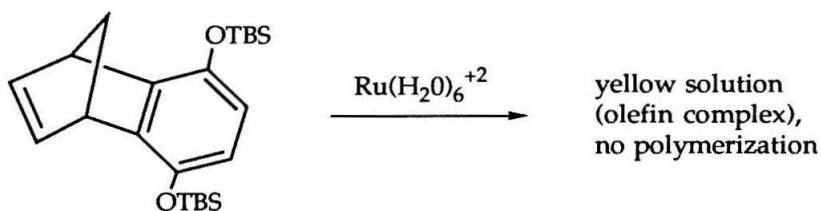


Figure 20: Attempts at aqueous ruthenium polymerization.

Unlike OsCl_3 , which polymerizes the dimethoxy [2.2.1] benzoquinone [2] as a black granular, insoluble solid, RuCl_3 and $\text{Ru}(\text{H}_2\text{O})_6^{+2}$ polymerize the same monomer in ethanol (Figure 21).

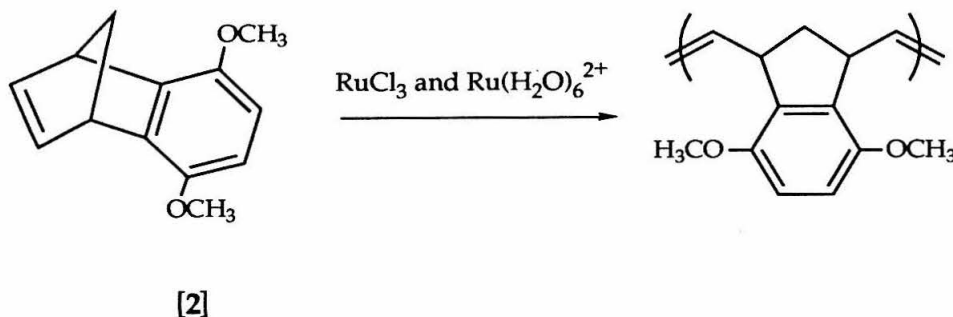


Figure 21: Aqueous polymerization of dimethoxybenzoquinone [2].

Polymer precipitation begins within 15 minutes at 55 °C and accumulates over 18 hours. The white flocculent polymer ($M_w = 38,000$, PDI 8.32) precipitates quantitatively from an amber polymerization solution at 55 °C. Few other polymerization parameters have been explored. While other work indicates often more successful results using degassed solvents and inert atmospheres, the affect of oxygen upon polymer molecular weight has not been investigated.

Reaction Chemistry

Considerable time and effort has been expended in the pursuit of electrically conducting polymers.¹⁹ Though we have polymerized interesting synthetic materials, our intention remains to find the most conductive state of these polybenzoquinones. These polymers, though, have inherent sites of saturation originating from the bridgehead positions of the monomer that must be removed to achieve extended polymer conjugation. Like other wide range semiconductors, polybenzoquinones are expected to exhibit electrical conductivity upon their oxidation or reduction (doping). These quinones are a class of well behaved compounds with highly reversible potentials, ideally suited for attempts at electrochemical (oxidative) doping and Bronsted acid (proton) doping.²⁰

Crystalline polymers encourage facile intra- and interchain carrier transport and narrow the effective band gap of the polymer. Aromatic groups along the polymer backbone often widen band gaps because of the

non-degenerate nature of the aromatic and quinoid states, though Wudl has shown that benzannulation successfully lowers the band gap of polymers by offering the aromatic resonance as an electron buffer between the nondegenerate energy states.²⁴

It has been suggested that unpaired electrons, upon aggregation of the polymer chains, may either localize or delocalize over the molecular sites, setting up a competition between the weak electron-electron interactions in the pendant electroactive groups.²² If the electrons delocalize, we may achieve electrical conductivity according to a charge-transfer mechanism or a hopping mechanism. The charge-transfer mechanism requires complete and long range electron delocalization, i.e., mobile charge carriers without an energy barrier to recombination. The hopping mechanism, though, requires discreet sites of electron delocalization and is often seen in amorphous polymers with pendant electroactive groups, including the polyalkylthiophenes and polypyrroles.²² If those same unpaired electrons localize on individual molecular sites, we may achieve a magnetically active polymer.²³

Polybenzoquinone-bis ketal chemistry (PBK, PNK)

In pursuit of electrically conductive organic materials, the hydrolysis, enolization, and oxidation of the polyquinone-bis ketal polymers (PBK, PNK) removes the saturated bridgehead centers to generate a fully conjugated backbone. Tautomerization of the polyquinones to polyhydroquinones removes these sites of saturation and is either slowly catalyzed by dilute acid, or rapidly achieved by base. When doped effectively, charge carriers develop along the polyquinone,

resembling a conductive polyacetylene with electroactive hydroquinones attached (Figure 22).

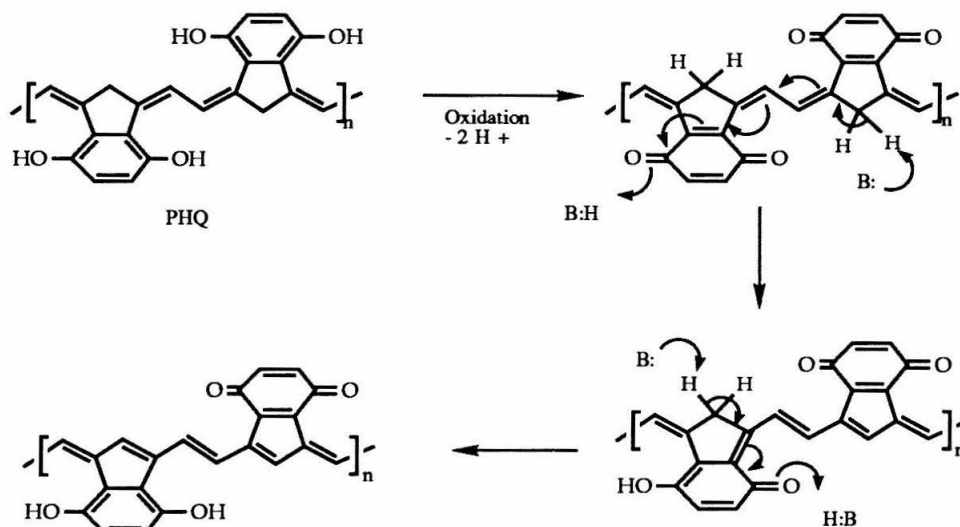


Figure 22: Proposed doping to highly conductive structures.

The polyquinone-bis ketals, **PBK** and **PNK**, were hydrolyzed by soaking films or powders in 15% HCl for 2-6 days to regenerate the quinone moieties from the latent quinones (Figure 23).²⁵ Treated films are shiny jet black and transmit orange when held up to light. The resulting polyquinones **PBQ** and **PNQ** are insoluble, brittle solids lacking optimal mechanical and conductive properties. Polyquinone structures are consistent with ¹³C CPMAS-NMR spectra. Carbonyl resonances at 188 and 184 ppm for **PBQ** and **PNQ** respectively, the disappearance of the methoxy peaks in the 50-60 ppm region, and the absence of ketal resonances at 90-100 ppm all confirm polymer hydrolysis. Additionally, each olefinic carbon is resolved in the **PBQ** sample with resonances at 150, 137, and 134 ppm.

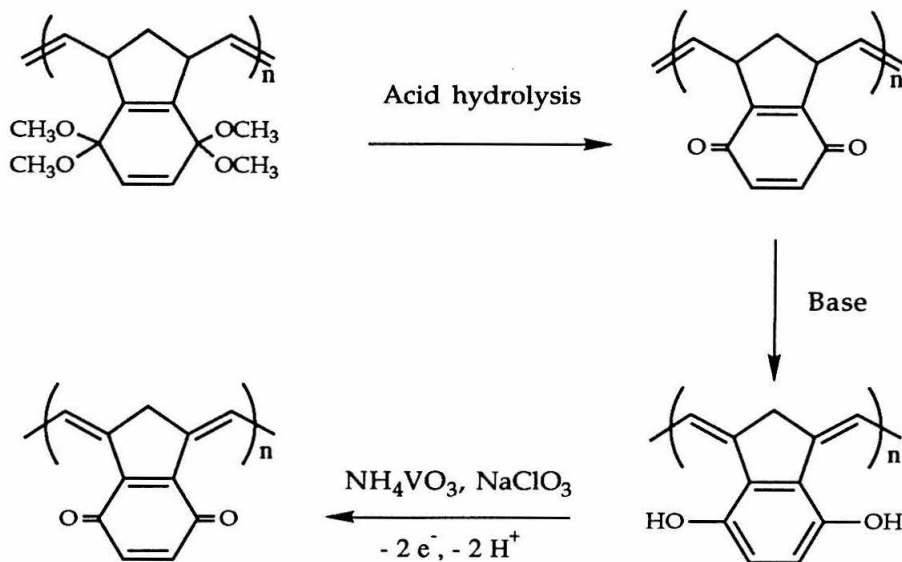


Figure 23: Hydrolysis and Oxidation of polybenzoquinone bis ketal.

Tautomerization of **PBQ** was investigated by infrared spectroscopy.¹⁶ This rearrangement broadens the polymer spectra and shifts the carbonyl band to lower energy, likely the result of extensive hydrogen bonding between quinone and hydroquinone units. Infrared spectroscopy also detects the an intense carbonyl stretching band at 1655 cm⁻¹ for PBQ and 1666 cm⁻¹ for PNQ and the absence of a sharp band at 2840 cm⁻¹, characteristic of methoxy groups. In addition, a number of strong ketal bands in the region of 1000 to 1200 cm⁻¹ are lost upon tautomerization, while the characteristic hydroquinone absorption appears at 3500 cm⁻¹.

Spectroscopic measurements support the proposed elimination in **PBK** as shown in Figure 23, though elemental analyses, IR spectroscopy, and residual ketal resonances in the ¹³C CPMAS-NMR indicate that polymer hydrolysis is not complete, but accompanied by elimination side reactions as well (Figure 24, 25).

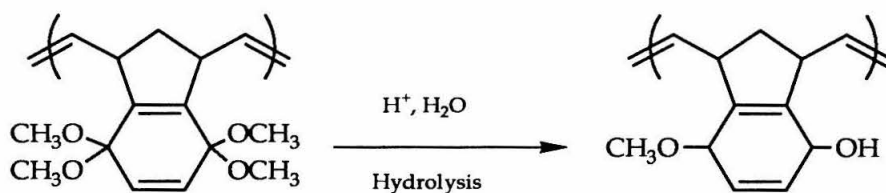


Figure 24: Polymer hydrolysis.

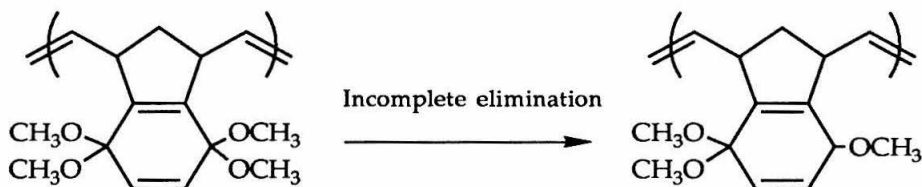


Figure 25: Incomplete polymer elimination.

Treatment of the precursor bis ketal polymer with strongly acidic aqueous solutions (concentrated HCl or HCl/Et₂O solution) results in methanol elimination products in addition to polyquinone formation. Thermal treatment of golden yellow **PBK** and **PNK** films produce insoluble, but pliable, burgundy red films. The facile elimination of methanol was characterized by thermogravimetric analysis and differential scanning calorimetry.

Differential scanning calorimetry of polybenzoquinone-bis ketal **PBK** shows two exotherms at 150 °C and 230 °C, believed to be the stepwise loss of methanol (Figure 26). Polynaphthoquinone-bis ketal **PNK** plots indicate a single, broad DSC exotherm from 210 °C to 280 °C. Thermogravimetric analyses of **PBK** and **PNK** display stepwise weight losses of 20% and 25%, respectively, at 250 °C, in keeping with the expected loss of two equivalents of methanol from the polymer.

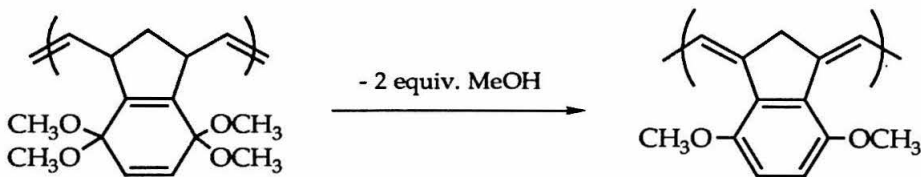


Figure 26: Thermal elimination of methanol.

Volatiles from the thermolysis of **PBK** (200 °C, 12 hr) were collected and identified as methanol. However, when **PNK** was subjected to the same procedure, other unidentifiable volatile compounds were collected along with methanol. Thermolysis at higher temperatures proves ineffective at driving the elimination to completion and results in the extrusion of unidentified orange and yellow solids.

The use of Lewis acid promoted methanol elimination was investigated (Figure 27). Polymers were codissolved with 0.1 eq. of a Lewis acid (ZnBr_2 , ZnI_2 , ZnCl_2 , AlCl_3 , and HgCl_2) and heated at 150 °C for 12 hours. In each case, the burgundy color, indicative of successful methanol elimination, appeared, but often turned brown upon exposure to air. While several Lewis acids seem to have lowered the onset temperature of elimination, only ZnCl_2 and HgCl_2 appear to have successfully driven the reaction to completion. Another approach, using acids and acid anhydrides (acetic and trifluoroacetic) to scavenge the eliminated methanol²⁶ was also successful, though particularly brutal upon polymer samples, as evidenced by elemental analyses.

Samples prepared by thermolysis of **PBK** at 200 °C for 12 hrs were readily doped with iodine to produce shiny black films. Films saturated with iodine (35% by weight) displayed conductivities of $4 \times 10^{-3} \text{ Scm}^{-1}$.

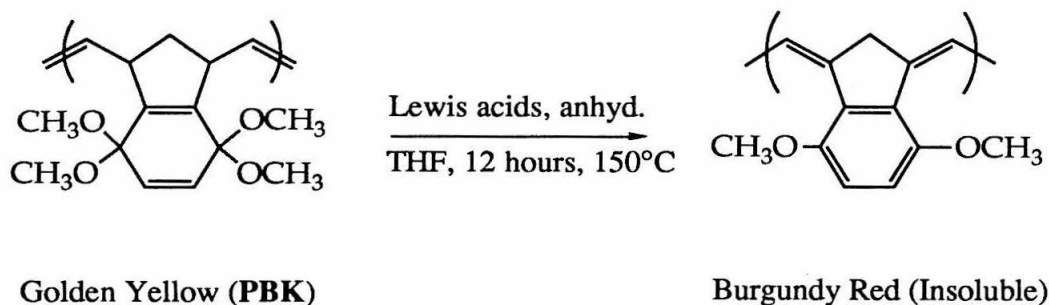


Figure 27: Catalyzed methanol elimination.

Polyquinone-bis silyl ether chemistry (PBS, PNS).

Similarly, the oxidation chemistry of the polyquinone-bis silyl ethers (**PBS**, **PNS**) has been investigated using electrochemical and chemical methods. Troubled by incomplete quinone-bis ketal hydrolysis, desilylation was attempted to improve polymer oxidation and offer a better chance at highly conductive materials.

The quinone-hydroquinone substrate displays a complex electrochemical behavior in buffered aqueous solution. Polymeric quinone-hydroquinone systems have great utility as special regenerable redox reagents. Bound to the surface by strong adsorption or covalent attachment, quinone modifiers act as immobilized, regenerable reagents held in an environment near the surface of the underlying conductor. Electrodes modified by polyquinones provide reliable voltammetric response and possess electrocatalytic activity over a wide pH range.²⁷

A thin polymer film of benzoquinone-bis silyl ether polymer (**PBS**) was deposited onto a glassy carbon electrode and electrochemically oxidized in a solution of acetonitrile/0.1 M TBABF₄. The irreversible oxidation wave at $E = +1.37$ V (vs. SCE) is consistent with polymer desilylation and oxidation to the polyquinone (Figure 28).

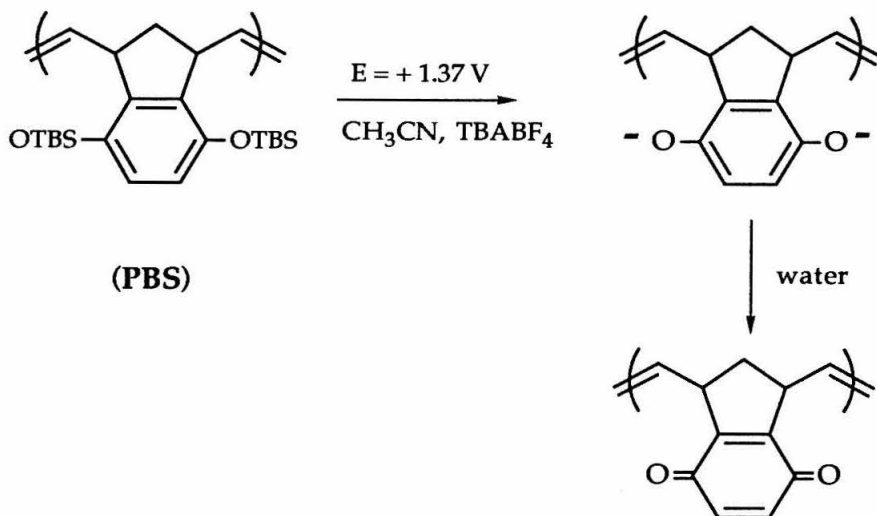


Figure 28: Electrochemical generation of quinone dianion.

When the same oxidized film was cycled through negative potentials, the reversible quinone reduction wave appeared and confirmed formation of the polyquinone (as proposed within the bis ketal reaction hydrolysis pathway). The unusual feature of this reversible quinone reduction wave is its appearance at $E = +0.35 \text{ V}$ (vs. SCE), 0.2 V less negative than that of benzoquinone. The dissimilarity of this potential with that of benzoquinone could be the result of an unusual (and unknown) (π)-system of the polymer. Interestingly, the reversible quinone reduction wave is seen only when small amounts of water are added to the electrolyte. The presence of oxygen in the electrolyte appears vital for successful oxidation, because no voltammetric waves are found when the same experiment is carried out under anhydrous solvent conditions.

In results that mimic the electrochemical findings, an anhydrous polymer solution was treated with an excess of tetrabutylammonium

fluoride (TBAF) at $-78\text{ }^{\circ}\text{C}$ (Figure 29). Soon after addition, a whitish/green solid falls out of solution, leaving behind a dark brown solution.

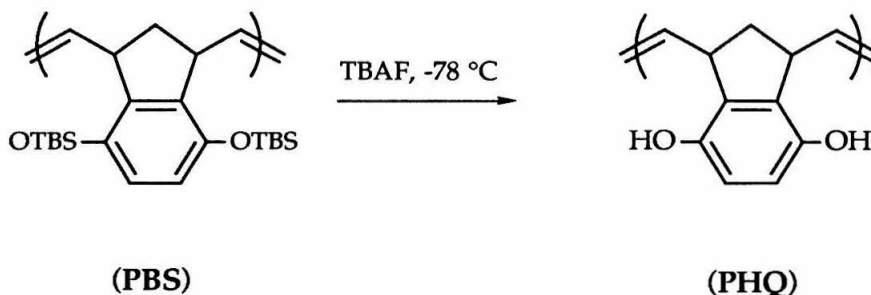


Figure 29: Treatment of bis silyl ethers with fluoride ion.

This solid, the quinone dianion salt, is soluble in acetonitrile and darkens immediately upon exposure to air. Filtration and dissolution in methanol immediately yields a black solution, that upon drying yields an insoluble black, shiny solid - the polyhydroquinone (PHQ).²⁸ Methanol quenches the dianion salt to yield the polyhydroquinone, not the naked polyquinone. In addition, ^{13}C -CPMAS NMR experiments confirm the incomplete elimination of silyl ethers from the polymer and the presence of saturated polymer centers. Though efforts at bulk polymer oxidation with ceric ammonium nitrate (CAN), etc. in wet solvents have resulted in black, insoluble, uncharacterized polymers there remain interesting applications for these soluble quinone dianions described earlier.

Proton doping, unlike most traditional dopants, neither degrades the polymer, nor induces charge defects within its structure, but instead yields a defect free, fully conjugated polymer backbone. It appears to be an equilibrium process, governed by the strength of acid and basicity of

solvent. The action of these non-oxidizing Bronsted (protonic) acids includes the direct protonation of the polymer backbone followed by an internal redox process that gives polarons as the predominant charge defects. Such a mechanism is similar to that proposed for the protonic acid doping of polyaniline.²⁹ An advantage that proton doping offers over conventional redox doping is the elimination of embrittlement and polymer degradation which often occurs upon "overdoping" with powerful redox dopants. Protonic acid doping

Given the appealing prospect of proton doping these materials to high electrical conductivities, polymer films of **PBK**, **PNQ**, and **PBS** were dipped into varying strengths of aqueous acid solutions. The golden yellow films darken upon acid exposure, but ketal and silyl ether stretches still appear in the IR spectra. The process is very slow, incomplete, and offers no advantage to the bis ketal hydrolysis. In spite of improved conjugation upon their oxidation, the electrical conductivities of these materials do not improve, upon doping, from their intrinsic conductivities of 10^{-6} - 10^{-7} S cm⁻¹. In preliminary conductivity studies the polybenzohydroquinone (**PHQ**,) displayed a conductivity of 5×10^{-4} S cm⁻¹ when saturated with iodine. Conductivity measurements remain in the semiconductor region, never besting 4×10^{-3} S cm⁻¹.

The present level of polymer conjugation is not sufficient for metallic conductivity. Extended conjugation is not achieved because sites of saturation remain along the polymer backbone, extended conjugation only appears below the spine. The oxidized hydroquinone polymers have not undergone further tautomerization to produce a polyacetylene backbone with higher conductivities (Figure 30) as depicted in Figure 18.

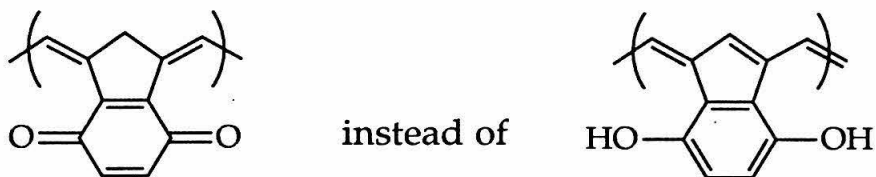


Figure 30: Incomplete tautomerization to polyhydroquinone.

Preliminary investigations into Bronsted acid doping have not improved polyquinone conductivities. Early efforts to facilitate charge transfer through proton hopping in the protonated quinones to mimic the doping results of polyaniline and polypyrrole have failed. Focus must return toward complete removal (chemical) of the saturated centers along the polymer backbone, since each methylene bridge interrupts a fully polyacetylene-like spine.

Polynorbornadiene-imine chemistry

Unlike the polyquinones, electroactive groups are already attached to the polynorbornadiene-imines (PAN). Pendant imines undergo two one-electron oxidations at moderate potentials without net oxidation or reduction of the polymer backbone.³⁰ The incorporation of these electroactive species within the polymer provides an opportunity to tinker with unpaired electrons on the molecular level. While it proceeds much like traditional chemical doping methods, electrochemical doping remains a more uniform and thorough treatment than chemical doping methods.

The electroactive moiety of our polynorbornadiene-imines (PAN) is an analog of N,N'-diphenyl-p-phenylenediamine (DPPD), the simplest oligomer of polyaniline (PANI). However, the redox chemistry of our

polymer differs significantly from that of DPPD. Our polynorbornadiene-imine gives a single two-electron wave separated by 250 mV under the same conditions that DPPD gives two one-electron waves separated by 250 mV (Figures 31, 32, 33, and 34).²¹

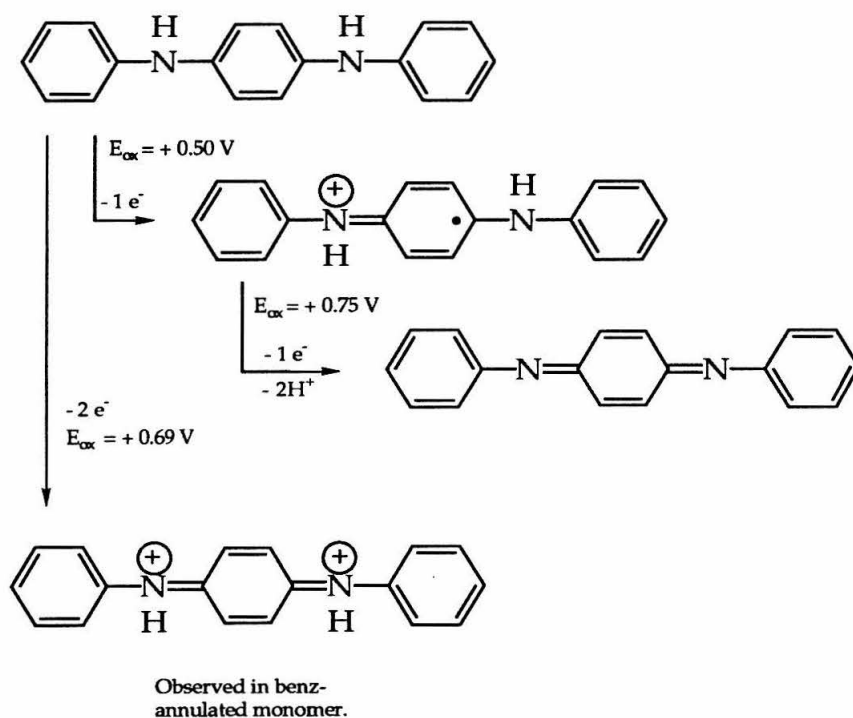


Figure 31: DPPD imine and amine electrochemistry.

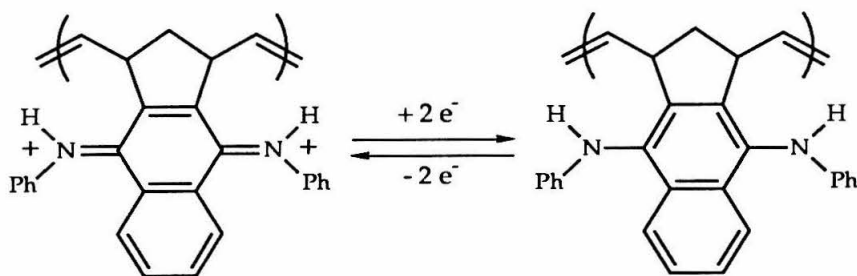


Figure 32: Electrochemistry of protonated polyimine.

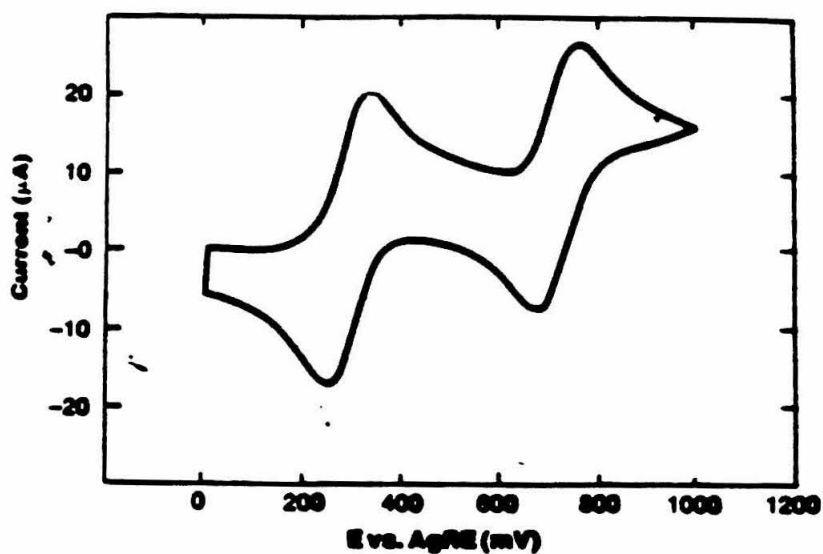


Figure 33: Electrochemistry of DPPD under Et_4NClO_4 in CH_3CN conditions.

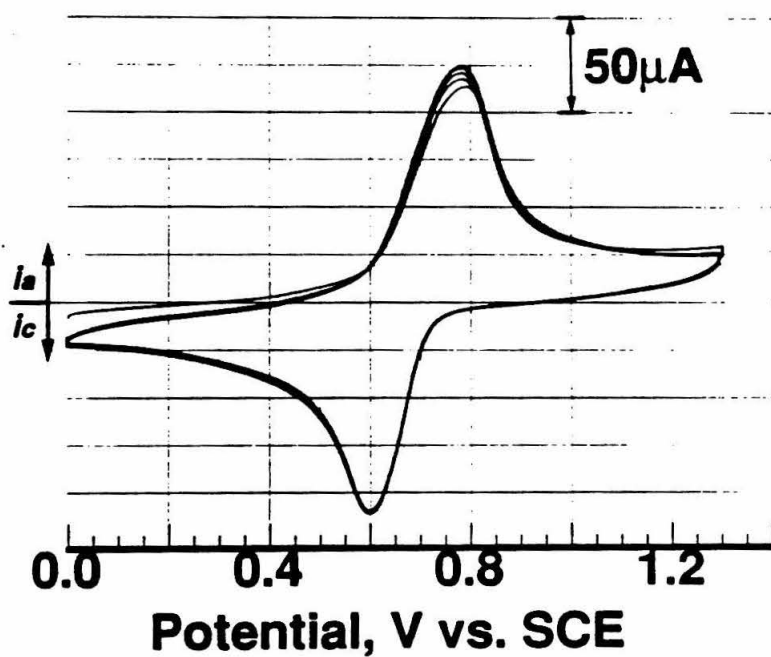


Figure 34: Electrochemistry of PAN under conditions of TBAP, HClO_4 , and CH_3CN on glassy carbon electrode, 50 mV/sec.

The two polyimines differ in the degree of stability of the one-electron product, the radical cation species. DPPD radical cations are spectroscopically observable, the polyimine radical cations (PAN) are not, though its dication is observable. The application of a potential across a polymer film shifts the electrochromic behavior of the polymer in the UV/Vis spectra. A UV/Vis shift out to 520 nm appears with formation of the protonated imine at +1.3 V (vs. SCE) from the UV/Vis transparent neutral amine (Figure 35). The polynorbornadiene-imine demonstrates the electrochromism of the imine/amine redox couple when electrochemically cycled and may be an indication of future switching-device prospects.

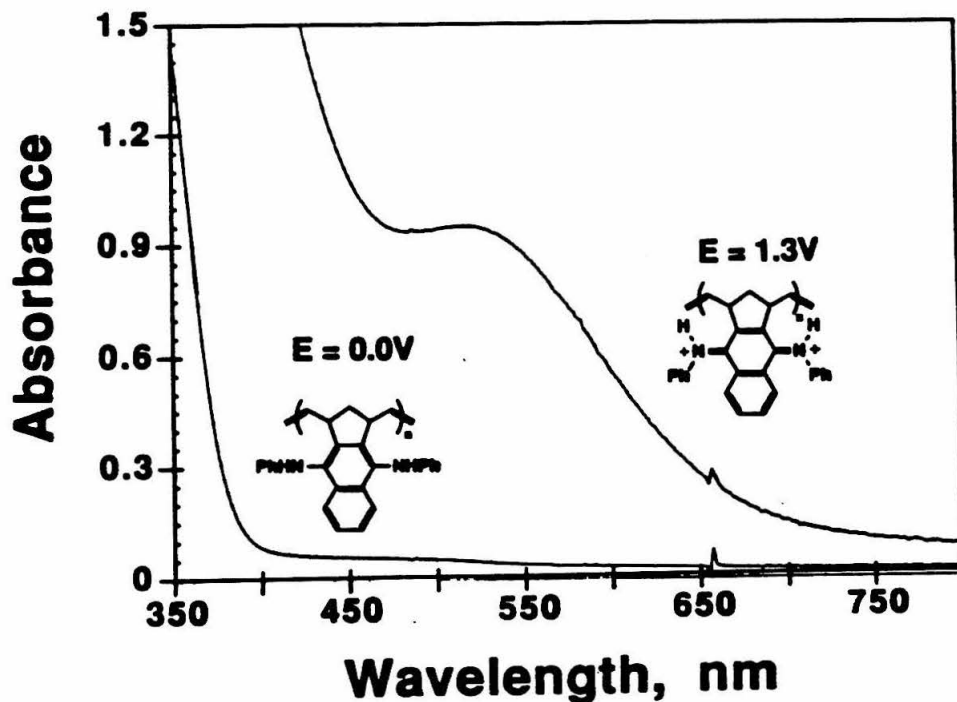


Figure 35: Electroactivity of (PAN) under conditions of TBAP, HClO₄, and CH₃CN on glassy carbon electrode, 50 mv/sec .

N,N'-diphenyl-*p*-phenylenediamine (DPPD) and *N,N'*-diphenyl-*p*-phenylenediimine (DPPI) mixtures disproportionate in solution when in the presence of a Bronstead acid and produce the DPDD radical cation ($+ \cdot$) (Figure 36). It is this disproportionation that is responsible for the protic acid generation of spins seen in polyaniline. Disproportionation attempts to chemically induce the radical cation in the polynorbornadiene-imine system, however, were unsuccessful. Solutions of polymer and amine do not disproportionate. The presence of the amine has no effect upon the UV/Vis spectrum of the protonated polynorbornadiene-imine.

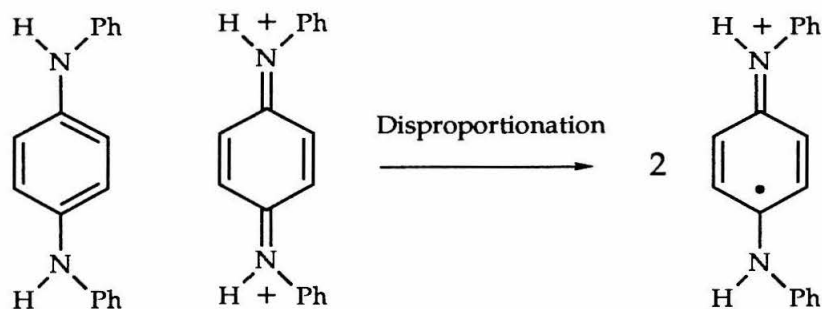


Figure 36: Disproportionation of DPPI and DPPD.

Interestingly, the voltammetry of the (monomer) norbornamine in aprotic media in the absence of a proton source does show the expected voltammetry with two one-electron step oxidations, but the two couples are separated by only 120 mV and the introduction of a proton source causes the voltammetry to change to the one two-electron wave seen for norbornanil in the presence of protic acid. Expectedly, the monomer and polymer imine is not electroactive at these potentials in the presence of a proton source.

Conclusions and Future Prospects

Polymers with the capacity to store, or switch electrochemically are a topic of continued interest. Via soluble precursor routes and ring-opening metathesis polymerization, quinone and imine redox units have been incorporated into well-defined, highly unsaturated, polymer structures. Hydrolysis and thermolysis of soluble polyquinone bisketals have been shown to produce insoluble materials with extended conjugation. While proton doping and tautomerism were envisioned as routes into intrinsically conducting materials, sites of saturation along the polymer chain hamper facile intrachain conduction. At present, these materials only display conductivities in the semiconducting region. Renewed efforts are needed to chemically remove the sites of saturation without disruption of the polymer backbone.

The polynorboraniline shows amazing electrochromicity. Though its radical cation remains elusive in our polymer system, the incorporation of such charge species provides an opportunity to tinker with unpaired electrons on the molecular level.

Quinone Experimentals:

General Considerations

All manipulations of air and/or moisture sensitive compounds were carried out using standard Schlenk or vacuum line techniques with argon as the flush gas. The argon was purified by passage through columns of activated BASF RS-11 (Chemlog) oxygen scavenger and Linde 4Å molecular sieves. Manipulation of air sensitive solids was performed in a Vacuum Atmospheres dry box equipped with a MO-40-1 purification train, a DK-3E Dri-Kool conditioner, and a Dri-Cold freezer. The catalyst dry train contained activated RidoxTM oxygen scavenger and Linde 11Å molecular sieves. In most cases involving the synthesis of these materials, glassware was dried in a 140 °C oven and subjected to vacuum while still hot.

¹H and ¹³C NMR were recorded on either a Jeol 400 GX (399.65 MHz ¹H), General Electric QE-300 Plus (300.199 MHz ¹H, 75.49 MHz ¹³C), or Bruker WM-500 (500.14 MHz ¹H) spectrometer. Chemical shifts were referenced to the solvent or to the residual protons of the solvent. Infrared spectra were acquired on both a Shimadzu IR-435 and Perkin-Elmer Series 1600 spectrometer. Infrared samples were either thin films or KBr pellets. Elemental analyses were performed by the California Institute of Technology Analytical Facility. Conductivity measurements were made with a home built Wnek probe or a commercially available Sigmatone sheet resistivity probe. Current was supplied to these probes by a Power Designs 605 precision power source and measured with a Keithley 160B digital multimeter. The voltage was monitored using a Fluke 895A

differential voltmeter. Thermal analyses were performed on a Perkin Elmer DSC-7 differential scanning calorimeter, TGA-7 thermogravimetric analyzer, and dual Tac 3/7 data stations. The thermal analysis system is driven by an IBM PS/2 computer equipped with standard Perkin Elmer software. Scanning rates for these analyses varied.

Polymer samples were run on a Millipore-Waters 150 C Gel Permeation Chromatography Spectrometer equipped with differential refractometer and a Waters 820 chromatographic data station. A home-built GPC station was also used and utilized Waters Unlustragel columns connected to a Knauer differential refractometer. Polymer solutions of various (~ 0.5 % w/v) concentrations were prepared using either spectral grade 1,2 dichlorobenzene, methylene chloride, or tetrahydrofuran. These solutions were filtered using 0.2 and 0.45 mm UnifloTM filters to protect the Unlustragel columns while sample injections of 0.2 ml and 1.0 ml/min flow rates were commonly used.

Solvents for all polymerizations were kept free of oxygen and moisture. Benzene was dried and deoxygenated with sodium benzophenone ketyl. Pentane was dried and deoxygenated after treatment with sulfuric acid for days. Tungsten alkylidene catalysts were either provided by departing group members or prepared from the published procedures (Introductory chapter, reference 5) and recrystallized from pentane. The large volume of hexane, pentane, and methanol used for precipitation of the polymer was degassed with an argon bleed for thirty minutes.

The Lewis acids, ZnI_2 and HgCl_2 were purified by heating at 100°C under vacuum for 12 hours prior to use. ZnCl_2 , ZnBr_2 , AlCl_3 , and the

acid anhydrides were used without further purification. Benzoquinone was recrystallized from ether before use, but the phenyl and methyl benzoquinones were used without purification.

Preparation of Cyclopentadiene-benzoquinone adduct [1].

This preparation works equally well for the synthesis of the benzoquinone, methylbenzoquinone, and phenylbenzoquinone adducts, as well as their naphthoquinone derivatives. Much of the bis ketal quinone chemistry is described by Tim Swager in his Thesis Dissertation, California Institute of Technology, 1988.

Cyclopentadiene (18.3 g, 0.278 moles) was added to benzoquinone (30 g, 0.278 moles) in 500 ml of ether at -15 °C. Once the reaction mixture warms to room temperature and stirs 3 hours, the ether is removed *in vacuo* to give a slightly yellowed solid. This solid is then dissolved in 500 ml methanol and a scoop of KHCO₃ added, gradually turning the solution brown. This mixture is stirred 12 hours and then methanol is removed *in vacuo* under dynamic vacuum to yield a thick black tar.

Preparation of Bicyclo[2.2.1]dimethoxybenzoquinone [2].

The hydroquinone (48.3 g, 0.278 moles) is dissolved in 300 ml of ethanol with heating, if necessary. Portions of dimethylsulfate (90.78 g, 0.72 mol) and sodium hydroxide (32 g, 0.80 moles) in 80 ml water are added in alternate portions over 50 minutes. With each addition, reflux is maintained, producing methyl ethyl ether. Once addition is complete, 10 grams of sodium hydroxide in 10 ml water are added with considerable exothermicity. The reaction is then refluxed for an additional 2 hours and

the ethanol distilled off, leaving 100 ml of solvent and brown sludge. This sludge is cooled and given an aqueous/ether workup. The ethereal layer is dried, evaporated to a brown solid, recrystallized and finally sublimed at 90 °C at 10^{-6} torr. The final sublimed product is collected as a white solid in 53% yield (27.7 g).

^1H (CDCl_3): 2.21 (2H, s), 3.78 (6H, d), 4.20 (2H, d), 6.45 (2H, d), 6.80 (2H, d) ppm. ^{13}C (CDCl_3): 148.55, 142.64, 140.10, 109.23, 69.79, 55.68, 46.78.

Preparation of Bicyclo[2.2.1]dimethoxynaphthoquinone [7].

The same procedures were followed as given above. This compound will be used in the synthesis of the imine monomers a bit later.

^1H (CDCl_3): 8.20 (2H, q), 7.55 (2H, q), 6.88 (2H, t), 4.43 (2H, m), 4.08 (6H, s), 2.30 - 2.40 (2H, m) ppm. ^{13}C (CDCl_3): 145.09, 141.43, 135.41, 127.62, 125.24, 121.80, 64.82, 61.80, 46.61 ppm.

Preparation of Benzoquinone-bis ketal monomer [3].

Electrochemical Oxidation: The dimethoxy adduct (12.5 g, 0.0612 moles) is dissolved in 1% KOH in methanol (200 ml), with small amounts of THF added to solubilize the solid. Two platinum gauze electrodes are immersed in the methanolic solution and the reaction is vented to a bubbler. A power supply provides the needed 6 volts for the oxidation and current changes are monitored with an in-line ammeter over the course of the five day electrolysis. During this time, the reaction mixture is monitored by thin layer chromatography (ether: hexane, 1:4). The species are easily identifiable. the R_f of the dimethoxy adduct is 0.4 - 0.5 and the bis ketal product decomposes (streaks) from 0 - 0.25. Completion is

determined by TLC and is followed with an aqueous/ether workup, trying to keep air exposure to a minimum. Upon removal of the remaining ether, a tacky yellow solid remains and readily sublimes at 80 °C, under dynamic (10^{-6} torr) vacuum, to a white crystalline solid. Multiple sublimations improve monomer quality.

Benzoquinone-bis ketal [3]: ^1H NMR (CDCl_3): 2.13 (2 H, t), 3.10 (6 H, s), 3.30 (6 H, s), 3.85 (2 H, q), 6.10 (2 H, s), and 6.85 (2 H, t) ppm. ^{13}C NMR (CDCl_3): 153.6, 142.2, 132.4, 95.1, 72.4, 50.9, 49.6 ppm. Elemental Analysis: C: 68.33 (68.18), H: 7.50 (7.65). Mass Spec.: M^+ 264, M^{+1} 265 (22 %), M^{+2} 266 (9 %).

Naphthoquinone-bis ketal [4]: ^1H NMR (CDCl_3): 2.23 (2H, m), 2.91 (6H, s), 3.08 (6H, s), 3.98 (2H, t), 5.93 (2H, t), 7.45 (2H, m), 7.67 (2H, m) ppm. ^{13}C NMR (CDCl_3): 155.0, 142.0, 137.7, 128.7, 126.1, 97.0, 72.0, 51.5, 49.8. Elemental Analysis: C: 72.70 (72.61), H: 6.90 (7.01).

Preparation of 1,4 Dihydro-5,8-dimethoxy-1,4-epoxynaphthalene [11].

The synthesis of this compound was attempted using the method of Cragg.¹¹ Sodamide (14.6 g) was ground (either under dry tetrahydrofuran or inside a dry box) and transferred to a three neck round bottom flask. Dry, freshly distilled furan (100 ml) and tetrahydrofuran (120 ml) were added at room temperature. The mixture was warmed to 50 °C and the 2,5-dimethoxybromobenzene (21 g) added dropwise. The solution was stirred at this temperature for 56 hours under argon, then cooled, filtered, and partitioned between water and ethyl acetate. The organic layer was dried, evaporated, and the residue chromatographed over silica gel with 10% ethyl acetate-petroleum ether. Silica gel is believed to have killed any

product around. ^1H NMR of the residue shows decomposition products. As a result, isolation of the benzofuran adduct remains unsuccessful.

Preparation of 1,4 Dihydro-5,8-dimethoxy-1,4-epoxynaphthalene [11].

The synthesis of this compound was attempted using the procedure of Pansegrau.¹¹ To a solution of 2,5 dimethoxybromobenzene (5 g, 0.023 moles) in 125 ml dry THF, cooled to $-78\text{ }^{\circ}\text{C}$, was added 18 ml of 1.6 M *n*-butyllithium solution (hexane). The mixture was allowed to stir for 30 minutes whereupon a slush developed, though no exotherm was apparent. Freshly distilled furan (25 ml) was added. Again, no exotherm or temperature increase occurred, but a white salt appeared. Stirred at room temperature for 8 hours, the solution became a clear yellow solution. This reaction mixture was poured into a saturated solution of NH_4Cl and the organic layer extracted with water, dried, and pumped down to yield a pale yellow crystalline solid. Unfortunately, this solid has been verified, by NMR as 1,4-dimethoxybenzene. ^1H (CDCl_3): 3.8 (6 H, s), 6.8 (4 H, s) ppm.

Preparation of Furan-benzoquinone adduct.

Furan (4.7 g, 0.069 moles) and benzoquinone (5 g, 0.0453 moles) were added together in 100 ml ether at $-15\text{ }^{\circ}\text{C}$. The solution was allowed to warm to room temperature and stirred for one day. No visible change was apparent. The ether was removed in vacuo to yield a dark green solid which was then promptly dissolved in methanol and a scoop of KHCO_3 was added. No exotherm or evidence of the enolization was apparent. The mixture was stirred for 12 hours and yielded a black, caked solid tar (in

particularly good yield) upon removal of the methanol. Infrared Spectroscopy (KBR pellet): 3415 (m,b), 3129 (m,b), 2950 (m, b), 2744 (m,b), 2632 (m,b), 2364 (w, s), 2331 (w, s), 1700 (s, s), 1653 (s, s), 1632 (s, s), 1510 (w, s), 1404 (s, s), 1307 (m, s), 1080 (m, s), 1006 (m, s), 980 (m, s), 890 (m, s), and 832 (m, s) cm^{-1} .

Preparation of Benzoquinone-bis(*t*-butyl-dimethyl)silyl ether monomer [5].

The ease of preparation of the bis tertiary butyldimethylsilyl ethers make them worthwhile to perform on a large (20 g) scale, including their chromatography workup. Both the benzoquinone and naphthoquinone derivatives are equally accessible with this procedure.

The rigorously clean Diels Alder adduct (20 g, 0.114 moles, 1.0 equivalent) is dissolved in bottled methylene chloride to give a clear, yellow solution. Upon addition of clean (filtered) triethylamine (33.4 mls, 0.240 moles, 2.1 equivalents) and DMAP (2.79 g, 0.023 moles, 0.2 equivalents), the reaction solution turns orange while remaining clear. The tertiary-butyldimethylsilyl chloride (39.64 g, 0.263 moles, 2.3 equivalents), dissolved up in methylene chloride, was added to the reaction mixture - returning the pot to the initial clear yellow color. The system was purged with argon, bottled up, and left to stir.

After 7 hours, the reaction mixture has darkened to a cloudy orange color. At 22 hours, a white crystalline, solid, NEt_3Cl , has crashed out in great abundance. Reaction is continually monitored by TLC. The bis silyl ether appears at a quick R_f (0.78) in 75 % EtOAc/hexane. At reaction's end, 4 days, the distinct product and starting material spots are visible on the TLC plate. Some crap remains at the origin (triethylamine, etc.). The

reaction mixture is extracted three times with 1 N HCl and dried over MgSO_4 . Rotovapping the organic layer yields a large quantity of clumpy orange solid that will not sublime cleanly, but which will chromatograph quite easily. A 10 cm flash column eluted with 20 % CH_2Cl_2 /hexane brings off the desired product ($R_f = 0.53$) as a colorless compound with 2 - 3 liters of solvent. The orange color seen earlier remains at the top of the column. Rotovapping the product to dryness yields a large quantity of fluffy white solid which sublimes sharply at 90 °C under flat dynamic vacuum to give a gorgeous white crystalline solid. The overall yield of the reaction, based on starting quinone, reaches 70 %.

^1H NMR (CD_2Cl_2): 6.76 (2H, s), 6.28 (2H, s), 4.03 (2H, s), 2.03 - 2.17 (2H, m), 0.99 (18H, s), 0.123 (6H, s), and 0.120 (6H, s) ppm. ^{13}C NMR (CD_2Cl_2): -4.30, 18.36, 25.83, 47.44, 69.68, 117.81, 141.99, 142.65, and 144.08 ppm. Elemental Analysis: C: 68.11 (68.30), H: 9.19 (9.40). IR (KBr): 2962 (m, s), 2861 (m, s), 1604 (w, s), 1481 (s, s), 1257 (s, s), 980 (s, s), 882 (s, s), 839 (m, s), 779 (s, s) cm^{-1} .

Preparation of Naphthoquinone-bis(*t*butyl-dimethyl)silyl ether monomer [6].

Similar reaction conditions for the synthesis of the bis silyl ether naphthoquinone. Again reaction time of 4 -5 days results in 60 % reaction yield. The brown clumpy reaction product is flash chromatographed using 20 % CH_2Cl_2 /hexane and cleanly removes the desired product ($R_f = 0.5$) away from impurities and unreacted starting materials. Sublimation of the white crystalline solid at 110 -115 °C under flat vacuum yields an immaculately white crystalline solid.

^1H NMR (CD_2Cl_2): 7.91 - 7.93 (2H, m), 7.33 - 7.35 (2H, m), 6.73 (2H, s), 4.15 (2H, s), 2.05 - 2.17 (4H, m), 1.12 (18H, s), 0.18 (6H, s), and 0.13 (6H, s) ppm.

^{13}C NMR (CD_2Cl_2): -3.80, 18.74, 26.23, 47.31, 65.92, 122.58, 124.39, 128.53, 134.50, 138.64, and 141.46 ppm. Elemental Analysis: C: 71.41 (71.60), H: 8.80 (8.80).

Preparation of Dehydro-naphthoquinone [8].

The bicyclo[2.2.1]dimethoxynaphthoquinone (5 g, 0.0198 mol) is dissolved up in acetonitrile and an aqueous solution of ceric ammonium nitrate (CAN) (32.6 g, 0.0594 mol), is added dropwise into the reaction mixture. Left to react for 2 hours, a bright yellow solid is filtered off from a cloudy, dingy yellow/orange solution. TLC (10 % ether/hexane) of this solution after an ether/water extraction indicates the absence of starting material. Extraction with ether/water and drying the organic layer yields a bright yellow solid (the norbornadiene-naphthoquinone) in 93 % yield.

Preparation of norbornadiene-naphthoquinone-imine monomer [9].

The synthesis of the imine monomer has been successful only with the naphthoquinone precursor. Reactions run with the benzoquinone are mired with side reactions presumably due to the acidic protons of the benzoquinone. Efforts to replace those aromatic protons on the benzoquinone with alkyl or halide substituents are continuing.

A benzene solution of the norbornadiene-naphthoquinone (2.0 g, 0.009 mol) and aniline (16.76 g, 0.180 mol) are loaded into a 250 ml round bottom flask, separately from the yellow TiCl_4 (3.42 g, 0.018 mol) solution in benzene. After the system is purged with argon and cooled to 0 °C, the TiCl_4 is added slowly through an addition funnel. The naphthoquinone derivative does not dissolve immediately, though addition of the TiCl_4

solution does turn the reaction a red color and thickens to a slurry. By reactions end, this slurry is a rust-colored suspension that is left to warm to room temperature under argon.

The reaction mixture is extracted with distilled water and chloroform, the organic layer dried and yields a red solid compound. Some additional yellow/orange solid crystallizes out of a concentrated chloroform solution. Column chromatography (10 % ether/petroleum ether) of the entire reaction mixture yields the desired product as a red, crystalline solid.

^1H (CDCl_3): 8.53 (2H, m), 7.62 (2H, m), 7.40 (10H, m), 7.18 (2H, m), 6.41 (2H, m), 2.93 (2H, m), 1.55 - 1.78 (2H, m) ppm. ^{13}C (CDCl_3): 153.95, 152.89, 151.81, 141.73, 133.80, 130.07, 128.62, 125.40, 124.19, 120.22, 68.75, 50.58 ppm. UV (CH_3CN): 312 nm (23,100) and 445 nm (7000). Elemental Analysis: C: 87.01 (87.10), H: 5.51 (5.40), N: 7.60 (7.50). M. p. 155 - 156 °C.

Preparation of Naphthoquinone-amine monomer [10].

An aqueous solution of sodium dithionite ($\text{Na}_2\text{S}_2\text{O}_4$) is added to an ether solution of the norbornadiene-naphthoquinone-imine. The reaction vessel is then shaken vigorously for some 4 hours. Upon completion, the organic layer has turned yellow. Extraction of the organic layer with ether/water yields a white solid.

^1H (CDCl_3): 7.98 (2H, m), 7.42 (2H, m), 7.21 (10H, m), 6.70 (2H, m), 4.03 (2H, m), 2.12 (2H, m) ppm. ^{13}C (CDCl_3): 141.62, 129.24, 125.63, 123.16, 118.39, 114.05, 65.48, 47.79 ppm. Elemental Analysis: C: 86.71 (86.70), H: 5.99 (5.90), N: 7.43 (7.50).

General Polymerization Techniques.

Extreme care was exercised to keep the system air and moisture free during polymerization. All glassware was pumped into the drybox hot and both monomer and catalyst were loaded into separate Schlenk tubes inside the drybox. Polymerizations were monitored by thin layer chromatography since the monomer decomposes with R_f 0 - 0.25 and the polymer sits at the origin. Aliquots of the polymerization solution were taken with a capillary tube under a heavy purge of argon and polymerization was terminated when no monomer streaking was observed. The polymer was precipitated from deoxygenated hexane after dilution of the polymerization solution with small amounts of methylene chloride.

All polymerizations are monitored for monomer consumption by thin layer chromatography and terminated upon completion. Monomer to catalyst ratios of typically 50 - 100 : 1 employed. Catalyst ratios as high as 250 : 1 have been attempted, but the higher ratios have resulted in polymer precipitations of "stickier" quality polymer and poorer reaction yields. Polymerizations run with monomer to catalyst ratios of 100 : 1 or 75 : 1 consistently give materials with high molecular weights and better material properties.

Polymerization of Benzoquinone bis ketal (PBK).

The bis ketal monomer (2.00 g., 7.58 mmoles) and tert-butyl tungsten alkylidene catalyst (43.4 mg., 0.0758 mmoles) are added together

in 5 ml of benzene. A color change from pale yellow or a golden yellow/orange occurs within minutes. The polymerization solution is viscous after 1.5 hours and polymerization is complete by 3 hours. The solution is then diluted with small amounts of benzene and methylene chloride and precipitated as an off-white powder from a large volume of hexane. The hexane is filtered off and the remaining solvent removed in vacuo overnight. NMR and elemental analysis samples were prepared after drying the polymer in a drying pistol heated with refluxing methanol.

^1H (CDCl_3): 1.60 (1H, b), 2.35 (1H, b), 3.10 (6H, b), 3.15 (6H, b), 3.60 (2H, b), 5.80 (2H, b), and 6.2 (2H, b) ppm. ^{13}C (CDCl_3): 144.8, 132.8, 130.2, 96.1, 51.8, 46.5, 42.0, 36.8 ppm. Elemental Analysis: C: 68.13 (68.18) H: 7.78 (7.65).

Polymerization of Naphthoquinone-bis ketals (PNK).

The procedure followed is that of the benzoquinone bis ketal polymerization above. A catalyst to monomer ratio of 1:100 is found most effective. The polymer precipitates in similar fashion, but takes a bit longer for polymerization to reach completion (8 hours).

^{13}C (CDCl_3): 145.8, 132.8, 129.6, 129.0, 125.9, 98.3, 51.6, 51.2, 46.9, 34.8 ppm. Elemental Analysis: C: 71.65 (72.61) H: 7.15 (7.01).

Polymerization of Benzoquinone-bis(*t*butyldimethyl)silyl ether (PBS).

The bis silyl ether is dissolved up in THF (or benzene) to give a clear, slightly yellowed solution. LKJ catalyst is dissolved up separately and added to the monomer to give a dark orange, but clear, polymerization solution. Left to stir at room temperature for 5 days,

continually monitored by TLC for presence of monomer ($R_f = 0.5$) and polymer ($R_f = 0.0$). Upon completion, precipitation in methanol or hexane gives a large quantity of off-white polymer.

^1H NMR (CHCl_3): 6.4 (2H, br), 5.7 (2H, br), 3.7 (2H, br), 2.4 and 1.8 (2H, br), 0.6 - 1.0 (18H, vbr), and -0.1 - 0.3 (12H, vbr) ppm. ^{13}C NMR (CHCl_3): -3.53, 18.50, 26.14, 40.50, 41.63, 46.00, 117.23, 132.00, 137.58, and 146.34 ppm. IR (nujol): 2949 (m, s), 2938 (m, s), 2858 (m, s), 1489 (s, s), 1304 (w, s), 1250 (m, s), 991, 879 (m, s), 832 (m, s), 778 (m, s), cm^{-1} .

Polymerization of Naphthoquinone(*t*butyldimethyl)bis silyl ether (PNS).

Polymerization of the naphtho-bis silyl ether follows the same procedure as above and is also similar to the polymerization of the bis ketal monomers.

^1H NMR (CHCl_3): 7.98 (2H, br), 7.60 (2H, br), 5.80 (2H, br), 4.40 (2H, br), 2.6 and 2.0 (2H, br), 0.95 (18H, br), 0.3 and -0.2 (12H, br) ppm. ^{13}C NMR (CHCl_3): 141.18, 132.93, 129.11, 123.60, 122.72, 42.3, 26.29, 18.61, -2.55, -3.45 ppm.

Polymerization of Naphthoquinone-imines (PAN).

Polymerization of these compounds followed the same procedures found with polymerization of the bis ketal and bis silyl ethers.

^1H (CDCl_3): A non-descript, broadened NMR spectra is obtained for the polymer and appears paramagnetic. However, the ^{13}C spectra is resolved. ^{13}C (CDCl_3): 154.52, 151.03, 146.02, 135.47, 128.42, 125.48, 124.14, 118.27, 48.0, 37.0 ppm. Elemental Analysis: C: 87.01 (83.90), H: 5.37 (5.40), N: 7.60 (7.50).

General Aqueous Polymerization Procedure

In a typical polymerization, the monomer and catalyst were degassed as solids in a test tube or Schlenk flask for 1 hour. Degassed water or a water/ethanol solution (~ 2 ml) was added to the flask under argon. Upon mixing, the reaction mixture was placed in an oil bath at 55 °C under argon. A white precipitate formed after 0.5 hours. After 2 days, the flask was removed from the oil bath and the polymer filtered through a glass frit and washed with methanol. The polymer was dried under dynamic vacuum at room temperature. The polymer is then dissolved and reprecipitated for NMR.

Polybenzoquinone-bis silyl ether: ^1H NMR (CH_2Cl_2): 6.4 (2H, br), 5.7 (2H, br), 3.7 (2H, br), 2.4 and 1.8 (2H, br), 0.6 - 1.0 (18H, vbr), and -0.1 - 0.3 (12H, vbr) ppm. ^{13}C NMR (CH_2Cl_2): -3.53, 18.50, 26.14, 40.50, 41.63, 46.00, 117.23, 132.00, 137.58, and 146.34 ppm.

Polymer hydrolysis of Polybenzoquinone-bis ketal (Polybenzoquinone) (PBQ).

All hydrolysis reactions were performed on either polymer films or powders without any regard to air exposure. The use of aqueous acidic and basic solutions is evidence of this fact. Film hydrolysis was carried out at room temperature using 250 ml lidded jars.

Films or powders of the polybenzoquinone bis ketal polymer were immersed in 10% and 15% HCl and 5% and 10% H_2SO_4 solutions for upwards of three weeks. By this time, films have turned a red/brown and are fragmented beyond use. Powders are jet black and easily collected. Treatment of the parent polymer with Ag_2O and ceric ammonium nitrate result in a dark brown/orange polymer.

Infrared Spectroscopy: 3500 (m vbr), 2920 (m s), 1655 (vs, br), 1588 (m, s), 1493 (s, s), 1453 (s, br), 1393 (w, s), 1318 (s, s), 1220 (s, br), 1075 (m, vbr), 967 (m, s), 830 (m, s), 673 (w, s) cm^{-1} .

Treatment of Polybenzoquinone-bis(^tbutyldimethyl)silyl ethers with fluoride.

The bis silyl ether polymer is easily dissolved in THF to give a clear tan colored solution. The solution is cooled to - 78 °C upon which a solution of TBAF in THF is added in several portions over a couple of minutes to the cooled, argon purged solution. No immediate indication of a reaction.

Soon after, however, the reaction mixture turns a murky green, and a white solid falls out of solution. As the solution warms to room temperature, it appears to be a dirty white/green solid accompanied by a dark colored solution.

Filtration indeed yields a green clumpy solid in good yield and a darker green/brown solution. The green solid dissolves immediately in methanol and turns immediately black. Further attempts to solubilize are fruitless. The black crystalline shiny solid is washed several times with THF and looks good.

Thermolysis of Polybenzoquinone bis ketals.

The polymer under investigation was loaded in specially designed, non greased, glassware and dissolved in a minimum of solvent (THF). The solvent was removed in vacuo and the vessel heated at 150 °C for upwards of 12 hours, resulting in an intractable, burgundy red solid.

Methanol Elimination from Polybenzoquinone bis ketals.

The polymer is dissolved in 5 ml of THF with 0.1 equivalents of either the Lewis acid or acid anhydride. Upon dissolution, the Lewis acids turned the golden yellow polymer solution a dark orange, while the trifluoroacetic anhydride swelled the polymer solution and immediately turned it black/red. As with the thermolysis, the solvent was removed under vacuum and the system heated for 12 hours at 150 °C. Once cooled, the intractable brown solids were rinsed several times with THF to remove residual acid and pumped dry again before analysis.

Quinone References:

- 1) *Synthetic Metals*. 1991, 25, 41 and references within.
- 2) K. Y. Jen, K. Y.; Odoodi, R.; Elsenbaumer, R. L. *Proc. of Am. Chem. Soc.; Div. of Poly. Mat. Sci. and Eng.* 1985, 53, 79. Sato, M.; Tanaka, S.; Kaeriyama, K. J. *J. Chem. Soc. Chem. Commun.* 1986, 873. Patil, A. O.; Ikenoue, Y.; Wudl, F.; Heeger, A. J. *J. Am. Chem. Soc.* 1987, 109, 1858. Askari, S. H.; Rughooputh, S. D.; Wudl, F.; Heeger, A. J. *Polymer Preprints*. 1989, 30(1), 157.
- 3) Edwards, J. H.; Feast, W. J. *Polymer J.* 1980, 21, 595. Gragon, D. R.; Karasz, F. E.; Thomas, E. L.; Lenz, R. W. *Synthetic Metals*. 1987, 20, 85. Gagnon, D. R.; Capistran, J. D.; Karasz, F. E.; Lenz, R. W.; Antoun, S. *Polymer J.* 1987, 28, 567. Han, C.; Lenz, R. W.; Karasz, F. E. *Polymer Commun.* 1987, 28, 261. Murase, I.; Ohnishi, T.; Noguchi, T.; Hirooka, M. *Polymer J.* 1987, 28, 229. Jen, K.; Jow, T. R.; Elsenbaumer, R. L. *J. Chem. Soc. Chem. Commun.* 1987, 1113. Ballard, D. G. H.; Couris, A.; Shirley, I. M.; Taylor, S. C. *Macromolecules*. 1988, 21, 294. McKean, D. R.; Stille, J. K. *Macromolecules*. 1987, 20, 1787. Feast, W. J.; Harper, K. *Polymer J.* 1986, 18(3), 161.
- 4) Patai, S.; Rappaport, R., Editors. The Chemistry of the Quinonoid Compounds. John Wiley and Sons. 1988. Peover, M.; Lindsey, A. *Chem. Ind.* 1961, 1273. Manecke, G.; Bahr, C.; Reich, C. *Angew. Chem.* 1959, 71, 646. Ezrin, M.; Cassidy, H. *Ann. N. Y. Acad. Sci.* 1953, 57, 79. Dalal, V. F.; Litt, M. H.; Rickert, S. E. *J. Poly. Sci.* 1985, 23, 2659.

- 5) Bryce, M. R.; Moore, A. J. *Tet. Lett.* **1988**, 29 (9), 1075. MacDiarmid A. G.; Chiang, J. C.; Richter, A. F. *Synth. Met.* **1987**, 18, 285. Huang, W.; MacDiarmid, A. G.; Epstein, A. J. *J. Chem. Soc. Chem. Comm.* **1987**, 1784. Wolf, J. F.; Forbes, C. E.; Gould, S.; Shacklette, L. W. *J. Electrochem. Soc.* **1989**, 136 (10), 2887. Shacklette, L. W.; Wolf, J. F.; Gold, S.; Baughman, R. H. *J. Phys. Chem.* **1988**, 88 (6), 3955. Epstein, A. J.; Ginder, J. M.; et al. *Synth. Met.* **1987**, 21, 63. McManus, P. M.; Yang, S. C.; Cushman, R. J. *J. Chem. Soc. Chem. Comm.* **1985**, 1556. Yue, J.; Epstein, A. J. *J. Am. Chem. Soc.* **1990**, 112, 2800. Lu, F. L.; Wudl, F.; et al. *J. Am. Chem. Soc.* **1986**, 108, 8311.
- 6) Polymerizations were attempted with a variety of catalysts including, OsCl_3 , RuCl_3 , IrCl_3 , ReCl_5 , WCl_6 : SnMe_4 and $(\text{CO})_5\text{W}=\text{C}(\text{OMe})\text{Ph}$.
- 7) Electrochemical oxidations of this type have been reviewed: Swenton, J. S. *Acc. Chem. Res.* **1983**, 16, 74, and references within. Swenton, J. S.; Bonke, B. R.; Chen, C.-P.; Chou, C. T. *J. Org. Chem.* **1989**, 54, 51.
- 8) Inagaki, T.; Lee, H. S.; Hale, P. D.; Skotheim, T. A.; Okamoto, Y. *Macromolecules.* **1989**, 22, 4641. Kobayahi, S.; Iwata, S. *J. Am. Chem. Soc.* **1990**, 112, 1265. Stern, A. J.; Swenton, J. S. *J. Org. Chem.* **1988**, 53, 2465. Vaughn, W. R.; Yoshimine, M. *J. Org. Chem.* **1957**, 22, 7. Meinwald, J.; Wiley, G. A. *J. Am. Chem. Soc.* **1958**, 80, 3667.
- 9) Oevering, H.; Paddon-Row, M. N.; et al. *J. Am. Chem. Soc.* **1987**, 109, 3258. Paddon-Row, M. N.; et al. *Tet.* **1986**, 42, 1779. Paddon-Row, M. N.; *Acc. Chem. Res.* **1982**, 15, 245. *Nippon Kagaku Kaishi.* **1987**, 684.

- 10) Cannizzo, L. F. California Institute of Technology Thesis. 1987.
- 11) Cragg, G. M. L.; Giles, R. G. F.; Roos, G. H. P. *J. Chem. Soc. Perkin I.* **1975**, 1339. Pansegrau, P. D.; Rieker, W. F.; Meyers, A. I. *J. Am. Chem. Soc.* **1988**, *110*, 7178. Rees, C. W.; West, D. E. *J. Chem. Soc. Perkin I.* **1970**, 583.
- 12) Willig, G.; Pohmer, L. *Chem. Ber.* **1956**, *89*, 1334. Ziegler, G. R. *J. Am. Chem. Soc.* **1969**, *89*, 446. Ziegler, G. R.; Hammond, G. S. *J. Am. Chem. Soc.* **1968**, *90*, 513.
- 13) Schaverien, C. J.; Dewan, J. C.; Schrock, R. R. *J. Am. Chem. Soc.* **1986**, *108*, 2771. Schrock, R. R.; Depue, R. T.; Feldman, J.; Schaverien, C. J.; Dewan, J. C., Liu, A. H. *J. Am. Chem. Soc.* **1988**, *110*, 1423.
- 14) Strauss, D. A.; Grubbs, R. H. *J. Mol. Cat.* **1985**, *28*. Gilliom, L. R.; Grubbs, R. H. *Organometallics*. **1986**, *5*, 721. Kress, J.; Osborn, J. A. *J. Am. Chem. Soc.* **1983**, *105*, 6346. Quignard, F.; Leconte, M.; Basset, J. M. *J. Chem. Soc. Chem. Commun.* **1985**, 1816. Schaverien, C. J.; Dewan, J. C.; Schrock, R. R. *J. Am. Chem. Soc.* **1986**, *108*, 2771. Schrock, R. R.; Depue, R. T.; Feldman, J.; Schaverien, C. J.; Dewan, J. C., Liu, A. H. *J. Am. Chem. Soc.* **1988**, *110*, 1423.
- 15) Klavetter, F. K.; Grubbs, R. H. *J. Am. Chem. Soc.* **1988**, *110*, 7807.
- 16) Swager, T. M.; Grubbs, R. H., unpublished results. Johnson, L. K., unpublished results.
- 17) Johnson, L. K.; Virgil, S. C.; Grubbs, R. H. *J. Am. Chem. Soc.* **1990**, *112*, 5384.
- 18) Ruthenium references

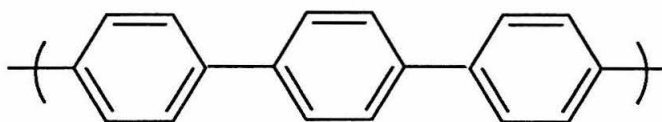
- 19) Skotheim, T. J., Editor. Handbook of Conducting Polymers. Marcel Dekker. New York. 1986.
- 20) Patai, S.; Rappoport, Z. The Chemistry of Quinonoid Compounds: Volumes 1 and 2. John Wiley and Sons. New York. 1988. Chiang, J. C.; MacDiarmid, A. G. *Synthetic Metals*. 1986, 13, 193. Reiss, H. *J. Phys. Chem.* 1988, 92, 3657.
- 21) Garito, A. F.; et al. *J. Org. Chem.* 1978, 43 (10), 2084. Enkelmann, V. *Angew. Chem. Int. Ed. Engl.* 1991, 30 (9), 1121. Wolf, J. F.; Forbes, C. E.; Gould, S.; Shacklette, L. W. *J. Electrochem. Soc.* 1989, 136 (10), 2887. Shacklette, L. W.; Wolf, J. F.; Gold, S.; Baughman, R. H. *J. Phys. Chem.* 1988, 88 (6), 3955.
- 22) Skotheim, T. A. Handbook of Conducting Polymer, Volumes 1 & 2. Marcel Dekker, Inc. New York. 1986. Cowan, D. O.; Wiygul, F. M. "The Organic Solid State". *Chemical and Engineering News*. July 21, 1986. p 28. Garito, A. F.; Heeger, A. J. *Accts. Chem. Res.* 1974, 7 (7), 232. Jerome, D. *Cond. Mat. News*. 1992, 1 (4), 11. Garito, A. F.; et al. *J. Org. Chem.* 1978, 43 (10), 2084.
- 23) Miller, J. *Synth. Met.* 1988, 27, 353. LeBlanc, Jr., O. H. in Physics and Chemistry of the Organic Solid State. Interscience. New York. 1967. p 123. Shchegolev, I. F. *Phys. Status Solidi*. 1972, 12, 9. Heeger, A. J.; Garito, A. F. *AIP Conf. Proc.* 1973, 10, 1476.
- 24) Wudl, F.; Kobayashi, M.; Heeger, A. J. *J. Org. Chem.* 1984, 49, 3382. Kobayashi, M.; Colaneri, N.; Boysel, M.; Wudl, F.; Heeger, A. J. *J. Chem. Phys.* 1985, 82, 5717. Bredas, J. L.; Heeger, A. J.; Wudl, F. *J. Chem. Phys.* 1986, 85, 4673. Kertesz, M.; Lee, Y. S. *J. Chem. Phys.* 1988, 88, 2609.

- 25) Stern, A. J.; Swenton, J. S. *J. Org. Chem.* **1989**, *54*, 2953. Fife, T. H. *Accts. Chem. Res.* **1972**, *5* (8), 264.
- 26) Shacklette, L.; Jen, K. Y.; Elsenbaumer, R., unpublished results.
- 27) Degrand, C.; Miller, L. L. *J. Electroanal. Chem.* **1982**, *132*, 163. Degrand, C.; Miller, L. L. *J. Electroanal. Chem.* **1981**, *117*, 267. Miller, L. L.; Van De Mark, M. R. *J. Am. Chem. Soc.* **1978**, *100*, 639. Degrand, C. *J. Electroanal. Chem.* **1984**, *169*, 259. Smith, D. K.; Tender, L. M.; Lang, G. A.; Licht, S.; Wrighton, M. S. *J. Am. Chem. Soc.* **1989**, *111*, 1099.
- 28) Corey, E. J.; Snider, B. B. *J. Am. Chem. Soc.* **1972**, *94*, 2549. Corey, E. J.; Venkateswarlu, A. *J. Am. Chem. Soc.* **1972**, *94*, 6190. Jung, M. E.; Lyster, M. A. *Org. Syn.* **59**, 35.
- 29) Wolf, J. F.; Forbes, C. E.; Gould, S.; Shacklette, L. W. *J. Electrochem. Soc.* **1989**, *136* (10), 2887. Huang, W.-S.; MacDiarmid, A. G.; Epstein, A. J. *J. Chem. Soc. Chem. Commun.* **1987**, 1784. Epstein, A. J.; Ginder, J. M.; Zu, F.; Woo, H.-S.; Tanner, D. B.; Richter, A. F.; Angeloupoulos, M.; Huang, W.-S.; MacDiarmid, A. G. *Synth. Met.* **1987**, *21*, 63. Reiss, H. *J. Phys. Chem.* **1988**, *92*, 3657. Han, C. C.; Elsenbaumer, R. L. *Synth. Met.* **1989**, *30*, 123. Kuzmany, H.; Sariciftci, N. S.; Neugebauer, H.; Neckel, A. *Phys. Rev. Lett.* **1988**, *60* (3), 212.
- 30) Garito, A. F.; et al. *J. Org. Chem.* **1978**, *43* (10), 2084. Enkelmann, V. *Angew. Chem. Int. Ed. Engl.* **1991**, *30* (9), 1121. Wolf, J. F.; Forbes, C. E.; Gould, S.; Shacklette, L. W. *J. Electrochem. Soc.* **1989**, *136* (10), 2887. Shacklette, L. W.; Wolf, J. F.; Gold, S.; Baughman, R. H. *J. Phys. Chem.* **1988**, *88* (6), 3955.

Chapter Two. Precursors to Polyparaphenylene

Introduction

Polyparaphenylene (PPP) is a structural, rigid-rod polymer with exceptional thermal and oxidative stability. Often crystalline with electrical conductivities approaching 500 S/cm (doped with AsF_5), PPP garners commercial interest for use in electrochemical cells, battery materials, static suppressors, and solid lubricants.¹



Polyparaphenylene (PPP)

This conjugated, insoluble, low molecular weight macromolecule often remains structurally uncharacterized because its synthesis often requires exotic solvents, including $\text{SbF}_5\text{-SO}_2$, butylpyridinium-chloride/ AlCl_3 , and trifluoromethane sulfonic acid. Different syntheses produce samples with different morphologies, so PPP properties are preparation-dependent.

The most economical method of PPP preparation is Kovacic's coupling of benzene using an $\text{AlCl}_3/\text{CuCl}_2$ catalyst (Figure 1). His preparation yields quantities of substantially linear, highly conductive polymer without numerous side reactions.

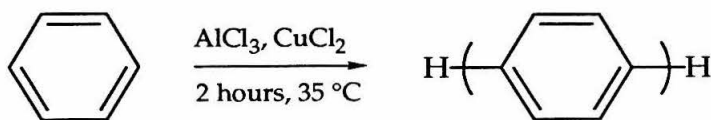


Figure 1: Kovacic's PPP preparation.

Other direct synthetic approaches, including the coupling of benzene dihalides, digrignards, and dilithio compounds (Wurtz-Fittig and Ullmann reactions), generate either ill-defined materials with a mixture of para, meta, and ortho linkages and crosslinks, or insoluble oligomers. These step growth processes synthesize low molecular weight materials with structural irregularities and low degrees of polymerization. Routes involving the polymerization and aromatization of cyclohexadienes often lack control over the amount of 1,2 and 1,4 polymer linkages because these methods require high temperature or strong oxidative dehydrogenations.²

The most promising PPP precursor polymer systems, however, rely upon the stereochemically controlled polymerization of functionalized cyclohexadiene diols (Figure 2).³ Using nickel catalysts, these functionalized cyclohexadienes are polymerized to yield soluble, high molecular weight materials which convert to PPP under mild thermal conditions.

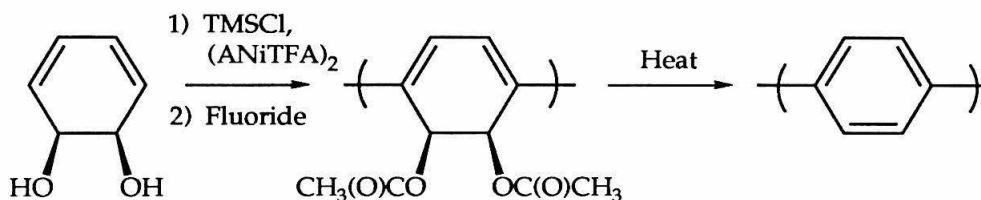


Figure 2: PPP carbonate precursor route.

Proposed Precursor Route

This chapter describes a new soluble precursor polymer route to polyparaphenylene (PPP) based upon the chemistry of 3,4-substituted cyclobutenes (Figure 3). These precursor polybutenamers undergo a final conversion, under mild reaction conditions,⁴ to insoluble PPP without destroying or disturbing the existing polymer structure. These

polybutenamers, regardless of their success in the PPP pathway, are of great interest because they incorporate high degrees of acid, oxygen, and heteroatom functionality into a soluble 1,4-poly(butadiene) structure.

The ring-opening metathesis polymerization (ROMP) of 3,4-substituted cyclobutenes yields soluble, high molecular weight polybutenamers, having the same repeat unit as substituted 1,4-poly(butadiene). Upon elimination, these polybutadienes undergo electrocyclic ring closure and spontaneous oxidation to native 1,4 PPP. Such electrocyclic ring closures are known to occur under mild conditions (~ 150 °C for 1,3,5 hexatriene) and yield a partially hydrogenated PPP substrate. All bis exo-methylenes, however, must be planar and cis to the polymer chain to drive the cyclization and oxidation of the precursor to completion. Stereochemical control during monomer synthesis and polymerization insures complete elimination, cyclization, and oxidation of the PPP precursors.

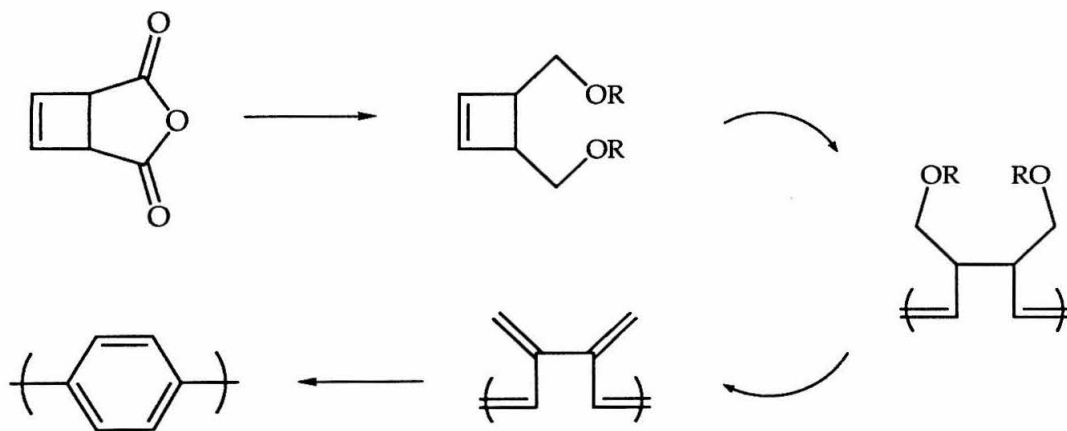


Figure 3: Proposed PPP precursor pathway.

The projected pathway also provides for the polymerization of neat dimethylene cyclobutene (DMCB). Isolation and entrapment of DMCB from pyrolysis reactions, however, is more dangerous given its high reactivity and penchant to form peroxide polymers upon exposure to air.

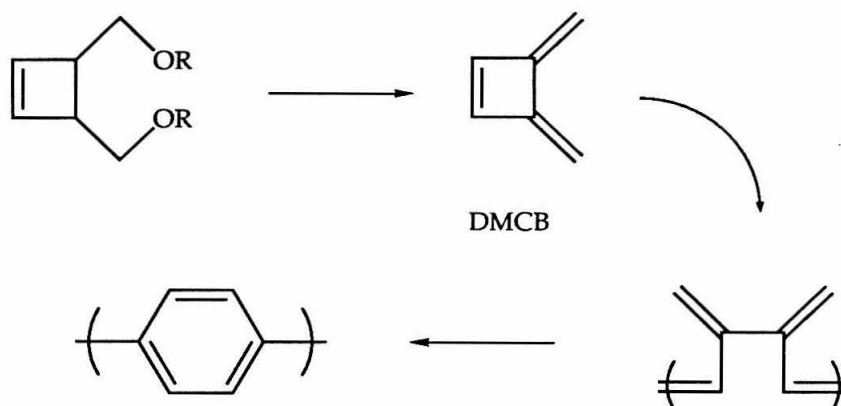


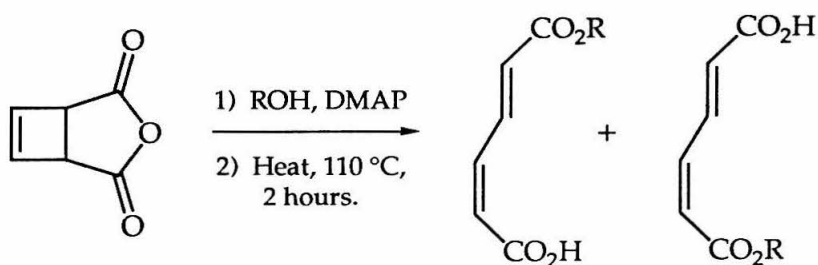
Figure 4: Polymerization of dimethylene cyclobutene (DMCB).

The ROMP of dimethylene cyclobutene, nonetheless, provides direct access into the synthesis of cross conjugated, highly unsaturated polymers and improves upon Ballard's PPP precursor methods because only a few polymer weight percent are lost upon electrocyclic ring closure and oxidation of the hydrocarbon precursor polymer to crystalline PPP.⁵ Ballard and Gin's functionalized precursors extrude nearly half the polymer's mass during conversions. Extrusion of acids, alcohols, and gases limits the utility of these methods while giving often fibrous and cellular materials.

This new synthetic approach to polyparaphenylene (PPP) precursors via polybutadienes (PBD) takes advantage of the ROMP-ability of cyclobutenes to generate 1,4 polymer linkages without 1,2 linkage defects. Their large strain energies, often exceeding 30 kcal/mole, provide a thermodynamic punch toward polymerization lacking in most other strained

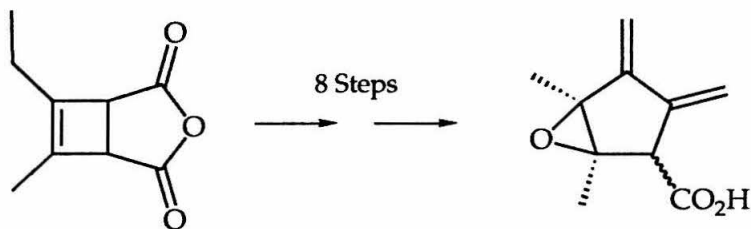
olefins. As a direct consequence, reaction between these 3,4-substituted cyclobutenes and our stable of increasingly tolerant ROMP catalysts presents some powerful opportunities in polymer and material chemistry.

Molybdenum, tungsten, vanadium, chromium, and classical Ti(IV) - Al(III) systems have ring-open polymerized cyclobutenes to give cis and trans 1,4-polybutadienes, yet there has been an amazingly small amount of research devoted to the polymerization of substituted cyclobutenes.⁶ Work on substituted cyclobutenes has focused, instead, upon the thermal conversion between cyclobutenes and butadienes, specifically the ratio of (E,Z) isomer formation in dissymmetric systems (Figure 5). In addition, these cyclobutenes have been synthesized as natural product precursors and other macromolecules of synthetic interest (Figure 6).⁷



Trost and McDougal, 1984.

Figure 5: (E,Z) isomer formation upon thermolysis.



Methylenomycin A

Scarborough and Smith, 1980.

Figure 6: Cyclobutene precursor to methylenomycin A.

Efforts within our own research group have included the polymerization of alkyl substituted cyclobutenes to 1,4-polybutadienes using functionality tolerant, tungsten, molybdenum, and ruthenium alkylidenes under both aqueous and anhydrous conditions.⁸ Polybutadiene not only has commercial usage in tires, conveyor belts, wire and cable insulation, footwear, and other soft rubber applications, but is also under investigation in academics for use in block copolymers, liquid crystal applications, and rubber technologies.⁹

The ROMP of substituted 3,4 cyclobutenes, unlike the addition polymerization of 1,3-butadiene, is a controlled polymerization of a reactive monomer that selectively polymerizes only 1,4 polymer linkages along the unsaturated polymer chain. According to the proposed pathway, a highly unsaturated and cross conjugated poly(methylenebutadiene) is the immediate precursor to the cyclized dihydro-polyparaphenylene. This polymer may arise either from the direct polymerization of dimethylene cyclobutene (DMCB), or from the elimination of functional groups from substituted

polybutadienes. The chemistry behind each pathway will be explored in further detail.

Dimethylene cyclobutene (DMCB)

The ROMP of dimethylene cyclobutene provides direct access into the synthesis of cross conjugated, highly unsaturated PPP precursor polymers. The thermal intramolecular rearrangement of 1,5 hexadiyne to dimethylene cyclobutene proceeds via an allene intermediate in 88 % yield (Figure 7).¹⁰

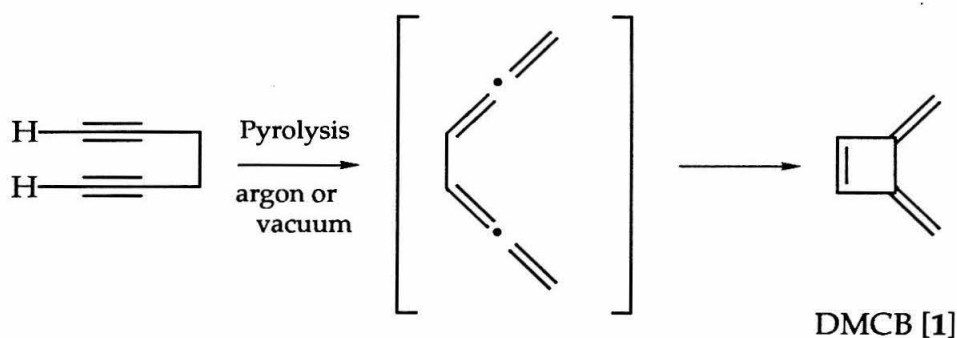


Figure 7: Pyrolysis of 1,5 hexadiyne.

The flash vacuum pyrolysis of 1,5 hexdiyne is carried out under either flow or static conditions that require a standard wide-bore tube furnace with quartz insert to insure volatilization and contact of the hexadiyne with the furnace hot zone. The gas phase reaction runs cleanly to completion over several hours under static vacuum at 232 °C. The static vacuum condition accomodates smaller scale (< 2 g) reactions and allows facile transfer of organic compounds without exposure to air. NMR confirms structural assignments of the exocyclic inboard and outboard protons at 4.67 and 4.75 ppm, respectively, as well as the olefinic singlet resonance at 6.96 ppm. Distillation readily separates the lower boiling DMCB (72 °C) from unreacted

hexadiyne (86 °C). The purification of dimethylene cyclobutene (DMCB) from unreacted 1,5-hexadiyne was attempted, but not pursued, given the explosive nature of neat (liquid) DMCB.

Dimethylene cyclobutene (DMCB) is a clear, colorless liquid that has (surprisingly) long term stability in the absence of air, though occasionally prone to room temperature polymerizations under argon. Upon exposure to air, however, DMCB rapidly polymerizes into hard, brittle, infusible, shock and heat sensitive peroxide polymers, $(C_6H_6O_2)_n$. Because of this reactivity, all quantities of DMCB are stored in solution, under argon, at subambient (-30 °C) temperatures.

Direct polymerization of DMCB into a soluble and well characterized polymer material remains doubtful. There is no evidence in the literature on the polymerization of this compound, though Tim Swager reported the polymerization of DMCB with a series of classical catalysts, including $WOCl_4/Sn(CH_3)_4$. His insoluble, tan, polymeric solids were highly crosslinked, colored materials with many saturated carbon centers (~ 45 %), indicating that polymerization of the highly reactive DMCB occurs by a non-ROMP mechanism. Infrared studies involving the polymeric vinylene (1849 cm^{-1}) groups eliminate both radical and cationic polymerization pathways, but do not offer any alternative polymerization mechanisms.¹⁶

Polymerizations of DMCB using titanium metallacycles and early tungsten alkylidene catalysts were unsuccessful, giving only indications of intramolecular catalyst deactivation and chain transfer processes.¹¹ Recent attempts have focused upon tungsten and molybdenum alkylidene polymerizations and have given quite different results. A solution of DMCB immediately turns dark red and opaque, instead of the expected golden

yellow, upon addition of $(^t\text{BuO})_2\text{W}(\text{CHC}(\text{CH}_3)_3)(\text{NPh}(2,6\text{-isoprop})_2)$. An insoluble black flocculent solid, different from Swager's tan colored solid, crashes out upon precipitation into methanol and remains uncharacterized. NMR spectra do not uncover evidence of DMCB polymerization, but only confirm the formation of dimethylcyclobutene among other reaction products.

Unlike the tempered reaction of the DMCB, the reaction of the hexadiyne alone with $(^t\text{BuO})_2\text{W}(\text{CHC}(\text{CH}_3)_3)(\text{NPh}(2,6\text{-isoprop})_2)$ is quite vigorous. Combination of milligram quantities of monomer and catalyst in benzene produces an exothermic reaction that produces a large quantity of insoluble, black residue. Shiny and reflective on some surfaces, the residue is believed to be polyacetylene.

The high reactivity and uncontrolled polymerization of the dimethylene cyclobutene made its elimination and isolation the less attractive precursor pathway into PPP. Efforts have focused upon the thermal elimination of functional groups from the polybutadiene polymers because the polymerization of 3,4-substituted cyclobutenes are significantly tamer reactions than those involving DMCB and bulk thermal elimination has been shown to be an effective method for cleanly removing solubilizing functional groups from a polymer precursor structure.¹²

Monomer Synthesis

Synthesis of 3,4-substituted cyclobutenes, pioneered by Hartmann and Criegee, begins with the [2 + 2] photoaddition of acetylene and maleic anhydride (or a maleimide derivative).¹³ Initially reported by Hartmann, photolysis of the acetone solution for 8 hours at -10°C with benzophenone as

a triplet sensitizer yields the desired photoadduct, cis-3,4-cyclobutenedicarboxylic acid anhydride in 10 % overall yield (Figure 8).

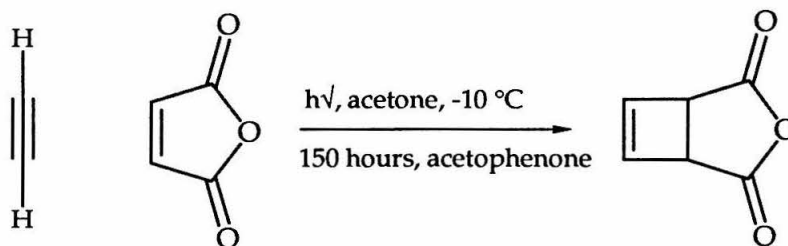


Figure 8: Photogeneration of cis-3,4-cyclobutenedicarboxylic acid anhydride.

Though the literature preparation calls for a 150-hour photolysis of a 1.7 M acetylenic solution, we found a significant loss of acetylene after only 8 hours of photolysis. Side reactions abound upon photolysis in the absence of acetylene. Photolysis generates not only the [2 + 2] maleic anhydride and acetone photoproduct (dimethyl oxetane), but also a large amount of radical anhydride polymer and bicyclopropyl isomers (Figure 9, 10). Vinyl radical and ring-opening polymerization reactions yield vast quantities of white flaky, insoluble, polymeric anhydrides in the absence of acetylene quantities.

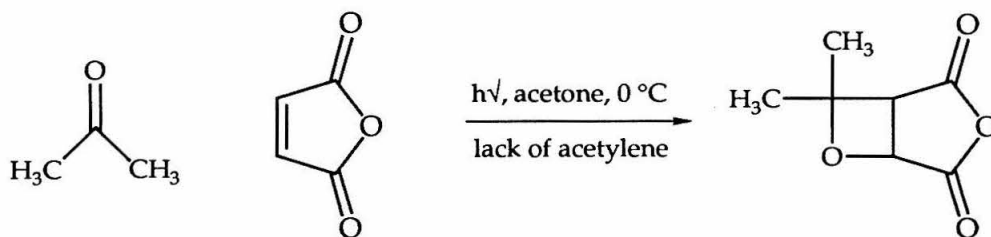


Figure 9: Dimethyl oxetane side reaction.

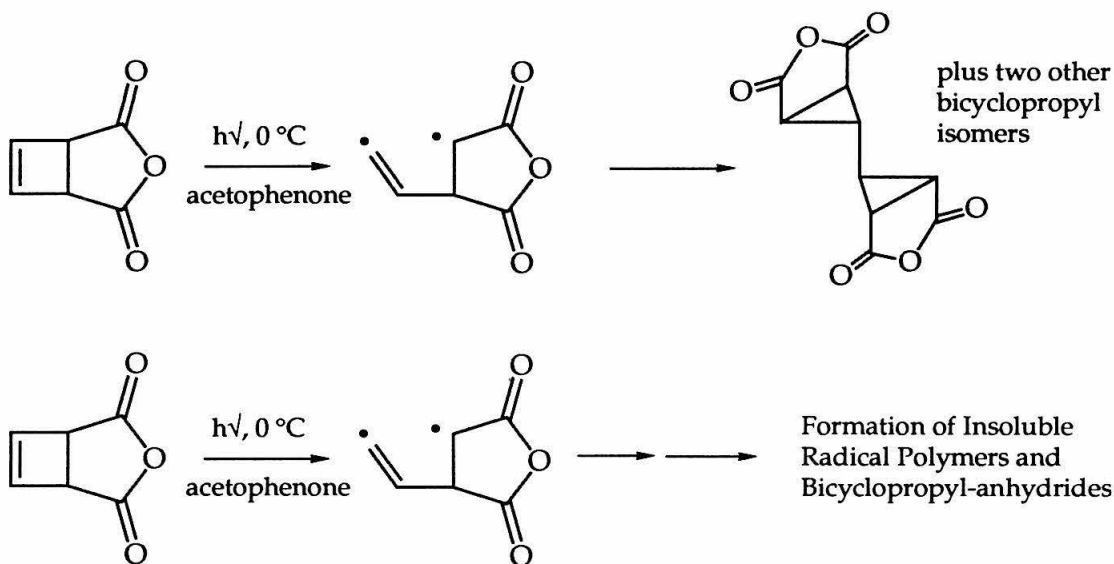


Figure 10: Photolysis (acetylene deficient) side reactions.

To remedy the loss of acetylene, reduce side reactions, and improve photoreaction yields, an acetylene sparge was employed to insure an acetylene-saturated reaction solution. While the prospect of an open acetylene cylinder within a photolysis set up is frightening, safety measures (blast shields, stainless steel fittings, tygon, and teflon tubing) have kept the situation under control.

The amount of dimethyl oxetane was also minimized by switching the reaction solvent from acetone to acetonitrile. While this doesn't eliminate oxetane formation completely (acetylene boils off from acetone in commercially available dewars - the most stable and safest way to handle the acetylene gas), the quantity of extraneous material is reduced without sacrificing acetylene solubility.

Photolysis at $-68\text{ }^{\circ}\text{C}$ optimizes the photoreaction and significantly reduces the amount of photogenerated side products. It is, however, unfeasible with our water-cooled photolysis lamp. Though our photoreactor

guarantees complete UV exposure, its design restricts the range of available reaction temperatures. Instead, by reducing reaction concentrations (≤ 0.54 M maleic anhydride), we drive the photolysis to completion and suppress the oxetane and polymer side reactions. At higher (1.02 M maleic anhydride, and above) concentrations, polymer formation inhibits photochemical completion by occluding the surface of the photolysis lamp.

Though benzophenone is the cited triplet sensitizer with a high photochemical threshold (69 kcal/mole) and long triplet lifetime (10^{-4} s), its presence in the reaction mixture complicated separation efforts. The anhydride, photoproduct, and benzophenoneone are all white solids with comparable boiling points at reduced pressure. Distillation of the semi-solid reaction mixture will not cleanly separate benzophenone from the reaction mixture distillate without great effort and loss of material. Attempts to react the benzophenone sensitizer selectively "away" from the cis-3,4-cyclobutenedicarboxylic acid anhydride, including NaBH_4 reduction, were unsuccessful. A different triplet sensitizer was required. Naphthalene (61 kcal/mole, 10^{-4} s), was not reactive enough to mediate the photoreaction, though acetophenone was found to not only mediate the photoreaction, but also simplify the reaction workup. Initially worry over acetophenone's "increased" triplet reactivity (71 kcal/mole, 10^{-4} s) was unnecessary because acetophenone-sensitized photoreactions yield clear, clean, uncomplicated reaction products.

The unfiltered UV irradiation of an acetylene-saturated acetonitrile solution at 0 °C for 8 hours with acetophenone sensitizer yields an "iced tea" colored solution, without evidence of any ring-opened side products.

Though the origin of discoloration is unknown, the reaction photochemistry is remarkably clean (Figure 11).

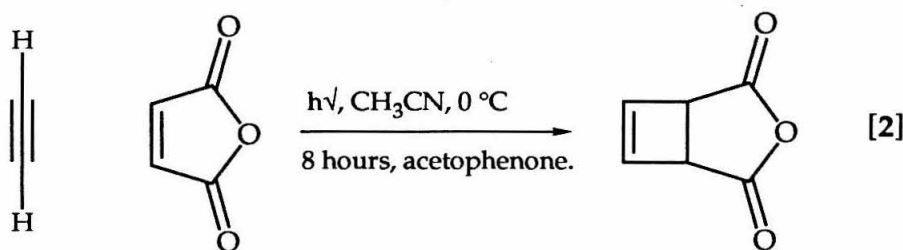


Figure 11: Photogeneration of cis-3,4-cyclobutenedicarboxylic acid anhydride.

Evaporation and concentration of the clear “iced tea” solution yields a bucketload of white solid and an orange reaction mixture sludge. Distillation of the reaction mixture at 50 °C under dynamic vacuum (10^{-6} torr) removes all unreacted maleic anhydride and acetophenone (a clear, colorless liquid) from the reaction. A second distillation at 80 - 90 °C under dynamic vacuum brings the cis-3,4-cyclobutenedicarboxylic acid anhydride product over as an off-white crystalline solid. Recrystallization from benzene and cyclohexane (1:1) gives the final product as a pristine, white crystalline (needles) solid. Because the oxetane and polymer side products are not soluble (or less soluble) in benzene, sonication and dissolution of the distillation pot (an orange caked solid at this point) in benzene removes additional anhydride from the sludge and improves the overall yield to ~20 %.

The proposed structure of structure of cis-3,4-cyclobutenedicarboxylic acid anhydride remains consistent with Nuclear Magnetic Resonance (NMR), Infrared spectroscopy (IR), and elemental analysis. While ^1H and ^{13}C NMR resonances are all sharp singlets, the IR vibrations at 1856 and 1790 cm^{-1} characteristically appear within a cyclic anhydride structure. The anhydride,

not surprisingly, is not a thermally stable compound. Thermal analysis (TGA) shows rapid decomposition of the compound to a blackened char with complete weight loss over the temperatures range of 100 - 210 °C.

While the photoadditions of 2-butyne, propenes, and 1-hexynes with maleic anhydride derivatives have been reported (and isolated in some cases)¹⁴, the photoreaction of simple unsubstituted acetylenes and anhydrides remains the research focus. The reaction chemistry of these substituted adducts must be left for exploration by others (Figure 12).

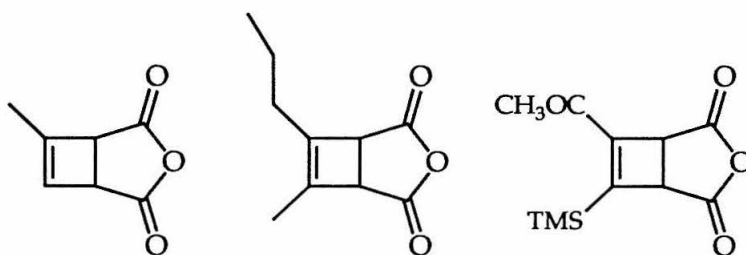


Figure 12: Photoproducts with substituted acetylenes.

Attempts at coupling acetylene with dihydrofurans, diacids, and diester 2-butenes have all been unsuccessful (Figure 13).

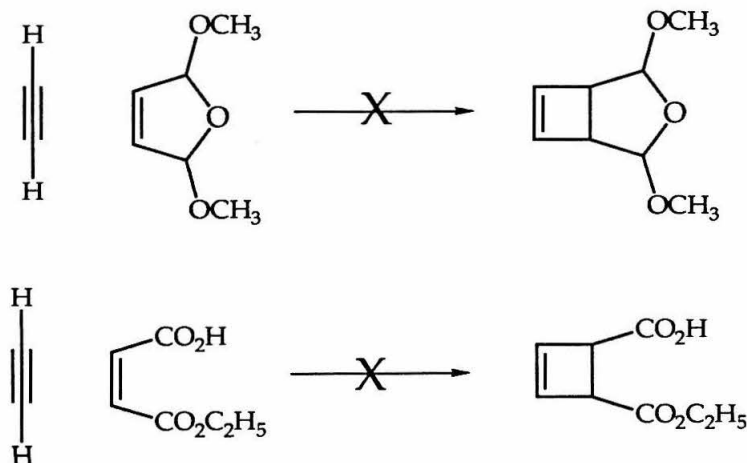


Figure 13: Unsuccessful photoadducts.

While these photoadducts might have presented synthetic shortcuts to the 3,4 substituted cyclobutenes, the photo-unreactivity of the 2-butenes and dihydrofurans is not surprising. Triplet energy absorbed by the butenes is probably used in fluxing between cis and trans conformations, instead of photoreacting with the acetylene.

The final, and possibly most interesting, photoproduct is the acetylene-N-methyl maleimide adduct (Figure 14).

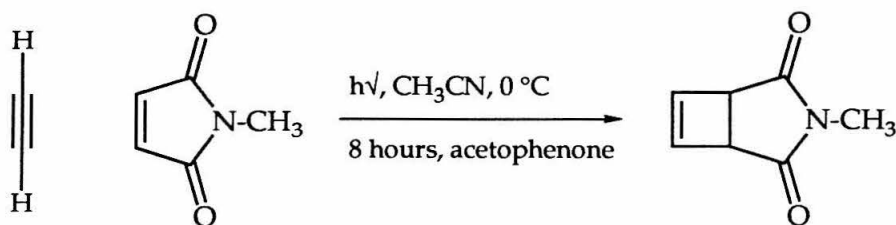


Figure 14: Protein conjugate monomer synthesis.

Generated under similar photolysis conditions as its maleic anhydride equivalent, great attention has been drawn to the ROMP polymer of this maleimide adduct as a potential substrate for the formation of catalytic protein conjugates.¹⁵ Since work into the polymerization of this compound has only begun, the full implication of this material will be discussed a bit later in the chapter.

The acetate, carbonate, and mesylate functionalized cyclobutenes have been targeted as PPP precursor polymers because their heteroatom functionalities remain compatible with ROMP conditions and eliminate under mild reaction conditions. Bulk thermal elimination has been shown to be an effective method for cleanly removing solubilizing functional groups from a polymer precursor. Though the cis-3,4-di(hydroxymethyl)cyclobutene-

monoethylester, cis-3,4-cyclobutenedicarboxylic-bis(dimethyl)amide, cis-3,4-cyclobutene-bis(trimethyl)silyl ether, along with several cyclobutene diesters have been synthesized, they proved unsuitable as polymer precursors and as a result, their polymerizations were not pursued (Figure 15).

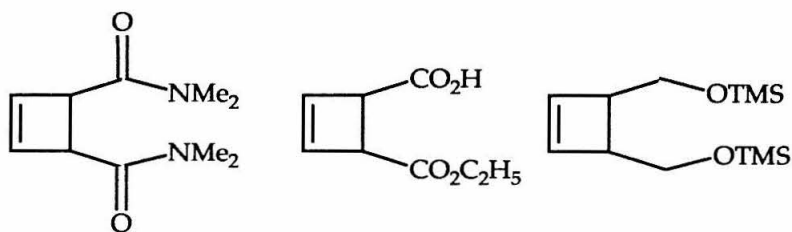


Figure 15: Unsuitable monomers for polymerization.

The LAH reduction of the cis-3,4-cyclobutenedicarboxylic acid anhydride gives the cis diol [3] in greater than 90 % yield as a clear, colorless oil (Figure 16).

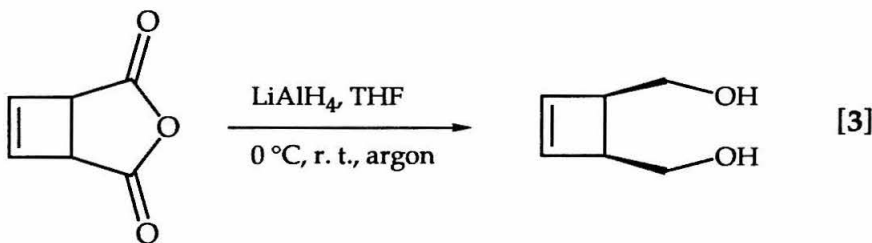


Figure 16: Reduction of cis-3,4-cyclobutenedicarboxylic acid anhydride [3].

NMR spectroscopy confirms the structure and purity of the cis diol that will elute on silica TLC plates, moving with $R_f = 0.70$ in a 75 % ethyl acetate/hexane solvent system. Anhydride reduction insures cis conformation upon the diol and upon subsequent compounds, and will simplify issues of polymer tacticity and microstructure.

Without further purification than a Fieser and Fieser aqueous workup, the diol is treated with acetic anhydride at room temperature for 24 hours and monitored by TLC (Figure 17). Elution of the dark sludge reaction mixture with 75 % ethyl acetate/hexane moves the diacetate compound [4] ($R_f = 0.85$) off a flash chromatography column of silica and away from unreacted diol and pyridine.

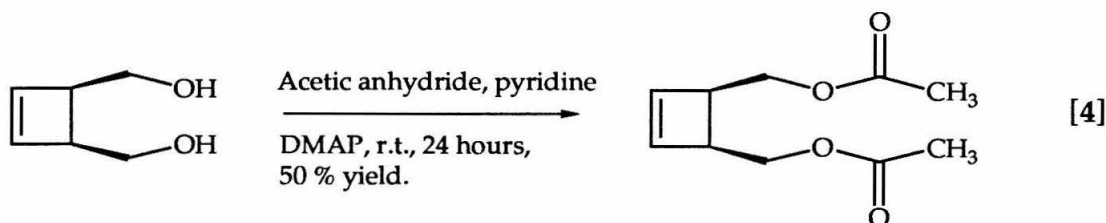


Figure 17: Synthesis of cis-3,4-di(hydroxymethyl)cyclobutene diacetate [4].

Remarkably crisp NMR spectra of the clear, pale yellow oil confirms the purity and structure of the cis-3,4-di(hydroxymethyl)cyclobutene diacetate [4]. Reaction yields, however, are a fair 50 % and based upon the starting diol.

Reaction conditions for the preparation of the cis-3,4-di(hydroxymethyl)cyclobutene) dicarbonate [6] (Figure 18) and cis-3,4-di(hydroxymethyl)cyclobutene) dimesylate [5] (Figure 19) monomers are similar and require the dropwise addition of an excess of methanesulfonyl chloride and methyl chloroformate at low temperature (-20 °C) because of the swift reactivity of those acid chlorides at room temperature.

With a 25 % ethyl acetate/hexane solvent system, flash chromatography of the striking yellow carbonate reaction mixture removes the pure dicarbonate ($R_f = 0.38$) off the column as a clear, colorless oil. The chromatographed oil crystallizes out of solution, or neat, into a white solid at

low temperatures ($-20\text{ }^{\circ}\text{C}$). The reaction proceeds in fair yields (60 %), based upon the amount of starting diol.

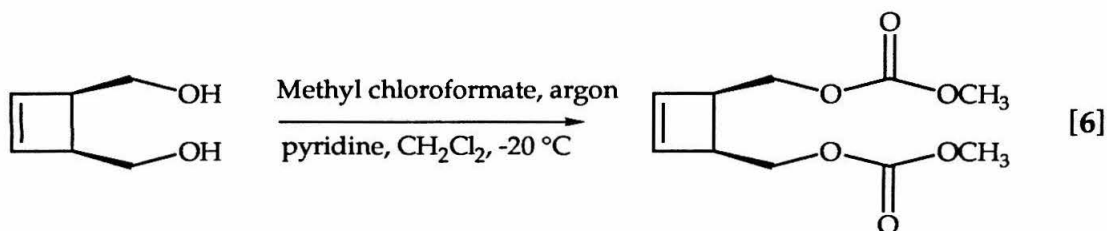


Figure 18: Synthesis of cis-3,4-di(hydroxymethyl)cyclobutene dicarbonate [6].

NMR spectra show a reasonably clean monomer, with some apparent baseline decomposition, olefins and characteristic carbonate methoxy groups appear at 6.09 and 3.72 ppm, respectively. IR spectroscopy confirms the structural assignments with C-H stretching frequencies appearing at 2860 - 2954 cm^{-1} along with the carbonyl and ether/ester vibrations at 1748 cm^{-1} and 1443 - 1261 cm^{-1} , respectively.

Thermal analysis (TGA and DSC) of the dicarbonate cyclobutene shows a broad exotherm at $180\text{ }^{\circ}\text{C}$ that coincides with its thermal decomposition. Upon a temperature of $255\text{ }^{\circ}\text{C}$, the compound has lost 77 % of its weight and has become a blackened soot.

The mesylate reaction does not require chromatographic purification. Instead, the dimesylate compound crystallizes from diethyl ether ($-20\text{ }^{\circ}\text{C}$), away from the orange reaction mixture, as a white crystalline solid. Reaction yields are particularly poor (30 - 50 %) and the compound does not appear to have any long term stability.

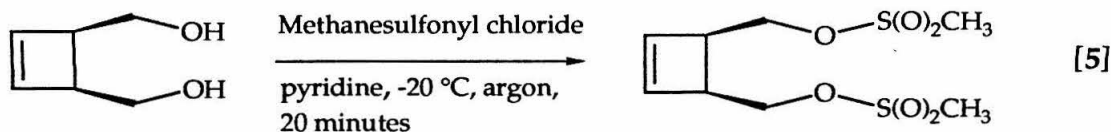


Figure 19: Synthesis of cis-3,4-di(hydroxymethyl)cyclobutene dimesylate [5].

NMR and IR spectroscopy again confirm the preparation of the cis-3,4-di(hydroxymethyl)cyclobutene dimesylate [5]. Sharp singlet resonances at 6.14 and 3.02 ppm correspond to the olefinic and methyl protons, respectively, of the compound. Aliphatic IR stretches at 2850 - 2980 cm^{-1} , along with the characteristic stretches of the methanesulfonyl group at 1450 cm^{-1} and 840 - 880 cm^{-1} identify the dimesylate cyclobutene. Thermal analysis shows degradation beginning at 100 $^{\circ}\text{C}$ and continuing until 300 $^{\circ}\text{C}$, with a 55 % weight loss. This elimination represents a partial loss of methanesulfonic acid from the compound before total decomposition at higher temperatures.

Given the thermal chemistry of these compounds, attempts were made to chemically and thermally eliminate two (2) equivalents of methanesulfonic and methanecarbonic acid from their respective monomers (Figure 20). Treatment of the dimesylate monomer with 1,8-diazabicyclo[5.4.0]undec-7-ene (DBU) in methylene chloride at room temperature darkens the solution, though there is no evidence of dimethylene cyclobutene (DMCB) formation after 24 hours. New methylene resonances expected at 4.67 and 4.75 ppm, accompanied by a shift of the olefin resonance to 6.96 ppm, never appear. Similar treatment of the dicarbonate monomer with DBU gives equally unsatisfying results.

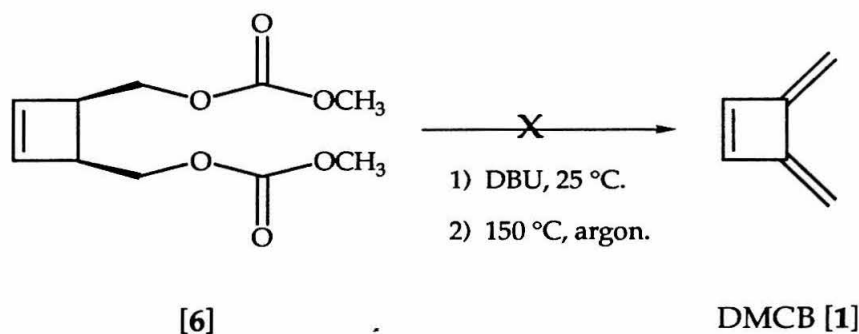


Figure 20: Generation of DMCB from [6].

The uncatalyzed pyrolysis of these 3,4-substituted cyclobutenes, however, show the stepwise loss of functional groups at low temperatures (100 °C). Thermal treatment of both *cis*-3,4-di(hydroxymethyl)cyclobutene) dimesylate and *cis*-3,4-di(hydroxymethyl)cyclobutene) dicarbonate monomers shows rapid loss of functionalities over the temperature range of 120 - 260 °C. This loss continues in the polybutadiene-carbonate until a carbon char remains at 260 °C, 17 % mass remains. A deep DSC exotherm at 156 °C (-9.45 kcal/mole) accompanies carbonate elimination (may include cyclization), while rapid decomposition, consistent with TGA thermograms, occurs at temperatures > 200 °C.

Attempts to trap DMCB during those elimination reactions, however, were unsuccessful because of the small quantities of material involved. IR analysis of these thermally treated solids, however, do not show any of the characteristic absorptions of 3,4-dimethylenecyclobutene (DMCB) or polyparaphenylene (PPP). These materials show a broad aliphatic and aromatic vibration $\sim 3000\text{ cm}^{-1}$ along with resonances at 1748 cm^{-1} and a non-descript shifts $< 1000\text{ cm}^{-1}$. The characteristic DMCB aliphatic and olefinic

stretches at $2950 - 3120\text{ cm}^{-1}$ and $1680 - 1710\text{ cm}^{-1}$, respectively, do not appear.

Efforts have refocused upon the polymerization of these 3,4-substituted cyclobutenes into PPP precursor polybutadienes and away from dimethylene cyclobutene (DMCB) because of its high reactivity and dangerous preparation. Substituted cyclobutene polymerizations with tungsten and molybdenum alkylidenes (Figure 21) are significantly tamer than those involving DMCB and may incur stereochemical control of the polymerization reaction.

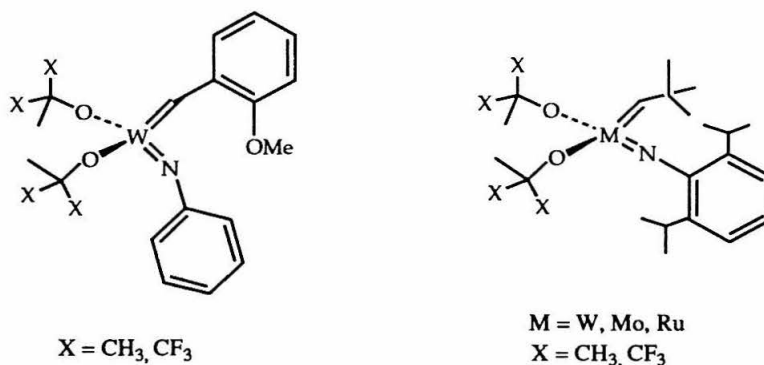


Figure 21: Non-Lewis acidic ROMP metathesis catalysts.

Polymerization

Cis-3,4-cyclobutenedicarboxylic acid anhydride.

Aqueous and organic polymerizations of the parent anhydride have been disappointing, given the success of ruthenium and molybdenum polymerizations of highly functionalized monomers, including 7-oxa norbornadieneanhydride. Amidst a slew of aqueous ruthenium ($\text{Ru}(\text{H}_2\text{O})\text{tos}_2$, RuCl_3 , K_2RuCl_5), organic ruthenium ($((\text{Cl})_2(\text{PPh}_3)_2\text{Ru}(\text{CHCHC}(\text{C}_6\text{H}_5)_2))$), tungsten and molybdenum catalysts

$((OC(CF_3)_2CH_3)_2M(CHPh(OCH_3))(NPh), M=W, Mo)$, nothing pitched at the cyclobutene anhydride gives an indication of polymerization, only catalyst deactivation and anhydride hydrolysis (Figure 22, 23).

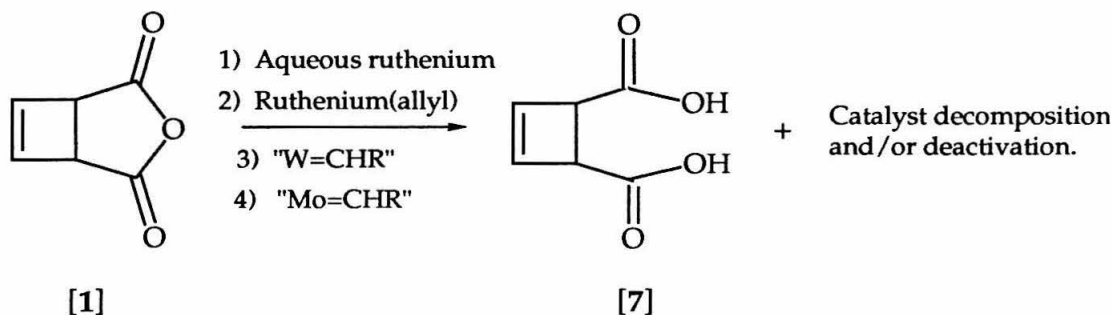


Figure 22: Unsuccessful polymerization of anhydride [1].

NMR spectra aqueous ruthenium polymerization solutions show nothing but the hydrolyzed anhydride. The $Ru(H_2O)tos_2$ solution turns yellow, but without substantial chemical shifts differences in the bound and unbound complex, no assessment can be made with regards to an isolable olefin complex. Even an activated polymerization solution ($Ru(H_2O)tos_2$ and 5,6-dimethoxymethyl-7-oxanorbornadiene) yields a clear yellow solution of hydrolyzed monomer.

(I)	$Ru(H_2O)tos_2$	1:1 Ethanol/water	Orange solution, no polymer.
(II)	K_2RuCl_5	1:1 Ethanol/water	Yellow solution, no polymer.
(III)	$RuCl_3$	Ethanol	Yellow/green solution, no polymer.

Figure: 23: Attempted aqueous ruthenium polymerizations.

In another development, a solution of the anhydride deactivates the golden brown ruthenium allyl catalyst $[(Cl)_2(PPh_3)_2Ru(CHCHC(C_6H_5)_2)]$. Though this ruthenium allyl complex is reported to be the most tolerant

toward oxygen functionalities, the anhydride and diacid cyclobutenes deactivate the ruthenium allyl catalyst without formation of a propagating carbene.

There is also no polymerization activity between these monomers and the tungsten $((OC(CF_3)_2CH_3)_2W(CHPh(OCH_3))(NPh))$ or molybdenum $((OC(CH_3)_2CF_3)_2Mo(CHC(Me_2Ph)(NPh))$ alkylidenes in d^8 -THF. Though tungsten decomposition is not unexpected, given the intolerance of tungsten alkylidenes to many heteroatom functionalities, a darkened, jade green molybdenum solution is an unexpected result and indicates catalyst decomposition.

Cis-3,4-di(hydroxymethyl)cyclobutene diacetate.

Returning to the polymerization of the series of diacetate, dimesylate, and dicarbonate cis-3,4-substituted cyclobutenes, the cis-3,4-di(hydroxymethyl)cyclobutene diacetate could not be polymerized with any catalyst under any conditions (Figure 24).

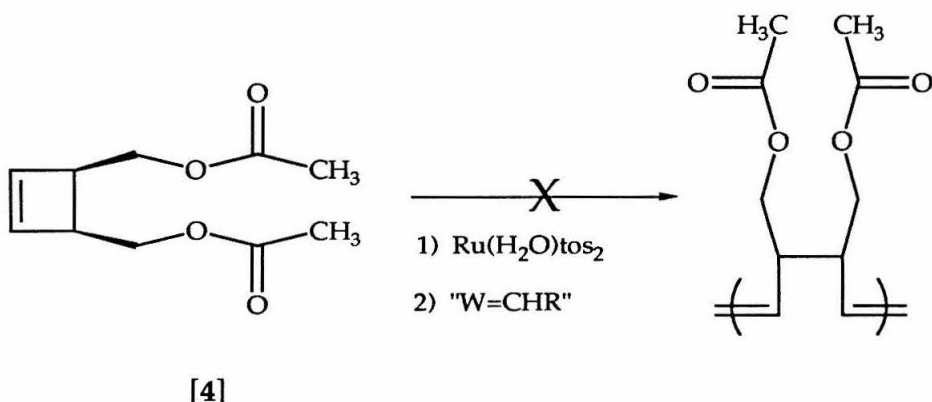


Figure 24: Unsuccessful polymerization of cis-3,4-di(hydroxymethyl)cyclobutene diacetate.

Aqueous ruthenium attempts again show promise, a 5,6-dimethoxymethyl-7-oxanorbornadiene-initiated catalyst solution of $\text{Ru}(\text{H}_2\text{O})\text{tos}_2$ in 1:1 ethanol/water turns a solution of catalyst and monomer a clear, yellow without polymerization. Indicative of a possible "olefin complex," the sharp singlet monomer resonances monomer do not, however, shift substantially upon Ru^{2+} addition to confirm a true isolable olefin complex. Polymerization attempts using tungsten alkylidenes yield inactive orange and yellow solutions of catalyst and unreactive monomer. No propagating species develop, no polymer forms.

Cis-3,4-di(hydroxymethyl)cyclobutene dimesylate.

Polymerization of the cis-3,4-di(hydroxymethyl)cyclobutene dimesylate, a substrate with more labile leaving groups has been more successful. Aqueous ruthenium catalysts (RuCl_3 and $\text{Ru}_2(\text{H}_2\text{O})_6\text{tos}_2$) polymerize the dimesylate cyclobutene in ethanol under argon at 55 °C. With Ru(II), a dirty off-white polymer falls out of the cloudy and dirty yellow aqueous solution in fair amounts over the course of days, whereas fine solid particles crash out of a similarly colored Ru(III) polymerization mixture.

Tungsten catalysts polymerize, at room temperature under argon, the cis-3,4-di(hydroxymethyl)cyclobutene) dimesylate into a sparingly soluble mass, not easily characterized (Figure 25). $(^t\text{BuO})_2\text{W}(\text{CHC}(\text{CH}_3)_3)(\text{NPh}(2,6\text{-isoprop})_2)$ and $(\text{OC}(\text{CF}_3)_2\text{CH}_3)_2\text{W}(\text{CHPh}(\text{OCH}_3))(\text{NPh})$ alkylidenes give clear orange polymerization solutions that darken slightly to golden brown solutions after 8 hours. Precipitation into pentane (or methanol) produces an off-white, insoluble, granular solid in very poor yield (< 5 %).

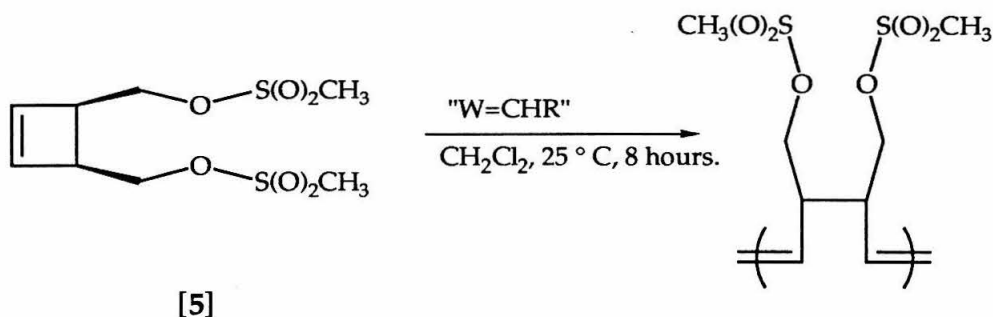


Figure 25: Polymerization of cis-3,4-di(hydroxymethyl)cyclobutene dimesylate.

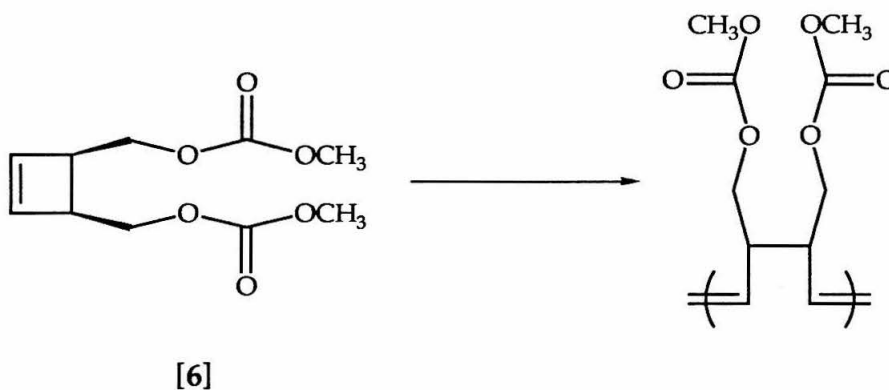
The proposed structure of poly(cis-3,4-di(hydroxymethyl)cyclobutene dimesylate) via the ring-opening metathesis polymerization of the appropriate cyclobutene is consistent with the available NMR, IR and thermal analysis data. NMR spectra show broadened resonances, though the metathesized olefin is significantly shifted upfield upon polymerization (6.14 to 5.65 ppm). The presence of the methylsulfonyl group at 2.32 ppm confirms incorporation of the mesylate group into the polymer structure. IR spectra of the polymer confirms the incorporation of mesylate groups within the polymer structure. The presence of methylsulfonyl groups (1450 cm^{-1}), ether functionalities (1260 cm^{-1}), and saturated carbons (2950 cm^{-1}) appear with a broadened aliphatic region (3300 cm^{-1}) and an unknown vibration at 2240 cm^{-1} .

TGA and DSC analysis of the polymer shows good thermal stability, while confirming elimination of the mesylate side groups with a sharp exotherm at $148\text{ }^{\circ}\text{C}$ (-2.3 kcal/mole) and 50 % polymer weight loss out to $500\text{ }^{\circ}\text{C}$ (Figure 29). NMR spectroscopy of the polymer supernatants show nothing but trashed monomer and scattered baseline activity.

Cis-3,4-di(hydroxymethyl)cyclobutene) dicarbonate.

Insoluble materials are not acceptable precursor polymers. While polymerization of the dimesylate cyclobutene was promising, the ability to produce soluble, well characterized polybutadienes depended upon the development of a tolerant molybdenum alkylidene catalyst.

The cis-3,4-di(hydroxymethyl)cyclobutene dicarbonate has been polymerized under both aqueous and organic conditions (Figure 26). Under standard aqueous conditions, the $\text{Ru}(\text{H}_2\text{O})_6\text{tos}_2$ polymerization solution turns from its initially pale purple color to a faint yellow at 55 °C. Within 6 hours, an off-white solid flocculent polymer falls out of solution and accumulates in great yield over the next 36 hours. NMR spectroscopy confirms synthesis of the ROMP polymer with a 60 (trans) : 40 (cis) olefinic structure and incorporation of diad-sensitive methine protons.



Catalyst	Solvent	Temp.	Time
$\text{Ru}(\text{H}_2\text{O})_6\text{tos}_2$	1:1 Ethanol/water	55 ° C	6 hours
$\text{Ru}(\text{allyl}) (\text{IV})$	CH_2Cl_2	25 ° C	N/A
$\text{W}(\text{OR}_{\text{F}_6})_2 (\text{II})$	CH_2Cl_2	25 ° C	N/A
$\text{Mo}(\text{OR}_{\text{F}_6}) (\text{I})$	CH_2Cl_2	25 ° C	1.5 hours

Figure 26: Aqueous and organic polymerizations of [6].

Attempts using K_2RuCl_5 , however, have been unsuccessful. The initial yellow polymerization solution darkens to an orange/brown within hours and catalyst decomposition is confirmed by NMR. A methylene chloride solution of carbonate and ruthenium(allyl) catalyst $(\text{Cl})_2(\text{PPh}_3)_2\text{Ru}(\text{CHCHC}(\text{C}_6\text{H}_5)_2)$ do not interact, though neither the monomer nor the catalyst decomposes. The clear yellow/brown solution develops a series of four new (propagating) carbenes at 17.52 - 17.63 ppm without any indication of polymer turnover. The monomer and catalyst carbene resonances remain unbowed and stable for ~ 1 day. This behavior hints at the great stability of the ruthenium(allyl) catalyst toward polymerization.

The activity of tungsten alkylidene catalysts toward the carbonate monomer is unexpected. With functionality similar to the cis-3,4-diacetate cyclobutene, conventional wisdom would hold that cis-3,4-dicarbonate cyclobutene would decompose the catalyst. However, the dicarbonate cyclobutene does, in fact, polymerize with $(\text{OC}(\text{CF}_3)_2\text{CH}_3)_2\text{W}(\text{CHPh}(\text{OCH}_3))(\text{NPh})$ at room temperature in an immediate and violent reaction. A thick red/brown "gel" coats the NMR tube. An NMR of the sample (admittedly thick and gooey with solids) shows a 10 % polymer yield, amidst quantities of unreacted monomer. The sample is pumped dry to yield a quantity of a yellow, insoluble, granular solid.

Combination of a couple of milligrams of metathesis catalyst, $(\text{OC}(\text{CH}_3)_2\text{CF}_3)_2\text{Mo}(\text{CHC}(\text{Me}_2\text{Ph})(\text{NPh}))$, and carbonate monomer in 0.5 ml CH_2Cl_2 solvent at room temperature gives a clear, golden yellow polymerization solution. Immediate polymerization is, in this instance, accompanied by a slight viscosity change in a golden orange and the appearance of new propagating carbenes (4) at 11.8 - 11.9 ppm. Bulk

polymerizations under the same room temperature conditions yield slightly yellowed polymers in good yield (80 %) after 1.5 hours, although polymerization continues for 6 - 8 hours. These conditions give the most reproducible results and allow neargram quantities of substituted polybutadiene to be synthesized.

^1H and ^{13}C NMR data depict a polymer with high trans content (trans : cis, 2.5 : 1) and unequal amounts of m and r diads (Figure 27). The sensitivity of the methine proton toward polymer stereochemistry results in the unequal distribution of m and r diads. These cis-disubstituted cyclobutene monomers have a plane of symmetry, thus insuring some structural uniformity upon polymerization. As a result, we must deal with the presence of m and r diads without having the additional burden of polymer head and tail tacticity (Figure 28). Stereochemical assignments, however, are neither complete nor conclusive.

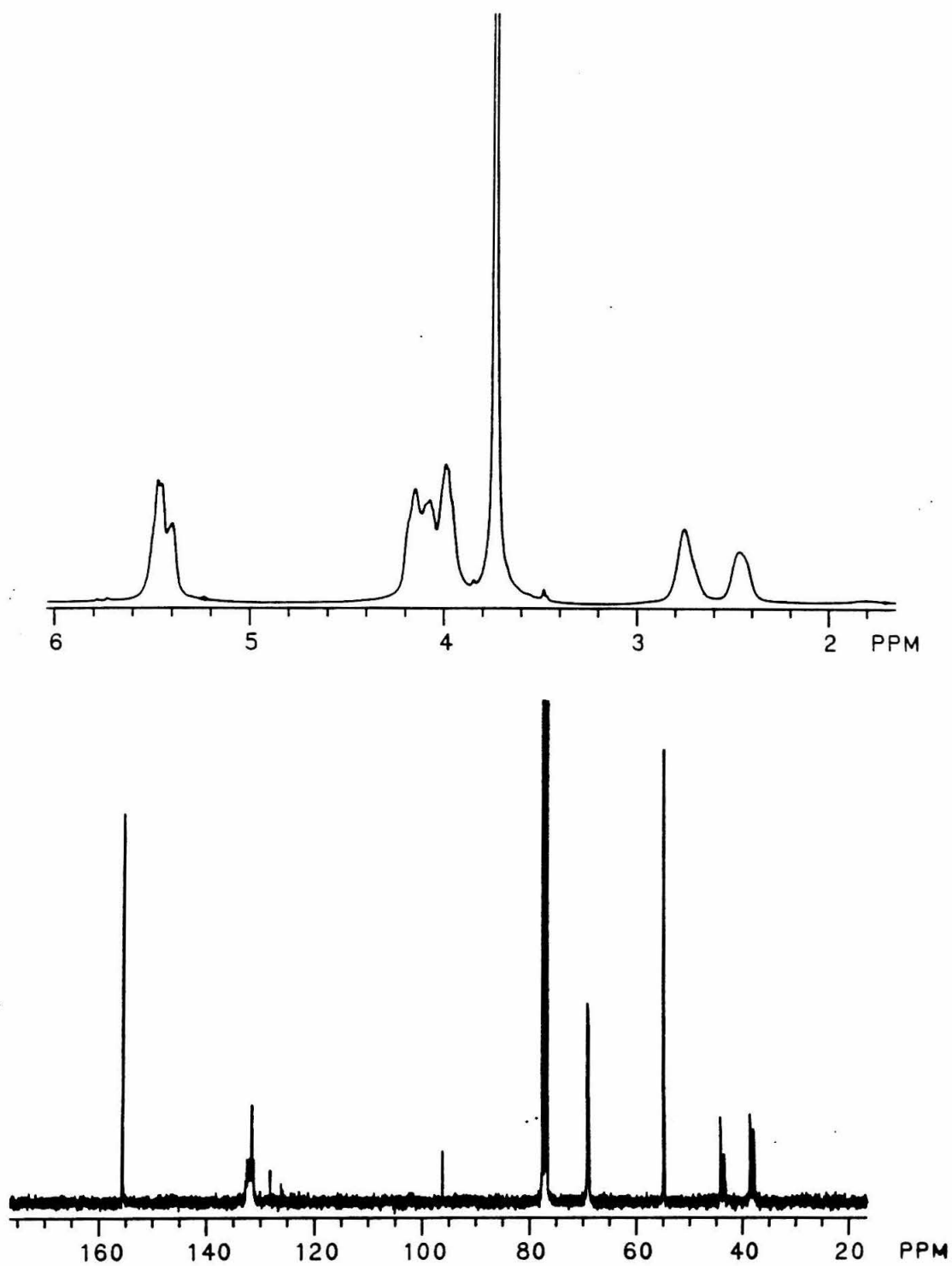


Figure 27: ^1H and ^{13}C NMR spectra of poly(3,4-dihydroxymethyl) cyclobutene dicarbonate.

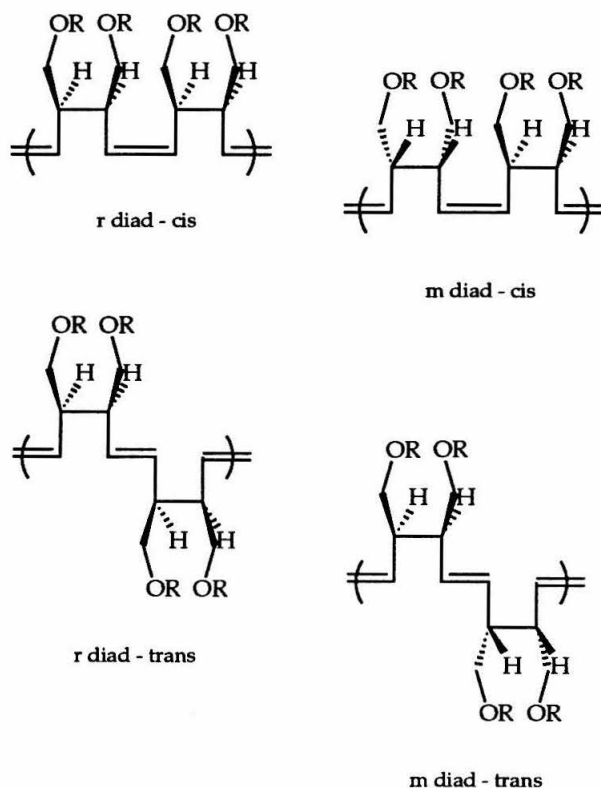


Figure 28: Proposed diad structures (based upon NMR data).

IR spectroscopy of the polymer confirms the incorporation of carbonate groups into the polybutadiene. Aside from broadened signals, the polymer vibrations remain largely unchanged with carbonyl and stronger ether/ester vibrations at 1750 cm^{-1} and $1380 - 1230\text{ cm}^{-1}$, respectively.

Gel Permeation Chromatography (GPC) of a representative poly(cis-3,4-di(hydroxymethyl)cyclobutene dicarbonate) sample shows a M_w of 60,000 (vs. polystyrene standards) (233 repeat units) with polydispersity index (PDI) of 1.74. DSC and TGA work on the polymer shows a T_g of $184\text{ }^{\circ}\text{C}$ and complete loss of the carbonate functionalities from $200 - 380\text{ }^{\circ}\text{C}$. The 52 % experimental weight loss mimics the 51.3 % theoretical loss corresponding to two equivalents carbonate for each repeat unit (Figure 29). Unlike the PPV

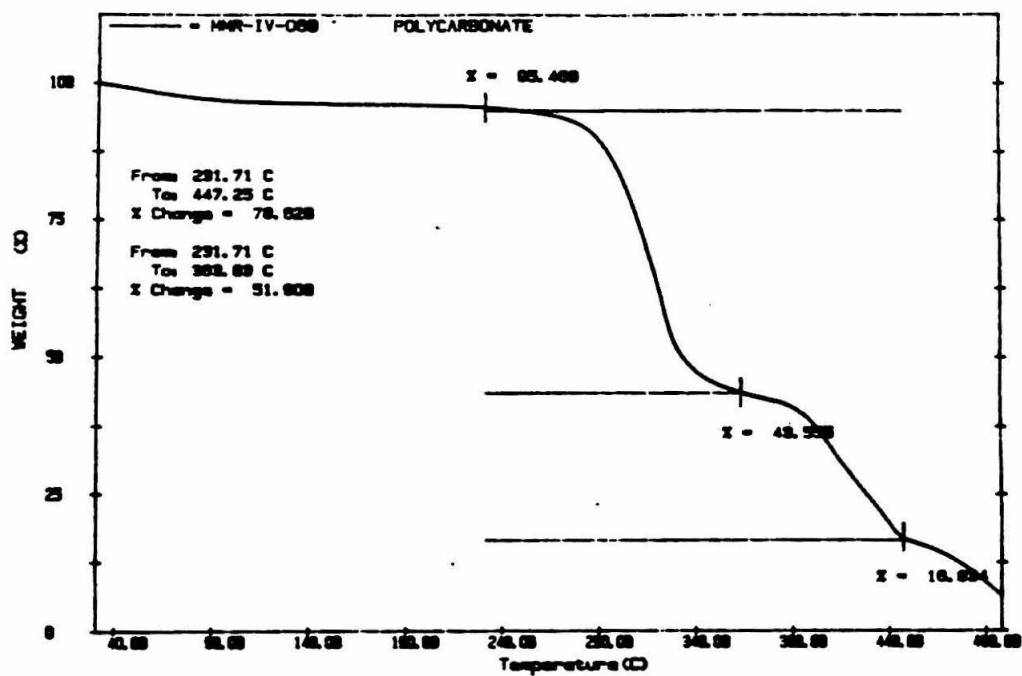
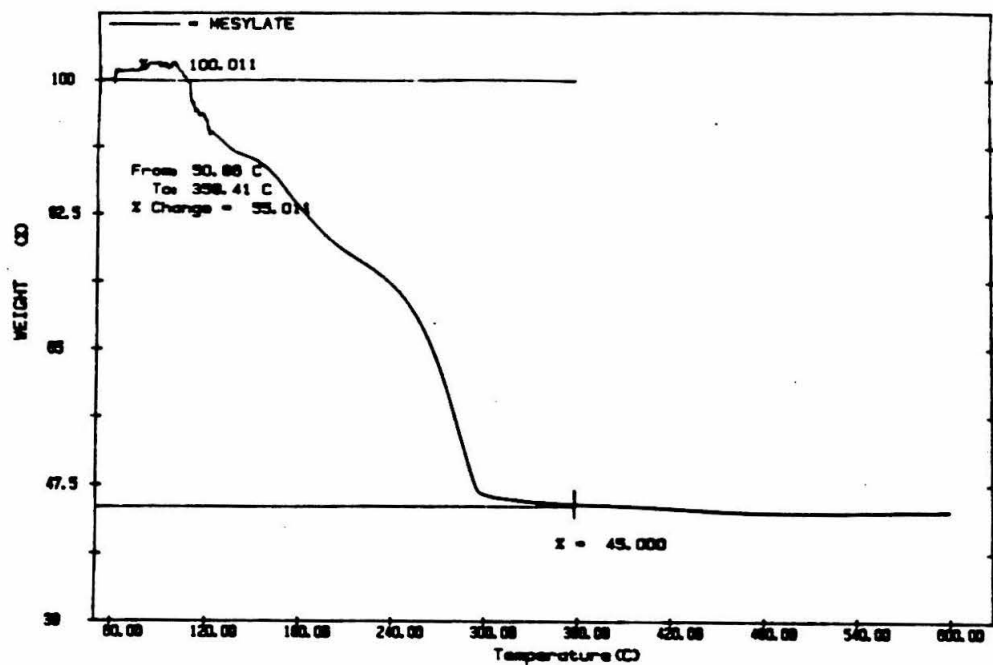


Figure 29: Thermal analysis (TGA) of dimesylate [5] and dicarbonate [6].

system, a thermal cis to trans isomerization of the polybutadiene remains undetected by IR and DSC.

In spite of promising soluble precursor polymers, work continued to increase the cis : trans polymer ratio in order to facilitate complete carbonate elimination and cyclization. Different polymerization catalysts alter the cis:trans polymer ratios, but do not fully suppress one isomer at the expense of the other.

It should also be noted that only the $(\text{OC}(\text{CH}_3)_2\text{CF}_3)_2\text{Mo}(\text{CHC}(\text{Me}_2\text{Ph})(\text{NPh}))$ catalyst polymerizes the 3,4-cyclobutene at room temperature. Attempts at low temperature ($-30\text{ }^\circ\text{C}$) polymerization led to jade green polymerization solutions without evidence of polymer. Additionally, polymerizations using non-fluorinated molybdenum catalysts $\text{Mo}(\text{t-BuO})_2$ and $(\text{ArO})_2\text{Mo}(\text{Me}_2\text{CH}(\text{Ph}))$ showed anomalous behavior (Figure 30). These room temperature polymerization solutions also turned green, but a low yield of polymer was recovered in each case.

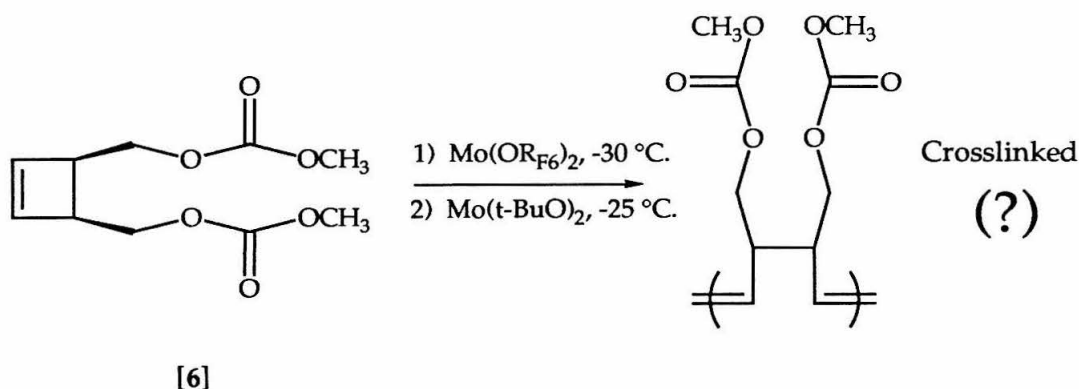


Figure 30: Unidentified polymerization behavior.

These sparingly soluble, high(er) molecular weight polymers resemble (analytically) the ROMP materials polymerized earlier though their elemental analyses show higher carbon content (6 %) and hydrogen content (1 %) than expected. These polymers are believed to be slightly crosslinked derivatives, based upon their similar NMR, IR, and thermal behavior. These polymers hint at an increased catalyst reactivity toward the carbonate functionality and decreased polymerization activity for reactions at low temperatures or using non-fluorinated molybdenum catalysts.

Attempts to chemically and thermally eliminate two (2) equivalents of methylcarbonic acid from these polymers were moderately successful. Precursor carbonate polymers show good thermal stability and decompose only at temperatures in excess of 360 °C. TGA weight losses (52 %) (Figure 29) mimic the theoretical loss of two methylcarbonic acid equivalents from the precursor polymer while collection of the pyrolysis volatiles proves largely inconclusive (Figure 31).

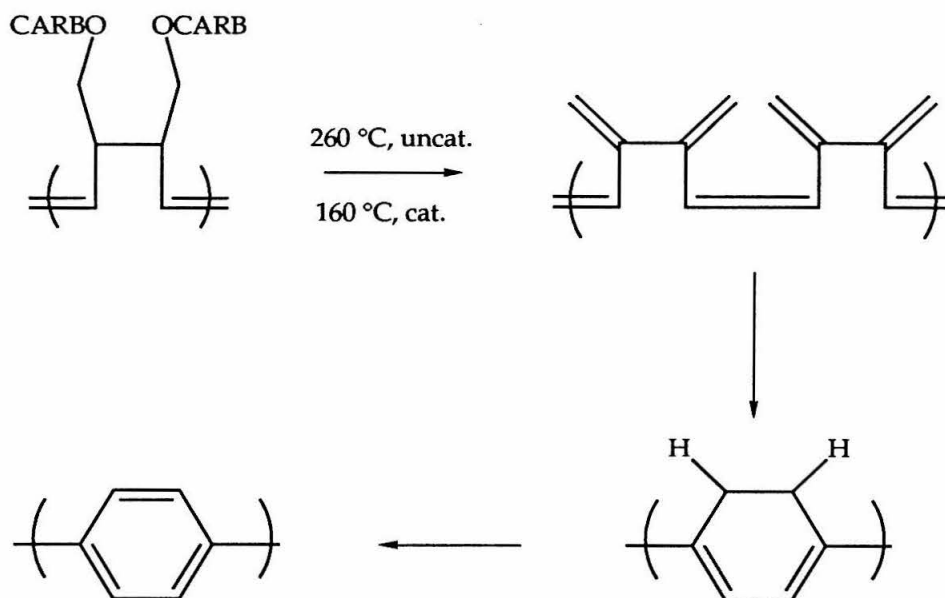


Figure 31: Full carbonate elimination toward PPP.

Uncatalyzed pyrolysis of dicarbonate polymer at 260 °C under flowing argon yields blackened, insoluble polymer solids. Infrared analysis of the solids confirm the complete loss of carbonate functionality from the polymer and disappearance of all ester and ether vibrations at 1750 cm^{-1} and 1258 cm^{-1} . The lack of PPP characteristic vibrations, including the strong band at 800 cm^{-1} , indicates that thermolysis at this temperature most likely degrades the polymer before 3,4-dimethylenecyclobutene (and polyparaphenylene) formation.

To combat polymer decomposition at thermolysis temperatures, carbonate elimination was found to be strongly catalyzed by the presence of octadecylamine (Figure 32). When present in catalytic amounts (5 -8 weight %), octadecylamine drops the onset of carbonate elimination 100 °C, to 160 °C. Bulk isothermal pyrolysis of the precursor carbonate polymer with amine at 160 °C under argon for 7 hours does not decompose the polymer structure.

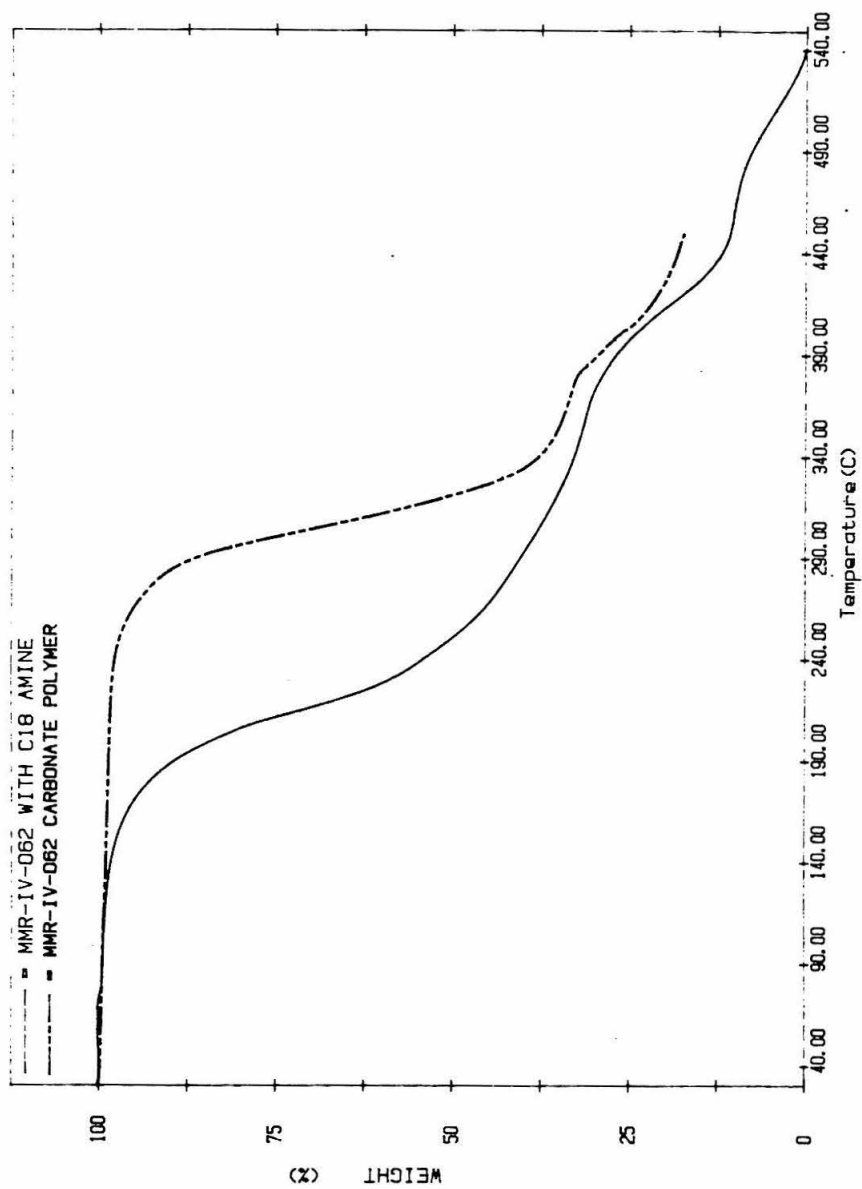


Figure 32: Catalyzed elimination of polymerized [6] with amine.

Unfortunately, it does not completely remove the carbonate functional groups from the polymer either (Figure 33).

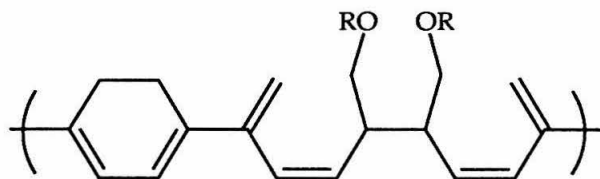


Figure 33: Incomplete polymer elimination.

Infrared and ^{13}C -CPMAS NMR analysis of the resulting orange solid confirm the presence of residual carbonate functionality due to incomplete elimination (Figure 34). Buried within the polybutadiene NMR resonances are (believed) PPP precursor shoulders at 134, 125, and 44 ppm which provide slight encouragement. Similarly, the PPP attributed stretches of 3450, 791, 740, and 691 cm^{-1} also accompany the many stretches (2961, 2903, 2858, 1749, 1448, 1385, 1258, and 960 cm^{-1}) characteristic of the carbonate polybutadiene polymer. There is, however, a marked absence of the principal PPP stretch at 803 - 805 cm^{-1} , characteristic of parasubstituted aromatics. Because of the incomplete elimination of carbonate functionality from the polybutadiene polymer, the results are inconclusive as to whether or not the cyclized PPP precursor is formed.

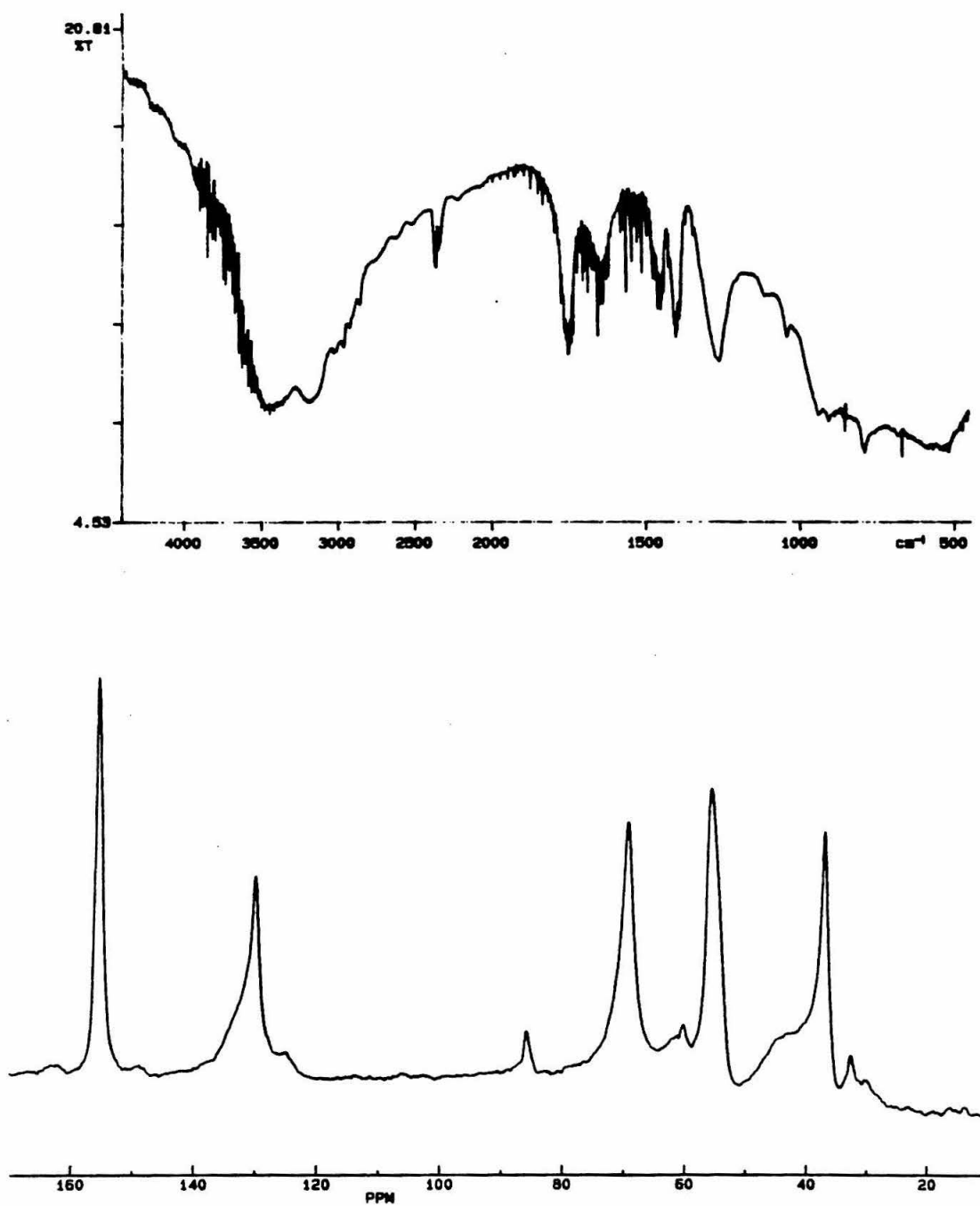


Figure 34: IR and ¹³C-CPMAS NMR of carbonate elimination products.

Conclusions and Future Prospects

The polymerization of substituted cyclobutenes was envisioned as a soluble precursor route into polyparaphenylene (PPP), an insoluble, rigid rod polymer. Towards that goal, highly functionalized 3,4-cyclobutenes have been polymerized with tungsten and molybdenum alkylidene ROMP catalysts, incorporating high degrees of acid, oxygen, and heteroatom functionality into the polymer structure. These precursor materials are soluble, high molecular weight polybutenamers with the same polymer repeat unit as similarly substituted 1,4-poly(butadienes). However, the proposed pathway to PPP requires the stereoregular polymerization of these bulky cyclobutenes to afford 100 % cis polymer. Despite catalyst changes and low temperature polymerizations, both cis and trans polymer appear in NMR spectra. Pyrolysis of these polybutadienes, even under catalytic conditions, yields polymeric solids with little similarity to PPP. With soluble precursor polybutadienes available, new approaches to the complete elimination and cyclization of these precursor polymers are required.

An interesting development to result from investigation into PPP via these cyclobutene precursors has been the attention drawn to the ROMP polymer of acetylene and N-methylmaleimide (Figure 35) as a potential substrate for the formation of catalytic protein conjugates.¹⁵

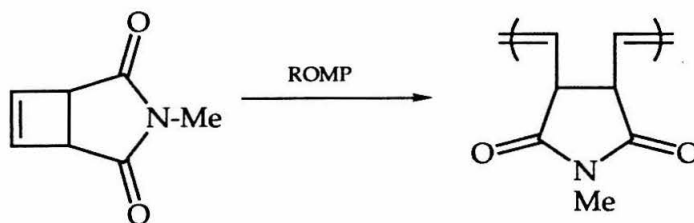


Figure 35: Protein conjugate polymaleimide.

Work continues on the synthesis of new organic-based materials for use in protein stabilization and peptide synthesis. Incubation of carbohydrate macromolecules with proteins give carbohydrate-protein conjugates (CPCs) of proteases (alpha-chymotrypsin, trypsin, and subtilisin) and endonucleases (EcoRI) that exhibit enhanced catalytic, proteolytic, and aqueous activity (Figure 36).

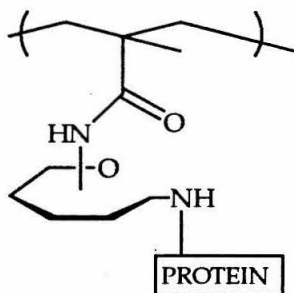


Figure 36: Carbohydrate-protein conjugates.

CPC(proteases) are used in the catalytic synthesis of peptide bonds and operate with high efficiency to give > 95 % dipeptide yields in THF, dioxane, and acetonitrile. CPC(proteases) and CPC(endonucleases) also cleave large proteins and nucleic acids in identical fashion as their native, non-conjugate proteins. The active site of the enzyme and the binding site of the antibodies are not significantly altered by CPC conjugates.

Given the increased structural stability and catalytic activity of CPC conjugates, new organic-based polymers are in demand. The incorporation of the ROMP polymer of the cyclobutene cyclic imide improves upon the existing radically polymerized methacryloyl polymer route and provides a well defined polymer backbone. Preliminary polymerization results indicate that this maleimide compound has similar reactivity as the anhydride

described earlier. As a consequence, the ROMP polymerization of the maleimide-cyclobutene may be difficult.

Cyclobutene Experimentals:

General Considerations

All manipulations of air and/or moisture sensitive compounds were carried out using standard Schlenk or vacuum line techniques with argon as the flush gas. The argon was purified by passage through columns of activated BASF RS-11 (Chemlog) oxygen scavenger and Linde 4Å molecular sieves. Manipulation of air sensitive solids was performed in a Vacuum Atmospheres dry box equipped with a MO-40-1 purification train, a DK-3E Dri-Kool conditioner, and a Dri-Cold freezer. The catalyst dry train contained activated Ridox™ oxygen scavenger and Linde 11Å molecular sieves. In most cases involving the synthesis of these materials, glassware was dried in a 140 °C oven and subjected to vacuum while still hot.

^1H and ^{13}C NMR were recorded on either a Jeol 400 GX (399.65 MHz ^1H), General Electric QE-300 Plus (300.199 MHz ^1H , 75.49 MHz ^{13}C), or Bruker WM-500 (500.14 MHz ^1H) spectrometer. Chemical shifts were referenced to the solvent or to the residual protons of the solvent. Infrared spectra were acquired on both a Shimadzu IR-435 and Perkin-Elmer Series 1600 spectrometer. Infrared samples were either thin films or KBr pellets. Elemental analyses were performed by the California Institute of Technology Analytical Facility. Conductivity measurements were made with a home built probe or a commercially available Sigmatone sheet resistivity probe. Current was supplied to these probes by a Power Designs 605 precision power source and measured with a Keithley 160B digital multimeter. The voltage was monitored using a Fluke 895A differential voltmeter. Thermal analyses were performed on a Perkin Elmer DSC-7 differential scanning

calorimeter, TGS-2 thermogravimetric analyzer, and dual Tac 3/7 data stations. The thermal equipment is driven by an IBM PS/2 computer running standard Perkin Elmer software. Scanning rates for these analyses varied.

Polymer samples were run on a Millipore-Waters 150 C Gel Permeation Chromatography Spectrometer equipped with differential refractometer and a Waters 820 chromatographic data station. A home-built GPC station was also used and utilized Waters Ultrastyrigel columns connected to a Knauer differential refractometer. Polymer solutions of various ($\sim 0.5\%$ w/v) concentrations were prepared using either spectral grade 1,2 dichlorobenzene, methylene chloride, or tetrahydrofuran. These solutions were filtered using 0.2 and 0.45 mm UnifloTM filters to protect the Ultrastyrigel columns while sample injections of 0.2 ml and 1.0 ml/min flow rates were commonly used.

Solvents for all polymerizations were kept free of oxygen and moisture. Benzene was dried and deoxygenated with sodium benzophenone ketyl. Pentane was dried and deoxygenated after treatment with sulfuric acid for days. The tungsten alkylidene catalysts were provided by departing group members, but were initially prepared from the published procedures (catalyst references) and recrystallized from pentane. The large volume of hexane, pentane, and methanol used for precipitation of the polymer was degassed with an argon bleed for thirty minutes.

Preparation of cis-3,4-cyclobutenedicarboxylic acid anhydride [2].

A 0.5 M solution of maleic anhydride (16 g, 0.163 mol) and acetophenone (6 g, 0.05 mol) was prepared using ~ 300 mls fresh-bottled

acetonitrile. The clear and colorless solution was freeze-pump-thaw-degassed three (3) times to insure water and air omission before being transferred, by cannula, into an argon swept, 250 ml Chem Glass photoreactor.

Once transferred, the photoreactor was cooled to -10 °C with an ice/water/salt bath and acetylene bubbled through the bottom of the solution for 30 minutes to insure an acetylene-saturated reaction solution. A vent bubbler was installed when the reaction vessel was loaded into the photolysis box. Unfiltered UV irradiation for 8 - 20 hours yields an iced tea colored solution often accompanied by a flocculent white, insoluble solid. Distillation at 50 °C, and again at 90 °C (under dynamic vacuum) and recrystallization from benzene and cyclohexane yields a crystalline white solid in 30 % overall yield.

^1H NMR (CDCl_3): 6.49 (2H, s) and 4.00 (2H, s) ppm. ^1H NMR (C_6D_6): 5.23 (2H, s) and 2.66 (2H, s) ppm. ^1H NMR (d^6 -acetone): 6.24 (2H, s), 3.91 (2H, s) ppm. ^{13}C NMR (CDCl_3): 169.13, 140.49, and 49.37 ppm.

Preparation of cis-3,4-di(hydroxymethyl)cyclobutene [3].

The white crystalline anhydride adduct was dissolved in THF (bottled, over sieves) to give a clear, colorless solution. Upon being purged with argon for 10 minutes, and cooled to 0 °C with ice and water, the commercially available solution of LAH in THF was added dropwise over the course of several minutes. The reaction is accompanied by gas evolution (H_2) and the

formation of lithium salts (salts will crash out of solution at low temperatures and may redissolve upon warming).

The reaction was left to stir and warm to room temperature and yielded a slightly yellow solution with discolored yellow and orange lithium salts. Workup according to Fieser and Fieser (equimolar amounts of water and 15% NaOH solution, followed by threefold excess of water) yields a thick, clear, colorless oil in greater than 60% yield. An additional 30% yield is obtained from the soxhlet extraction of the lithium salts in THF for 2 days. Greater than 90% overall yield. Unsuccessful recrystallization (literature).

^1H NMR (CDCl_3): 6.03 (2H, s), 3.74 - 3.85 (4H, m), and 3.22 - 3.24 (2H, m) ppm. ^1H NMR ($\text{d}^6\text{-DMSO}$): 6.12 (2H, s), 4.64 - 4.66 (2H, br), 3.50 - 3.53 (4H, m), and 2.97 - 2.98 (2H, m) ppm. ^{13}C NMR (CDCl_3): 137.27, 61.73, and 48.02 ppm.

Preparation of cis-3,4-di(hydroxymethyl)cyclobutene diacetate [4].

The cis- diol (1.03 g, 9.0×10^{-3} moles, 1 eq.), pyridine, and acetic anhydride (2.07 g, 2.03×10^{-2} moles, 2.25 eq.) were combined at room temperature to give a slightly yellowed, clear solution. The subsequent solid addition of DMAP (2.25 g, 1.84×10^{-2} moles, 2.04 eq.) turns the reaction solution nearly opaque, though it remains clear. The reaction is left to stir for 24 hours at room temperature and monitored by TLC. The dark opaque crude reaction mixture is chromatographed (75 % EtOAc/hexanes to obtain a yellow oil (among other compounds) as the desired product. Overall yield approaches 50 %.

^1H NMR (CDCl_3): 6.07 (2H, s), 4.14 - 4.16 (4H, m), 3.18 - 3.22 (2H, m), and 2.01 (6H, s) ppm.

Preparation of cis-3,4-di(hydroxymethyl)cyclobutene dimesylate [5].

The clear, colorless diol (0.65 g, 5.7×10^{-3} moles, 1.00 eq.) is dissolved up in dry pyridine (over CaH_2) to give a clear, but distinctly dark yellow/orange, solution. The reaction solution is cooled to 0°C and swept with argon for twenty (20) minutes. The mesyl chloride (1.47 g, 1.3×10^{-2} , moles, 2.25 eq) is syringed slowly over several minutes time, immediately turning the clear reaction mixture bright orange/yellow. A white granular solid generated during the reaction thickens the reaction mixture. The mixture is left to stir and warm to room temperature.

The liquid decants off and evaporation yields an orange/yellow, clear semi-solid. The dimesylate compound dissolves in diethyl ether and further decanting and evaporation yields a white solid. The overall reaction yield approaches 50 %.

^1H NMR (CHCl_3): 6.14 (2H, s), 4.33 - 4.39 (4H, m), 3.38 - 3.41 (2H, m), and 3.02 (6H, s) ppm. ^{13}C NMR (CHCl_3): 137.60, 68.71, 44.69, and 37.66 ppm.

Preparation of cis-3,4-di(hydroxymethyl)cyclobutene dicarbonate [6].

A slightly yellowed solution of the diol (1.47 g, 0.13 mol), pyridine (4.08 g, 0.0516 mol), and dry methylene chloride is cooled to -20°C (dry ice

and acetone) and swept with argon for twenty minutes to insure a system free of air. When complete, methyl chloroformate (4.87 g, 0.0516 mol) is added to the reaction solution DROPSWISE over the course of forty (40) minutes. The reaction solution clouds upon contact with the formate, evidence of a successful reaction. Upon completion of formate addition, the reaction is left to stir under argon and warmed to room temperature.

Soon after formate addition, a white solid (pyridine -HCl) crashes out from the reaction mixture, leaving behind a striking clear yellow solution. Additional amounts of pyridine and chloroformate may be required (after filtering off the white solid) to drive the reaction to completion. Extraction and drying over MgSO_4 yields a clear, colorless organic layer which evaporates down to a slightly yellow oil. Further cleanup (column chromatography, 25 % EtOAc/hexanes, $R_f = 0.38$) gives a clear and colorless oil.

^1H NMR (CHCl_3): 6.09 (2H, s), 4.21 - 4.25 (4H, m), 3.72 (6H, s), and 3.23 - 3.27 (2H, m) ppm. ^{13}C NMR (CHCl_3): 155.44, 137.56, 67.11, 54.58, and 44.08 ppm. IR spectroscopy (KBr): 2954, 2907, 2860, 1748, 1443, 1384, 1261, 1108, 955, 790, and 744 cm^{-1} .

Preparation of cis-3,4-cyclobutenedicarboxylic-bis(dimethyl)amide.

A dry THF solution of white crystalline solid anhydride and ECC [1-(3-dimethylaminopropyl)-3-ethylcarbodiimide hydrochloride] were combined at room temperature. Shortly after addition, the solution turns purple at the sites of undissolved ECC. The dimethylamine is gradually added and mixed.

While the solids partially dissolve, a reaction mixture slurry remains. Left to react for two (2) hours at room temperature. Cleanup involves an ether/water extraction and evaporation.

Preparation of cis-3,4-cyclobutenedicarboxylic acid.

The anhydride was added to 20 mls of a 1:1 methanol/water solution to give a two-phase system. To this reaction mixture, 40 mls of a 0.25 M NaOH solution was added at 0 °C. At this point, everything solubilizes to give an orange solution.

Reaction was left to stir for one (1) hour. After the hour, the methanol/water is distilled off at 72 °C and the volume of reaction solution reduced some 20 mls. When cooled to room temperature, the solution is neutralized (actually made slightly acidic) - the endpoint indicated by a color change in the solution from orange to yellow. This solution was extracted and dried to yield an off-white solid.

An alternative method is to leave the anhydride exposed to the ambient elements for months. It will hydrolyze naturally to the diacid compound.

^1H NMR ($\text{d}^8\text{-THF}$): 6.17 (2H, s), 3.80 (2H, s), and 10.85 (2H, s) ppm. ^1H NMR (C_6D_6): 5.67 (2H, s) and 3.39 (2H, s) ppm. ^{13}C NMR ($\text{d}^8\text{-THF}$): 171.84, 137.47, and 49.94 ppm. IR spectroscopy (KBr): 3110, 2724, 2609, 2528, 1699, 1423, 1402, 1303, 1220, 907, 830, 771, 709, and 652 cm^{-1} .

Preparation of 3,4-dimethylenecyclobutene (DMCB) [1].

The experimental apparatus for the flash vacuum pyrolysis was fashioned from the device used extensively by Huntsman. While this set up was successful, the contact time was too short and often resulted in incomplete conversion of the diyne.

My flow (or static) system uses a standard Hoskins (Model FD 303 A) tube furnace with a 2" bore along with a 48 cm quartz tube with 30 mm inner diameter fitted on both ends with a male 24/40 standard taper joint. Specially designed adapters connecting standard Kontes (2 mm) schlenks allow vacuum and argon service hookups. The furnace temperature was controlled with a Variac and Omega thermocouple and temperature gauge.

The 1,5 hexadiyne, a clear, colorless liquid, is repeatedly (8 times or so) freeze-pump-thaw-degassed to insure the omission of air and moisture. At room temperature, the diyne is volatilized at 232 °C within the tube furnace. The furnace core temperature drops to 218 °C from 232 °C (static system) when the diyne has entered. After chasing the diyne back into the furnace for several hours, the furnace contents (including product) are condensed into another Kontes receiver flask for analysis.

^1H NMR (CHCl_3): 6.72 (2H, s) olefin, 4.68 (2H, s) outboard, and 4.57 (2H, s) inboard ppm.

General Polymerization Techniques.

Extreme care was exercised to keep the system air and moisture free during polymerization. All glassware was pumped into the drybox hot and

both monomer and catalyst were loaded into separate Schlenk tubes inside the drybox. Polymerizations were monitored by thin layer chromatography since the monomer decomposes with R_f 0 - 0.25 and the polymer sits at the origin. Aliquots of the polymerization solution were taken with a capillary tube under a heavy purge of argon and polymerization was terminated when no monomer streaking was observed. The polymer was precipitated from deoxygenated hexane after dilution of the polymerization solution with small amounts of methylene chloride.

All polymerizations are monitored for monomer consumption by thin layer chromatography and terminated upon completion. Monomer to catalyst ratios of typically 50 - 100 : 1 employed. Catalyst ratios as high as 250 : 1 have been attempted, but the higher ratios have resulted in polymer precipitations of "stickier" quality polymer and poorer reaction yields. Polymerizations run with monomer to catalyst ratios of 100 : 1 or 75 : 1 consistently give materials with high molecular weights and better material properties.

Polymerization of cis-3,4-di(hydroxymethyl)cyclobutene dicarbonate [6].

^1H NMR (CHCl_3): 5.46 (2H, b), 3.97 - 4.07 (4H, b, m), 3.73 (6H, s), 2.46 (2H, b), 2.75 (2H, b) ppm. ^{13}C NMR (CHCl_3): 155.68, 155.43, 131.43, 68.93, 68.82, 54.66, 44.02, 43.20, 38.44, 37.82 ppm.

Cyclobutene References:

- 1) Kovacic, P.; Jones, M. B. *Chem. Rev.* **1987**, *87*, 357 and references within. Elsenbaumer, R. L.; Shacklett, L. W., in Handbook of Conducting Polymers, Skotheim, T. A., Ed. Marcel Dekker, Inc. New York. 1986. Gorman, C. B.; Grubbs, R. H. *Conjugated Polymers: The Interplay Between Synthesis, Structure, and Properties. Conjugated Polymers: The Novel Science and Technology fo Conducting and Nonlinear Optically Active Materials*. Bredas, J. L.; Silbey, R., eds. 1991.
- 2) Soubiran, P.; Aeiyaeh, S.; Aaron, J. J.; Lacaze, P. C. *J. Electroanal. Chem.* **1988**, *251*, 89 and references within. Kovacic, P.; Jones, M. B. *Chem. Rev.* **1987**, *87*, 357. Tour, J. M.; Stephens, E. B. *J. Am. Chem. Soc.* **1991**, *113*, 2309. Yamamoto, T.; Hayashi, T.; Yamamoto, Y. *Bull. Chem. Soc. Jpn.* **1978**, *51*, 2091.
- 3) Ballard, D. G. H.; Courtis, A.; Shirley, I. M.; Taylor, S. C. *J. Chem. Soc. Chem. Commun.* **1983**, 954. Ballard, D. G. H.; Courtis, A.; Shirley, I. M.; Taylor, S. C. *Macromolecules.* **1988**, *21*, 294. Gin, D. L.; Conticello, V. P.; Grubbs, R. H. *J. Am. Chem. Soc.* **1992**, *114*, 3167.
- 4) Stevens, M. P. Polymer Chemistry: An Introduction. Oxford University Press. Oxford. 1990.
- 5) Ballard, D. G. H.; Courtis, A.; Shirley, I. M.; Taylor, S. C. *J. Chem. Soc. Chem. Commun.* **1983**, 954. Ballard, D. G. H.; Courtis, A.; Shirley, I. M.; Taylor, S. C. *Macromolecules.* **1988**, *21*, 294. Gin, D. L.; Conticello, V. P.; Grubbs, R. H. *J. Am. Chem. Soc.* **1992**, *114*, 3167.

- 6) Stevens, M. P. Polymer Chemistry: An Introduction. Oxford University Press. Oxford. 1990. Ivin, K. J. Olefin Metathesis. Academic Press. New York. 1983.
- 7) Rondan, N. G.; Houk, K. N. *J. Am. Chem. Soc.* **1985**, *107* (7), 2099. Winter, R. E. K. *Tet. Lett.* **1965**, (17), 1207. Criegee, R. *Angew. Chem., Int. Ed. (Engl.)*. **1968**, *7* (8), 559. Hake, H.; Landen, H.; Martin H. D. *Tet. Lett.* **1988**, *29* (50), 6601. Buechele, J. L.; Weitz, E.; Lewis, E. D. *J. Chem. Phys.* **1982**, *77* (7), 3500. Landan, H.; Margraf, B; Martin, H. D.; Steigel, A. *Tet. Lett.* **1988**, *29* (50), 6507. Squillacote, M.; Semple, T. C. *J. Am. Chem. Soc.* **1990**, *112*, 5546. Ingham, S.; Turner, R. W.; Wallace, T. W. *J. Chem. Soc. Chem. Commun.* **1985**, 1664. Trost, B. M.; McDougal, P. G. *J. Org. Chem.* **1984**, *49*, 458. Scarborough, R. M., Jr.; Toder, B. H.; Smith, A. B., III. *J. Am. Chem. Soc.* **1980**, *102* (11), 3904. Griffin, G. W.; Kirschenheuter, G. P. *Tetrahedron*. **1985**, *41* (11), 2069.
- 8) Wu, Z.; Wheeler, D. R.; Grubbs, R. H. *J. Am. Chem. Soc.* **1992**, *114*, 146.
- 9) Kovacic, P.; Jones, M. B. *Chem. Rev.* **1987**, *87*, 357 and references within. Elsenbaumer, R. L.; Shacklett, L. W., in Handbook of Conducting Polymers, Skotheim, T. A., Ed. Marcel Dekker, Inc. New York. 1986.
- 10) Huntsman, W. D.; Wristers, H. J. *J. Am. Chem. Soc.* **1963**, *85*, 3308. Huntsman, W. D.; Wristers, H. J. *J. Am. Chem. Soc.* **1967**, *89*, 342. Blomquist, A. T.; Maitlis, P. M. *Proc. Chem. Soc.* **1961**, 332. Huntsman, W. D.; DeBoer, J. A.; Woosley, M. H. *J. Am. Chem. Soc.* **1966**, *88*, 5846. Braverman, S.; Duar, Y. *J. Am. Chem. Soc.* **1990**, *112*,

5831. Cava, M. P. Cyclobutadiene and Related Compounds. 1967.
Raphael, R. A.; Sondheimer, F. *J. Chem. Soc.* **1950**, 120.
- 11) Swager, T. M. California Institute of Technology. Thesis. 1988.
- 12) Gin, D. L.; Conticello, V. P.; Grubbs, R. H. *J. Am. Chem. Soc.* **1992**, 114, 3167. Conticello, V. P.; Gin, D. L.; Grubbs, R. H. *J. Am. Chem. Soc.* **1992**, 114, in press.
- 13) Scharf, H. D.; Mattay, J. *Liebigs Ann. Chem.* **1977**, 772. Criegee, R.; Zirngibl, U.; Furrer, H.; Seebach, D.; Freund, G. *Chem. Ber.* **1964**, 97, 2942. Hartmann, W. *Chem. Ber.* **1969**, 102, 3974. Brauman, J. I.; Archie, W. C., Jr. *J. Am. Chem. Soc.* **1972**, 94, 4262. Scharf, H. D.; Korte, F. *Angew. Chem.* **1965**, 77, 452.
- 14) Birkofer, L.; Eichstadt, D. *J. Organomet. Chem.* **1986**, 307, 279. Schenck, G. O.; Steinmetz, R. *Bull. Soc. Chim. Belg.* **1962**, 71, 781. Koltzenburg, G.; Fuss, P. G.; Leitich, J. *Tet. Lett.* **1966**, (29), 3409. Scharf, H. D.; Mattay, J. *Liebigs Ann. Chem.* **1977**, 772. Criegee, R.; Zirngibl, U.; Furrer, H.; Seebach, D.; Freund, G. *Chem. Ber.* **1964**, 97, 2942. Hartmann, W. *Chem. Ber.* **1969**, 102, 3974.
- 15) Wang, P.; Hill, T. G.; Wartchow, C. A.; Huston, M. E.; Oehler, L. M.; Smith, M. B.; Bednarski, M. D.; Callstrom, M. R. *J. Am. Chem. Soc.* **1992**, 114, 378. Callstrom, M. R.; Bednarski, M. D. *MRS Bulletin*. **1992**, 17 (10), 54.

Chapter Three. Preparations to Organic Ferromagnets

Introduction

All materials respond to an externally applied magnetic field. The behavior of a substance in that magnetic field is used to classify that system. While there are at least 14 different types of magnetic behavior, we will focus upon diamagnetism, paramagnetism, and ferromagnetism.¹

Diamagnetism arises from the interaction of the paired electrons in filled molecular orbitals with an externally applied magnetic field. Since the majority of all molecules have paired electrons, diamagnetism is a common molecular property. All other magnetic behavior implies the presence of unpaired electrons in a molecule. The interactions (or lack of them) among these unpaired electrons determines the type of magnetic material and resultant behavior. These couplings often include a mixture of intra- and intermolecular interactions.

Paramagnetic substances are characterized by random orientations of the magnetic moments in a material resulting from the spin angular momenta of unpaired electrons (Figure 1). As a consequence of these random moments, these materials display a zero overall magnetic moment in the absence of an external magnetic field.

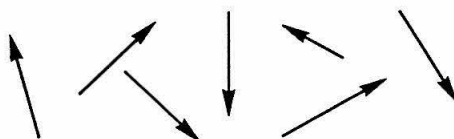


Figure 1: Paramagnetic spins: zero overall magnetic moment.

Though there is no interaction between neighboring spin centers, the application of an external magnetic field aligns the spins parallel to the direction of the magnetic field. At elevated temperatures, the thermal energy of the system opposes and disrupts the parallel alignment of the radicals in the magnetic field, rendering the material diamagnetic. This is the basis of the Curie Law, one of the first fundamental theories of paramagnetism.

Ferromagnetic substances are characterized by the parallel orientation of magnetic moments of the unpaired electrons (Figure 2). Unlike the non-communicative nature of paramagnetic centers, ferromagnetic coupling of electrons results in the energetic stabilization of the high spin state (all spins parallel) and gives rise to a permanent magnetic moment in the material.



Figure 2: Ferromagnetic spins: non-zero overall magnetic moment.

A true ferromagnet has a spontaneous magnetization in the absence of an externally applied magnetic field and has the physical characteristics of a metal. At elevated temperatures, electron spin magnetic moments randomize, the thermal energy having overcome the coupling between magnetic moments, and the ferromagnetic material behaves paramagnetically. The communication between spin centers has been lost. Strength and thermal stability are related to the number of parallel spins and the magnitude of the energetic coupling between those spins.

High spin behavior, and magnetism in general, is a consequence of exchange interactions. Exchange is a quantum mechanical phenomenon that

has no classical counterpart. To control the intra- and intermolecular magnetic couplings among paramagnetic centers (the qualitative and quantitative aspects of spin-spin interactions) in structures with stable high spin states is to control the magnetic properties of these materials. Molecular based ferromagnetism must contain not only molecules with magnetic moments, but also a means to couple those moments to one another in parallel (high spin) fashion. It is a bulk, macroscopic property that requires magnetic interactions in three dimensions.

The design of molecular ferromagnetic materials is an area of increasing theoretical and experimental interest.² Work on ferromagnetic materials is not new, and several theoretical models have been proposed to describe this magnetic behavior. Each model approaches the design of molecular ferromagnetic materials a bit differently, but each attempts to control electron interactions in these molecular spin-containing systems.

There are several theoretical models for the design of ferromagnetic polymers:

- 1) Hund's Rule.
- 2) McConnell Spin Exchange Model.
- 3) Charge Transfer Model.
- 4) Polaronic Ferromagnetism Model.
- 5) Topological Coupling Model.

In 1963, McConnell proposed that controlled stacking of organic, conjugated π radicals with opposite sign spin densities should lead to construction of a high spin system with intermolecular ferromagnetic coupling.³ Experiments show a certain degree of ferromagnetic ordering is achieved among polycarbenes with the McConnell Spin Exchange Model, but

there exists no evidence of bulk ferromagnetic ordering in other solids. Iwamura and Itoh's polycarbenes have shown intramolecular high spin behavior (Eff. magnetic moment = 9.08, $S = 8.1$), above 2.1 K, while Kinoshita's galvinoxyl mixtures have shown intermolecular organic ferromagnetic coupling between as many as six separate molecules (Figure 3).⁹

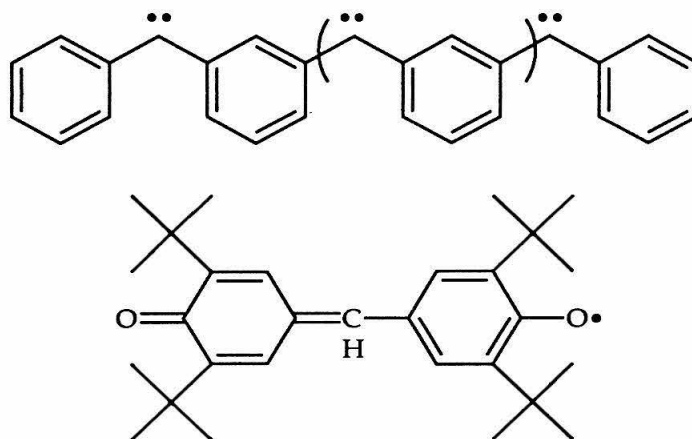


Figure 3: High spin polycarbene and galvinoxyl materials.

The McConnell approach, however, is limited by the ability to correctly pack and arrange radical structures over large distances. The uncertain composition and magnetic qualities of these polymers emphasize the increased need for rationally designed, well defined systems.

The Charge Transfer Model involves alternating donor-acceptor stacks in the solid state which interact to form a ferromagnetic-coupled material at low temperatures (Figure 4).⁴ Miller's ferricinium/TCNE molecules exhibit spontaneous magnetization and hysteresis below 5 K, although attempts to extend this work have failed with closely related donor and acceptor molecules.⁵

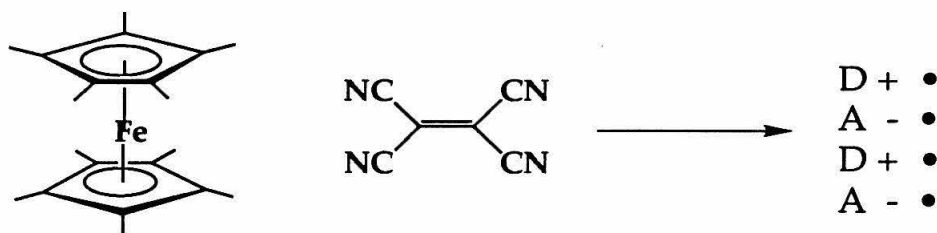


Figure 4: Miller's charge transfer materials.

The Polaronic Ferromagnetism Model is another approach to polymer-based magnetic materials. The model conceptually breaks ferromagnetic polymers down into monomers and coupling units (Figure 5). Monomer units contain localized magnetic moments, while the coupling units couple the two spin units to which they are attached.

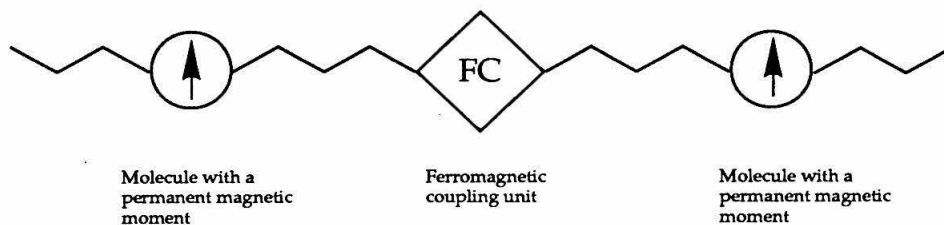


Figure 5: Polaronic ferromagnetism model.

The spin units are polarons generated by the oxidative doping of conjugated polymers. The magnetic high spin work in the Dougherty laboratory, which focuses upon the Polaronic Ferromagnetism Model, has shown promise with the poly(meta-phenyleneoctatetraene) (PMPOT) and cyclobutadiyl systems (Figure 6).⁶

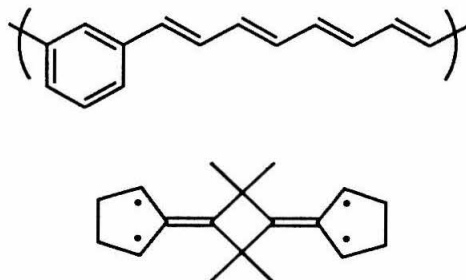


Figure 6: Polaronic coupling and polymer systems.

The development of completely organic magnetic materials presents an intellectual challenge that redefines the frontiers of organic synthesis, electronic structure theory, and materials chemistry. Organic magnets offer new insights into the nature of magnetism and lead to the development of materials with unique optical, electrical, and magnetic properties, though it remains unlikely that organic magnetic materials will ever replace the conventional magnetic materials.

A number of organic polymers have been synthesized with stable radical substituents incorporated within their structure. However, most of those unpaired spins were magnetically localized and behaved as polymer-bound monoradicals. Though several solids have been found to possess weak ferromagnetic intermolecular interactions, there are no ferromagnets.⁷ By contrast, the Topological Coupling Model predicts a class of organic compounds will have interesting magnetic properties by virtue of its topology.⁸ Based upon a theoretical investigation of high spin ground states for neutral molecules in conjugated alternant π -electron networks, Ovchinkov concluded that theoretical evidence supported high spin organic molecules.

Work on purely organic systems, including Iwamura's polycarbenes,⁹ has been limited by irreproducible synthetic and magnetic results, poor

reaction yields, and scant theoretical support. In most organic molecular solids, the unpaired electrons interact weakly, and often antiferromagnetically. Such solids are either bulk paramagnets or, if the antiferromagnetic interactions lead to long range coupling, antiferromagnets.⁷ For example, in spite of the local threefold symmetry considered important for three-dimensional ferromagnetic exchange, only a few percent of Torrance's 1,3,5-triaminobenzenes shows strong magnetic properties (Figure 7).¹⁰

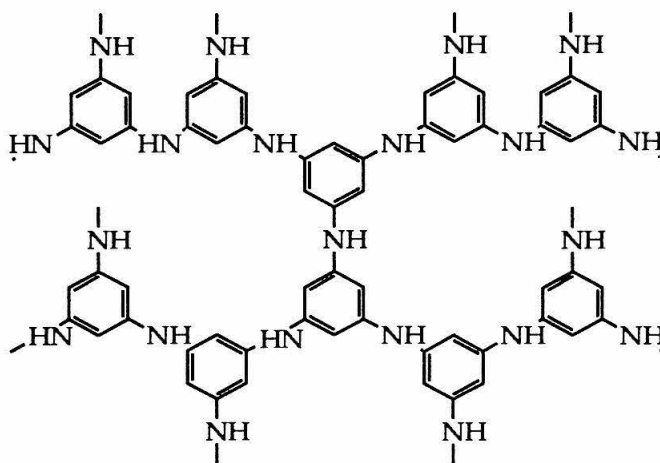


Figure 7: Ferromagnetically active 1,3,5-triaminobenzene.

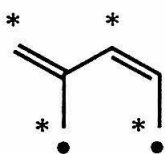
The polymer has an effective magnetic moment up to approximately 420 °C that does not recover upon cooling. Such unstable magnetism indicates irreversible structural changes in the polymer. However, the recent ferromagnetic behavior of inorganic/organic systems has led to a renewed interest in the development of organic molecular ferromagnets.

Parallel spin alignment of unpaired electrons by through-bond interaction has been discussed theoretically.⁸ Ovchinikov's topological model, in particular, has great utility in the design and prediction of high spin

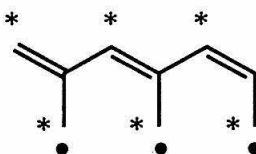
alternant molecules because the spin state of such molecules is simply calculated. It is quite easy to design, on paper, large molecules with high spin multiplicities. Such exercises led to the proposition that a polymer's spin state could be directly proportional to the number of monomer units. For every unit cell with an extra (*), an overall spin state of $S = n/2$ is predicted for the material (Figure 8).

These polymer structures are typically alternant hydrocarbons, i. e., π conjugated molecules whose atoms are subdivided into starred (n^*) and unstarred (n°) carbon atoms so that no two starred or unstarred spin positions are adjacent. The spin quantum number (S) of the macromolecule can be derived from the number of starred π centers (n^*) and unstarred ones (n°). At $n^* = n^\circ$ the total spin is zero, and the ground state is a singlet. For an alternant π -conjugated macromolecule, if there is a difference between n^* and n° , the full spin of the molecule is more than zero.

$$\text{Total Spin (S)} = \frac{\# \text{ starred} - \# \text{ unstarred}}{2}$$



$$S = 1$$



$$S = 3/2$$

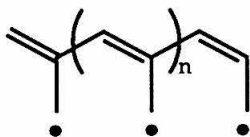


Figure 8: Ovchinikov's device for high spin molecules.

However, this model has several drawbacks in its application to bulk molecular ferromagnetism. First, it presents no mechanism for the intermolecular communication between high spin fragments. It relies solely upon strong one-dimensional coupling with weak two- and three-dimensional coupling. Bulk ferromagnetism is achieved only if spin-containing macroscopic ferromagnetic domains are formed amidst three-dimensional communication among spin sites. Secondly, this model is a theoretical model. While it has held true for single organic molecules, it remains largely untested in polymer systems.

To test the claims and postulates of this model, an organic-based ferromagnetic polymer was designed around the ring-opening metathesis polymerization (ROMP) of 3-diphenylmethylene cyclobutene and presents distinct advantages over classical metal based magnetic systems. Doping, the generation of charged species along the polymer, generates a radical spin ($1/2$) on every monomer unit in the polymer chain, resulting in a fully conjugated polybutenamer polymer (i. e., polyacetylene) with active spin centers every five (5) carbons apart(Figure 9). This polybutenamer has the same polymer repeat unit as a similarly substituted 1,4-poly(butadiene).

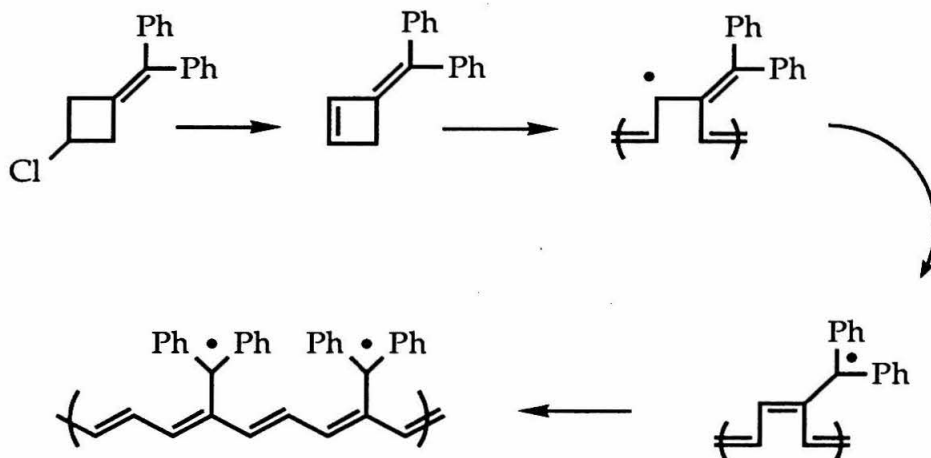


Figure 9: Proposed route into ferromagnetic materials.

Synthesis and Polymerization

Synthesis of the diphenylmethylenecyclobutene begins with the radical chlorination of the commercially available starting material, 1,1-cyclobutanedicarboxylic acid (Figure 10).

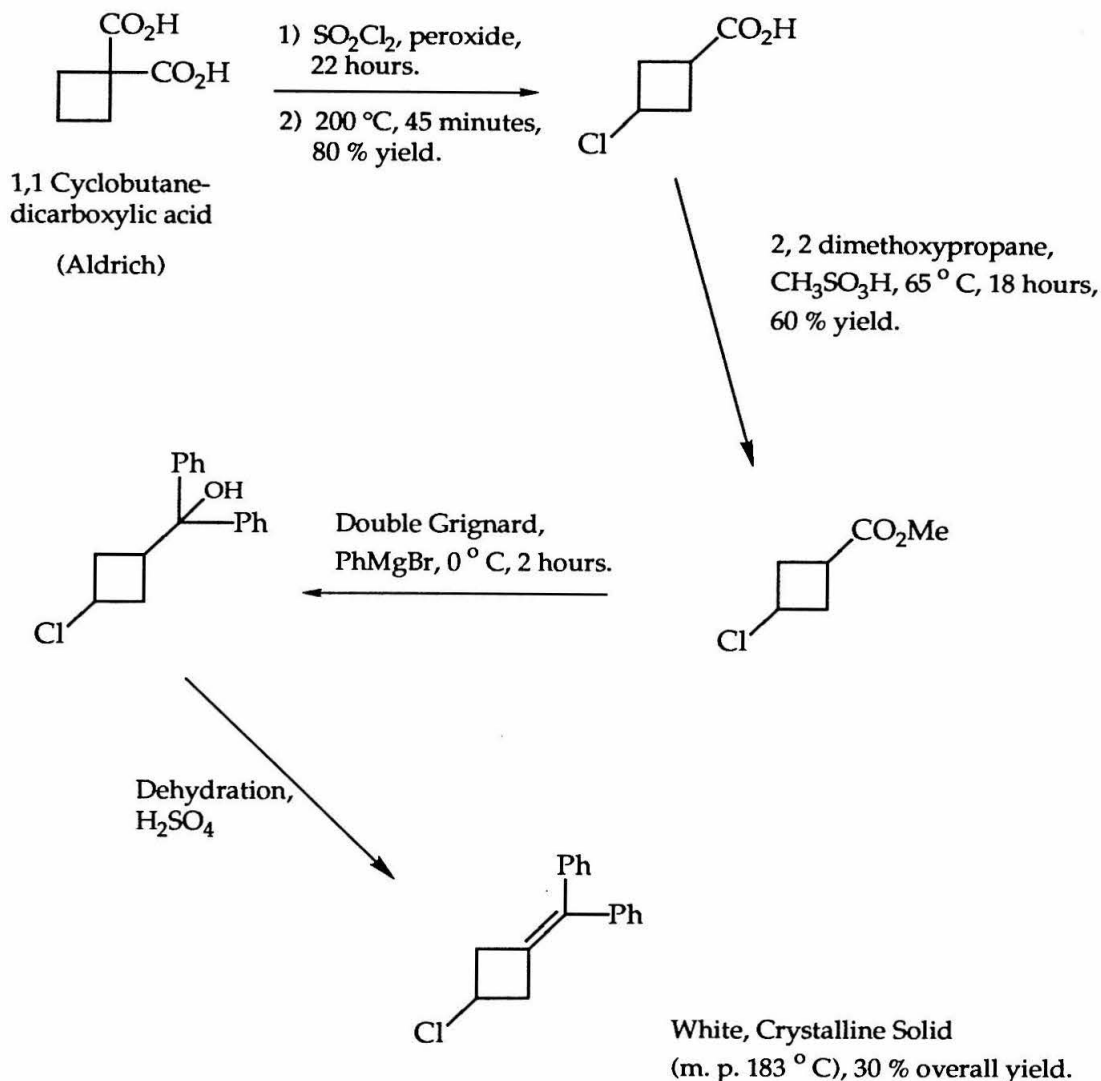


Figure 10: Synthesis of 3-diphenylmethylene-1-chlorocyclobutane.

The reaction of the commercially available diacid with sulfuryl chloride effects cyclobutane chlorination in 80 % yield after moderate decarboxylation conditions.¹¹ Distillation of the dark reaction mixture provides a clear and colorless, analytically pure oil. Esterification of the 3-chlorocyclobutane with 2,2-dimethoxypropane at 65°C yields the methyl ester as a clear oil.¹² The

reaction of two equivalents of grignard reagent with this ester at 0 °C cleanly yields the tert-butanol product.¹³ Flash chromatography and recrystallization provide the white, crystalline, 3-diphenylmethylene-1-chlorocyclobutane monomer; 60 % yield over two steps.

High spin ground states do not always imply instability. A high spin π electron network might be stabilized by "external" functional groups attached to the network. As a consequence, the synthesis of these compounds has been extended to alter phenyl ring sterics and electronics (Figure 11). Addition of a second, different, aryl grignard yields the appropriately functionalized chlorocyclobutane solid.

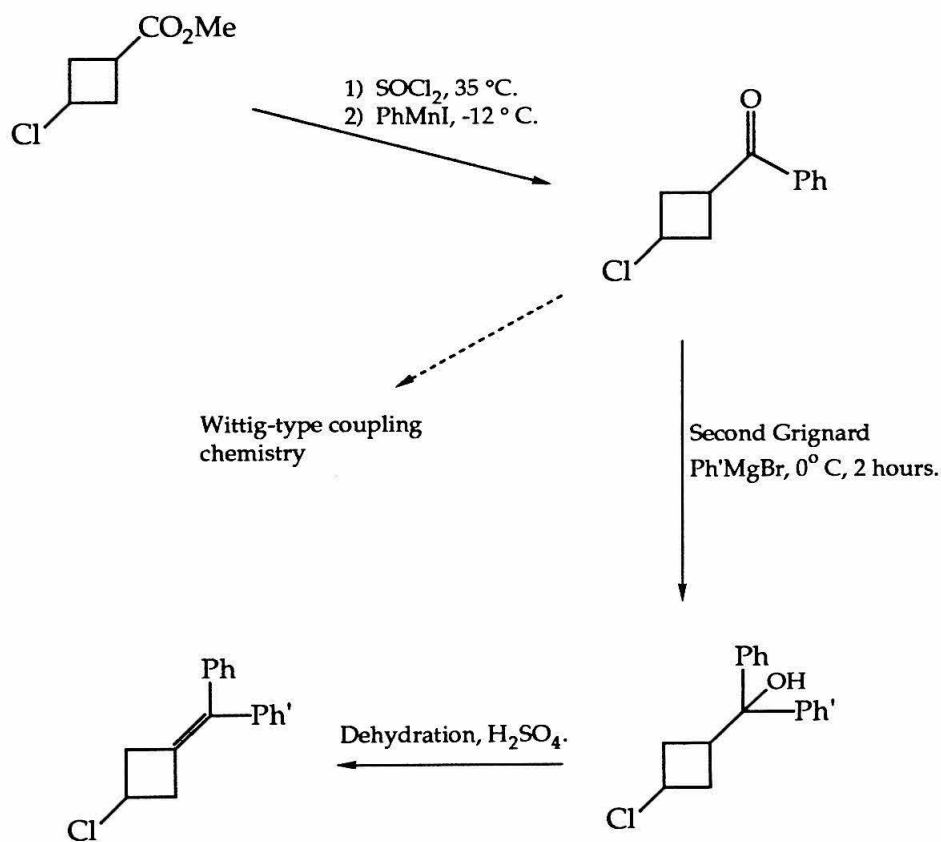


Figure 11: Modified synthesis of phenylcyclobutanes.

A series of para-substituted halide, thiol, galvanoxyl, silyl ether, and amino phenyl cyclobutanes have been made in order to test the effects of these substituents upon the bulk magnetic and polymerization behaviors of these materials (Figure 12).

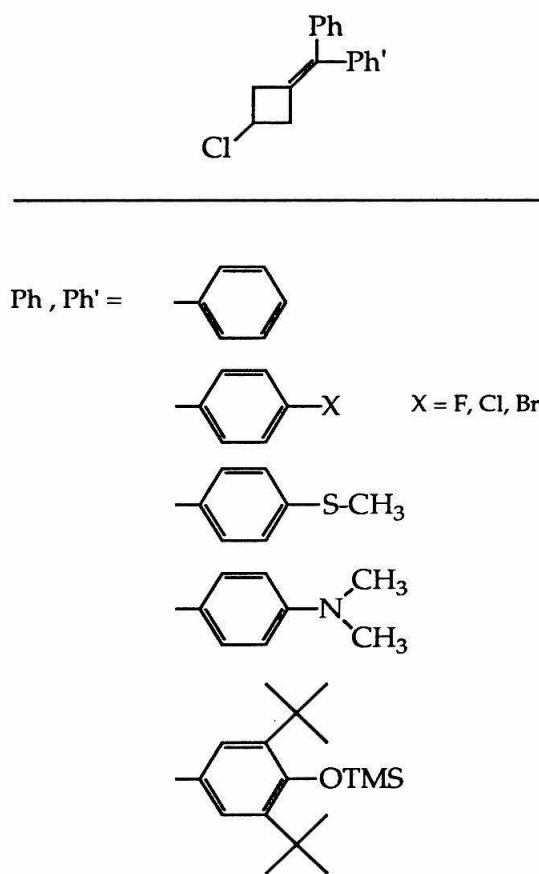


Figure 12: Substituted phenyl cyclobutane monomers.

The 3-diphenylmethylene-1-chlorocyclobutane compound is our precursor monomer which, upon reaction with base, yields the ROMP-able cyclobutene (Figure 13).

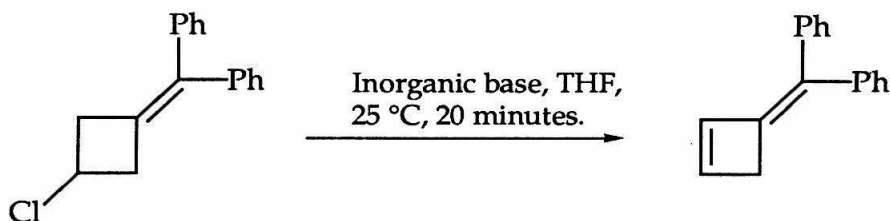


Figure 13: Elimination to yield ROMP-able cyclobutene.

A variety of inorganic bases [sodium amide (NaNH_2), sodium hexamethyldisilazide (HMDS), potassium hydride (KH), lithium diisopropylamide (LDA), and sodium hydride (NaH)] cleanly eliminate chlorine from the precursor monomer in 20 minutes at room temperature.

The diphenylmethylene cyclobutene was first polymerized using Grubbs' dimethyl titanocene metallacycle in benzene at 70 °C (Figure 14).¹⁴

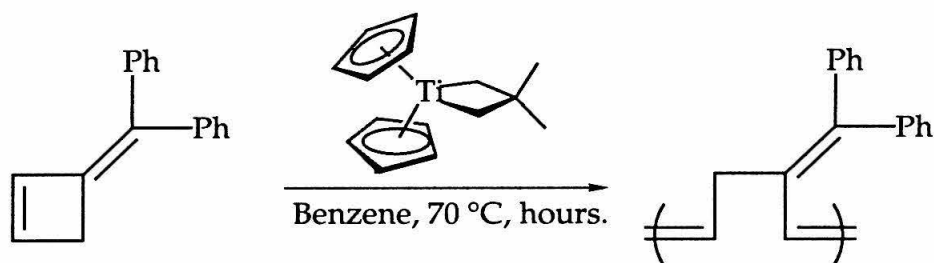


Figure 14: Titanium ROMP polymerization.

The yellow/green polymeric solid was completely soluble in organic solvents and showed a clean NMR spectrum after only several hours at room temperature. As the olefin resonances of the monomer decreased in intensity, broad polymer peaks arose from the spectrum baseline. Although the titanocenes polymerize this cyclobutene, the resulting materials are low molecular weight, yellow and green solids and are produced in low yield.

Initial tungsten alkylidene polymerizations also yielded low quality, low molecular weight solids and were marred by large losses of olefin and uncontrolled polymerization reactions (Figure 15).

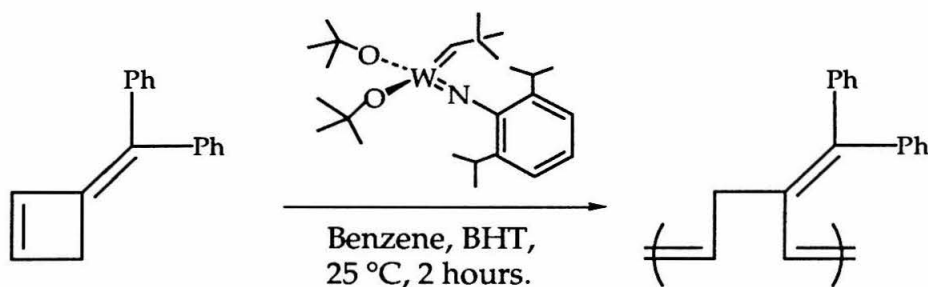


Figure 15: Early tungsten alkylidene polymerizations.

$[(t\text{BuO})_2\text{W}(\text{CHC}(\text{CH}_3)_3)(\text{NPh}(2,6\text{-isoprop})_2)]$ polymerized the cyclobutene olefin, in the presence of BHT, to yield a soluble, fine white, wispy polymer ($M_w = 8000$, PDI 1.6). Though a fair polydispersity, the low degree of polymerization (33 repeat units) and low reaction yield prevented any accumulation of clean polymer for doping. 2,6-di-tertbutyl-4-methylphenol (BHT) was present in all early elimination and polymerization reactions in an effort to quench the high reactivity of the cyclobutene monomer. While BHT does not react directly with the tungsten alkylidene catalyst, its presence in these early efforts might have, nonetheless, affected the polymerization activity of the metal.

Recent work has focused upon BHT-free tungsten alkylidene polymerizations, wherein the cyclobutene is generated in situ. The isolated cyclobutene is a colorless, highly reactive, viscous oil, unlike its white crystalline chloride precursor. Purification from the sodium salts generated in the elimination reaction remains a waste of time and materials when

experiments indicated the compatibility of the alkylidene catalysts with the salts.

Thus, the more economical approach to polymerization is the in situ generation of the cyclobutene monomer. The ability to generate the monomer in the presence of an inorganic base and tungsten alkylidene catalyst improves reaction yields and eliminates the earlier use of BHT as an anti-oxidant. This "one pot" approach allows the controlled ROMP of a reactive, strained cyclic monomer and eliminates the loss of time and materials involved in monomer purification. Room temperature polymerization of 3-diphenylmethylenecyclobutene yields a soluble, high molecular weight polymer in 6 hours. Precipitation into methanol separates all lingering sodium salts and reaction impurities from the polymer solids. In addition, the reaction appears unaffected by the rate or order of premonomer, inorganic base, and catalyst addition.

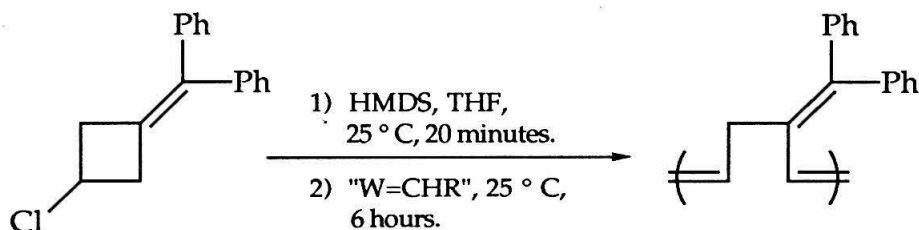


Figure 16: "One pot" elimination and polymerization.

The most reproducible polymerization results are achieved using a "one pot" recipe of the precursor chloride monomer, hexamethyldisilazide base, and $[\text{OC}(\text{CF}_3)_2\text{CH}_3)_2\text{W}(\text{CHPh}(\text{OCH}_3))(\text{NPh})]$ catalyst, in THF, at 25°C (Figure 16). Left to eliminate for some 40 minutes before addition of catalyst (often a 50 - 120 : 1 catalyst to monomer ratio), the simplicity of reaction allows convenient preparations of over 1 gram of clean polymer. Quenching

and precipitating the polymerization in methanol or pentane after 2 hours gives a slightly yellow, soluble, high molecular weight, diamagnetic polymer in 70 % yield.

Polymer characterization by NMR indicates a high (>90 %) cis polymer content and predominantly head to tail linkages as a consequence of the bulky diphenyl methylene groups. All NMR resonances are well resolved, multiplets (except for aromatic ring resonances) and shifted slightly from their respective monomer resonances (Figure 17). NMR spectroscopy also shows indications of other (lesser) polymer structures apparently sensitive to the polymer methylene region (2.5 - 3.0 ppm (^1H) and 30.6 and 38 ppm (^{13}C)). GPC analysis occasionally depicts a second, low molecular weight fraction in addition to the broader, high molecular weight polymer fraction. Even though catalyst amounts remained relatively consistent, polymer molecular weights and polydispersities vary wildly, apparently indicative of a highly reactive, non-living, polymer system (Figure 18).

MMR-III-018	$M_n = 22,100$ $M_w = 84,000$ $\text{PDI} = 3.81$	MMR-III-068	$M_n = 290,000$ $M_w = 514,000$ $\text{PDI} = 1.77$
MMR-III-026	$M_n = 83,000$ $M_w = 230,000$ $\text{PDI} = 2.74$	MMR-III-080	$M_n = 800$ $M_w = 1,100$ $\text{PDI} = 1.40$
MMR-III-028	$M_n = 116,000$ $M_w = 313,000$ $\text{PDI} = 2.70$	MMR-III-084	$M_n = 261,000$ $M_w = 420,000$ $\text{PDI} = 1.60$
MMR-III-040	$M_n = 150,000$ $M_w = 352,000$ $\text{PDI} = 2.35$	MMR-III-090	$M_n = 930,000$ $M_w = 5.5 \text{ Million}$ $\text{PDI} = 5.94$
MMR-III-062	$M_n = 11,000$ $M_w = 62,000$ $\text{PDI} = 5.81$	MMR-III-094 (Fluoro)	$M_n = 31,000$ $M_w = 175,000$ $\text{PDI} = 5.62$

Figure 18: Successful "one pot" polymerizations.

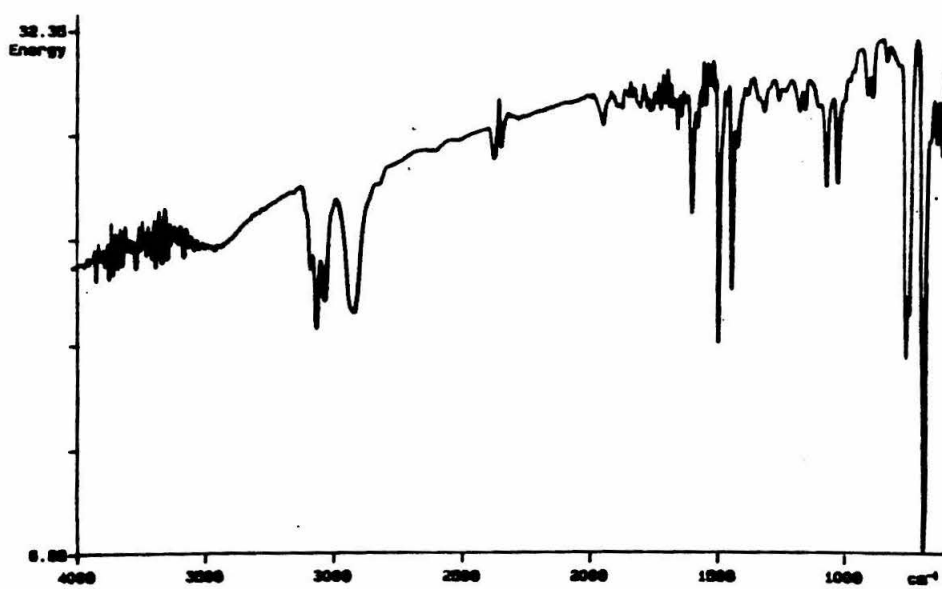
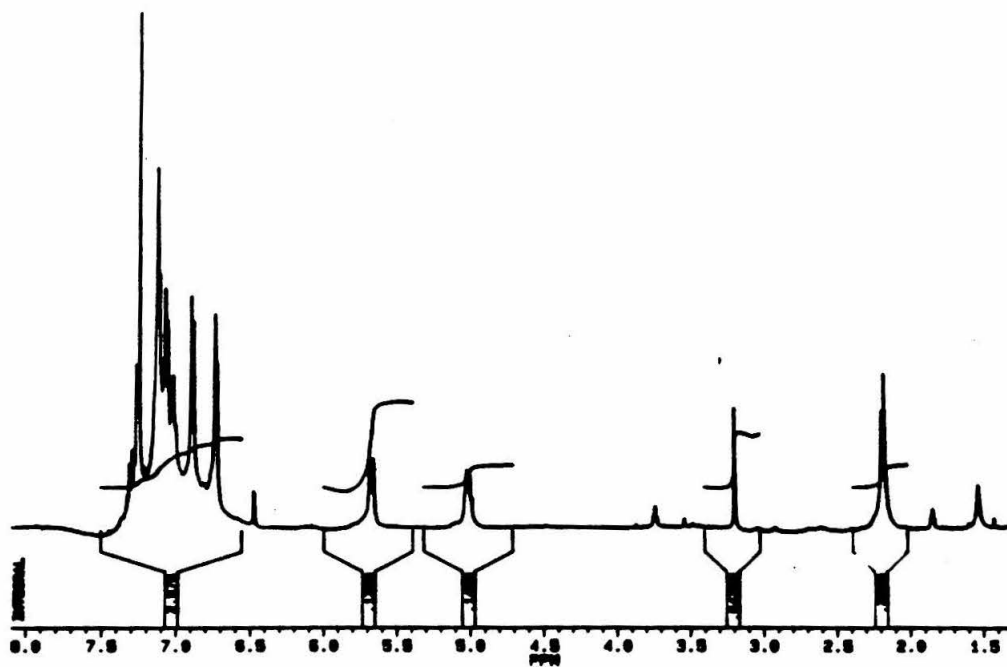


Figure 17: ^1H NMR and IR spectra of poly(3-diphenylmethylenecyclobutene).

TGA and DSC results show (Figure 19) the thermal stability of the polymer to 200 °C before degradation to a blackened char occurs (52 % weight remains at 430 °C, 30 % at 550 °C). An unidentified, sharp, irreversible exotherm of - 5.3 kcal/mole appears at 220 °C and may indicate a cis to trans isomerization. The high solubility of these polymers in common organic solvents facilitates their doping as precipitated white powders or thin films.

All low temperature (-78 °C) polymerizations failed. These attempts at a controlled polymerization often resulted in partial catalyst decomposition and sparingly soluble, polymer solids. Highly aromatic, polymer solids with broad molecular weight ranges (8000 - 350,000 vs. polystyrene standards) and broader polydispersity indices (2.0 - 6.5) emerged from these polymerization solutions (Figure 20), which had lost their distinctive orange/yellow shade and turned green .

MMR-III-020	$M_n = 5,500$ $M_w = 36,000$ PDI = 6.49
MMR-III-048	$M_n = 22,000$ $M_w = 56,000$ PDI = 2.57
MMR-III-072	$M_n = 92,000$ $M_w = 190,000$ PDI = 2.08

Figure 20: Unsuccessful polymerizations (amorphous NMR spectra).

Disturbingly, this amorphous, nondescript polymer resembles the desired ROMP polymer in many respects. While ^1H NMR shows a highly aromatic polymer without any discriminating olefinic or methylene resonances, ^{13}C NMR shows a structurally similar polymer structure with broader resonances than the ROMP polymer (Figure 21).

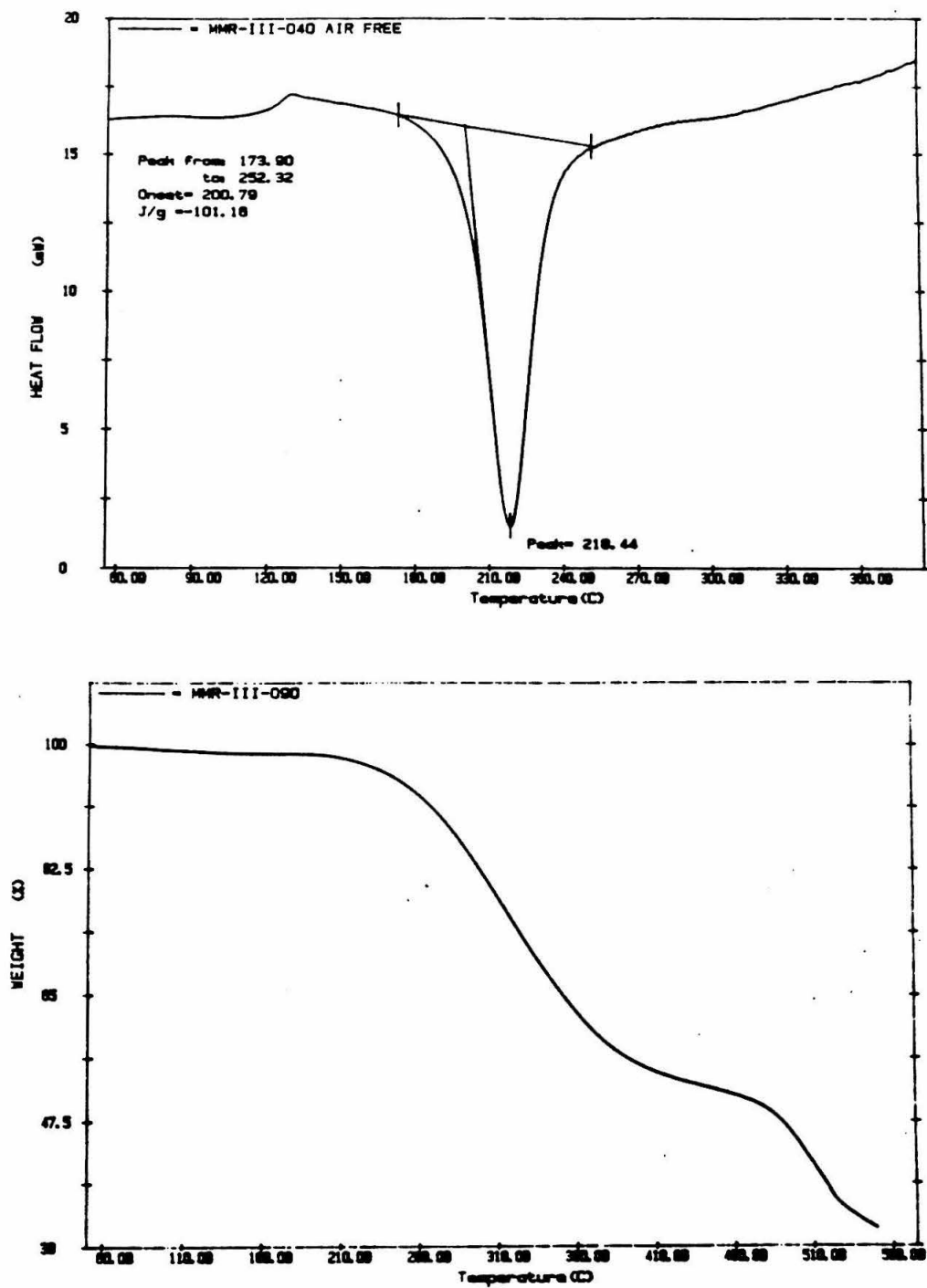


Figure 19: Thermal analysis (TGA and DSC) of poly(3-diphenylmethylenecyclobutene).

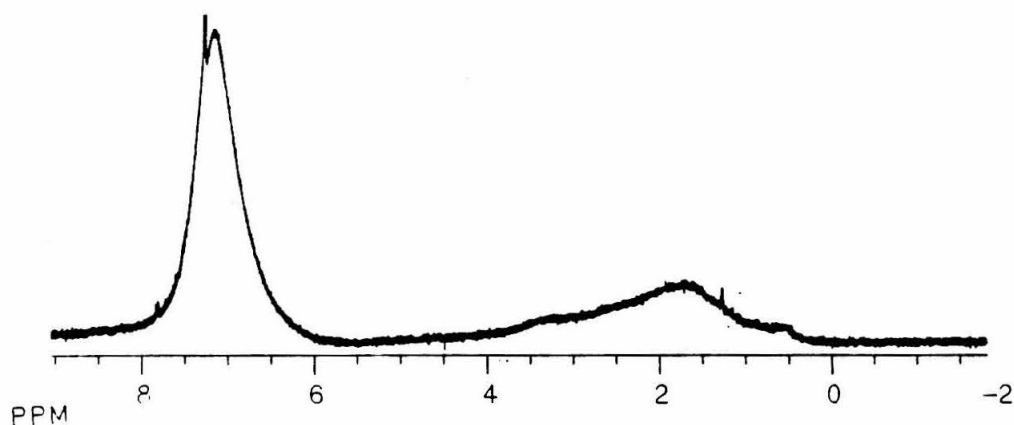


Figure 21: Amorphous, non-descript ^1H NMR of poly(3-diphenylmethylenecyclobutene).

With the exception of a DSC exotherm mentioned earlier, analysis (IR spectroscopy, elemental analysis, TGA, NMR, SQUID) of both the desired ROMP polymer and the amorphous, nondescript solid has remained consistent. The polymer is not believed to be a radically polymerized solid, but instead may simply be a slightly cross linked derivative of the ROMP polymer. Slight polymer crosslinking, or an occasional paramagnetic impurity, would broaden the ^1H NMR spectrum.

Doping Efforts

The ring-opening polymerization of 3-diphenylmethylenecyclobutene yields soluble, high molecular weight polymer that exhibits reproducible ferromagnetic activity upon chemical treatment. Doping, the generation of charged species along the polymer, generates a radical spin ($1/2$) on every

monomer unit in the polymer chain, resulting in a fully conjugated polybutadiene polymer (i. e., polyacetylene) with active spin centers every five carbons apart (Figure 22).

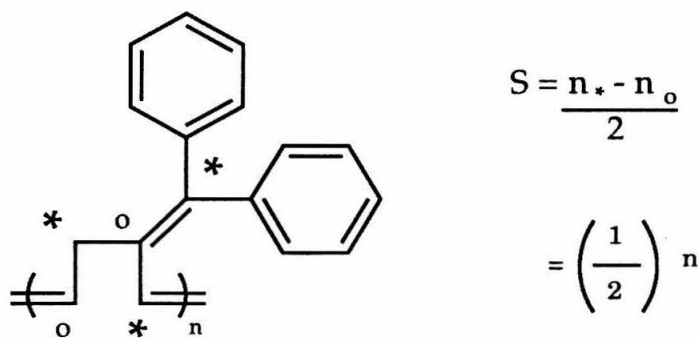


Figure 22: Ferromagnetic organic polymer design.

Such a relationship between the radical centers diminishes their tendency to recombine and encourages ferromagnetic coupling between them. More importantly, these radical centers resemble trimethylenemethane and diphenylmethyl radicals - radical systems analogous to the well known and very stable triphenylmethyl radical (Figure 23).¹⁵ As a consequence of their structural topology, these stable spins should be ferromagnetically coupled (in one dimension) to provide a magnetically active polyradical structure.

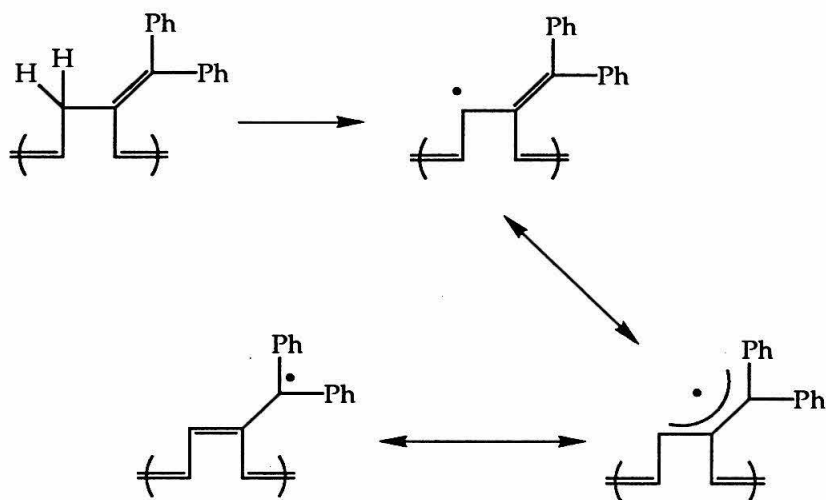


Figure 23: General doping approach to magnetic materials.

Polymer solubility facilitates the exposure of these white powders and thin films to chemical dopants. All polymer doping efforts were performed on clean, well characterized, diamagnetic ($< 10^{17}$ unpaired spins) polymer samples to insure that any change in the magnetic and/or physical characteristics upon treatment would be attributed to doping and not to simple side reactions.

Polymer samples were dissolved in an organic solvent (usually CH_2Cl_2), and then the dopant was added and allowed to react for a specified amount of time. Because of concern that methanol might quench developing spin centers, doped polymer solutions were precipitated into swirling pentane before bulk magnetic measurements with the SQUID were taken. The added benefit of soluble, doped materials allows us to investigate physical, chemical, and structural changes of the magnetic polymer upon doping. In every instance of successful doping, the ^1H NMR polymer spectrum depicted the amorphous, nondescript polymer seen earlier (Figure 21). This behavior seems consistent with the presence of paramagnetic

centers within the polymer and bodes well for our efforts at generating spins within the polymer.

With these efforts, we're simply looking for changes in the bulk magnetic properties of these materials upon chemical treatment. The magnetization induced in a polymer is proportional to the strength of the externally applied magnetic field: $M = \chi H$. The magnetic susceptibility of the sample, χ , is defined as the extent to which the material is susceptible to induced magnetization and can be defined in terms of molar susceptibility, χ_m .

Temperature and external field dependence of magnetization and susceptibility of these materials have been investigated (piecemeal) with the SQUID (Superconducting Quantum Interference Device). Magnetization is measured directly by a SQUID at 1.8 K and the raw data are fit to the Brillouin function, generating a spin value (S) and number of spins present in the doped polymer sample. Analysis of these magnetic experiments allows us to distinguish between ferro-, para-, and diamagnetic behavior.¹

The generation of charged species within the polymer (i.e., doping) has been attempted through:

- 1) Oxidation of the polymer.
- 2) Deprotonation of the polymer backbone.
- 3) Hydrogen atom abstraction.
- 4) Solution electrochemistry.

Direct polymer oxidation, successful in the doping of organic conductive polymers, was envisioned as a route into polymeric radical cations and attempted with a variety of oxidants, including air, iodine, ferricinium salts, lead dioxide, and silver oxide (Figure 24).

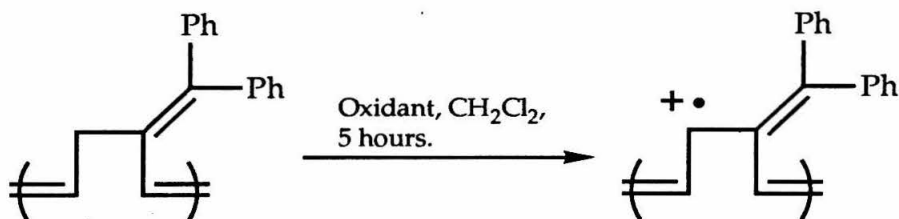


Figure 24: Oxidative doping of polymer.

Attempts at heterogeneous polymer oxidation involving lead dioxide (PbO_2) and silver (II) oxide (AgO) were unsuccessful. Benzene solutions of the polymer were left in contact (even sonicated) with the oxidants for some 22 hours without any indication of polymer oxidation or paramagnetism.

Iodine addition turns the polymer solution a dark, but clear, burgundy red color. The mixture gives no indication of oxidation until precipitation yields a distinctly yellow polymer solid. Magnetic results indicate a slightly paramagnetic solid. The spin value of $S > 0.5$ is indicative of some ferromagnetic coupling among the spins in the sample. A broadened NMR accompanies a newly paramagnetic iodine-doped solid with low, but acceptable, S values and number of radical spins generated.

MMR-III-070 (Iodine)

$$S = 1.07$$

$$\# = 1.18 \times 10^{20} \text{ spins/mole monomer}$$

This was the first evidence of a successful doping of a diamagnetic polymer to a paramagnetic (arguably ferromagnetic) material.

An inert DMF solution of polymer and $\text{Cp}_2\text{Fe BF}_4$ gives a similar maroon solution. Left to stir under argon for 12 hours, the reaction solution

turns orange. Precipitation into methanol yields a white flocculent, diamagnetic polymer solid in low yield.

Direct deprotonation of the polymer backbone with a variety of inorganic bases (NaH, HMDS, LDA, LAH, etc.) did not generate magnetically active materials. Though the doubly allylic methylene protons appear especially susceptible to attack, no reaction was observed (by NMR) when polymer films were treated with *tert*butyllithium or methyllithium. Additionally, no deuterium is incorporated into the polymer when the alkyl lithium reactions are quenched with deuterium oxide.

Other efforts have focused upon the reactivity of these doubly allylic protons of the polymer. Reaction sequences involving N-Bromosuccinimide (NBS) bromination and elimination and a Rajca-type sequence have been carried out with disappointing results (Figures 25, 26). The Rajca sequence is a rationally designed effort to generate neutral radicals along the polymer chain.¹⁶

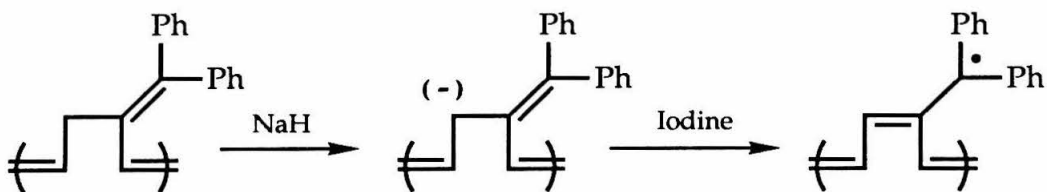


Figure 25: Rajca-type attempt at neutral radical generation.

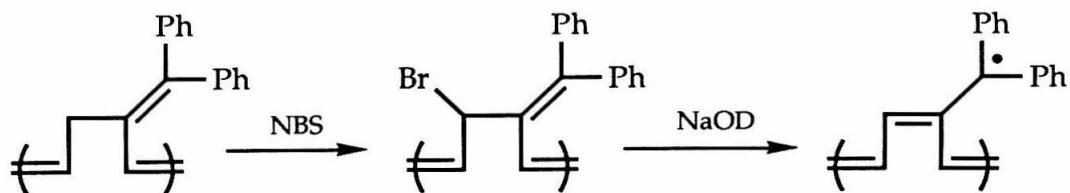


Figure 26: Allylic deprotonation and radical generation.

Deprotonation using a standard base, followed by anion oxidation by iodine to the neutral radical, have given red-orange polymeric materials with ambiguous and irreproducible magnetic results. EPR indicates the qualitative presence of radicals within the polymer structure, without providing structural details of the radical species.

The most desired synthetic route to magnetically active materials remains the photochemical abstraction of a neutral hydrogen atom to generate a neutral radical center on the polymer (Figure 27). Photolysis of these polymer solutions generates magnetically active spin centers but at a cost to the polymer structure. Reproducible magnetic data is accompanied by extreme polymer degradation. Early attempts to photogenerate a neutral radical with tertbutyl peroxide were inconclusive.

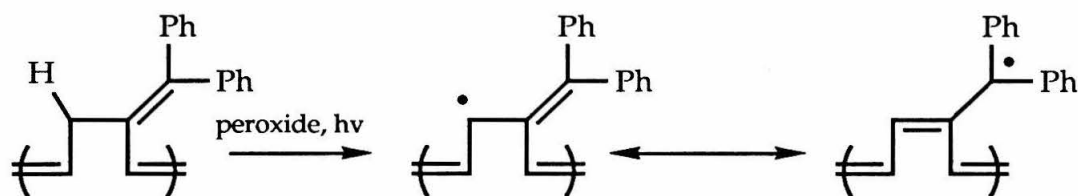


Figure 27: Hydrogen abstraction.

Treatment of the polymer in a benzene glass at 77 K showed a broadened EPR signal of 110 G (peak to peak width), as compared to the EPR spectra of the untouched polymer, 3300 G and 10 G peak separation. However, without any fine structure, the photochemical processes responsible for the broadened signal remain unidentified. A similarly broadened EPR signal is observed when photochemical radicals are generated photochemically with AIBN.

Polymer treatment with benzoquinone and DDQ provides alternative methods for photochemical hydrogen atom abstraction.¹⁷ Unfiltered UV

photolysis of a benzoquinone/polymer solution yields an opaque, dark brown solution that, upon precipitation into pentane, yields a flaky black, soluble solid in low yield. NMR and SQUID experiments indicate a paramagnetic, possibly hysteretic, material. The paramagnetic signal, number of spins, and S values are low, but the results are encouraging.

MMR-III-075 (Benzoquinone + hv)

$$S = 2.59$$

$$\# = 1.78 \times 10^{21} \text{ spins/mole monomer}$$

DDQ reactions proceed similarly. Combination of reactants at room temperature gives an orange solution or filthy yellow green mixture with formation of a black solid soon after addition of the DDQ oxidant. Precipitation gives a low yield of a trashy, but soluble, dark green polymer solid. This solid remains soluble in conventional organic solvents, but no structural determination could be made with NMR. SQUID measurements are irreproducible, but hint at paramagnetic behavior at 2 K.

Treatment of the polymer with an excess of iminium salt (structure) at room temperature yields a clear purple solution, which within minutes of addition darkens to a beautiful clear emerald green solution. Polymer precipitation and drying yields a deep, dark blue solid in quantitative yield. GPC analysis of the polymer shows extensive chain degradation as a consequence of this photolysis. A sample of molecular weight 420,000, PDI 1.6 is reduced to a material with molecular weight 35,000, PDI 20 after iminium salt and photolysis treatment.

MMR-III-088 (Iminium salt)

$$S = 0.90$$

$$\# = 3.16 \times 10^{21} \text{ spins/mole monomer}$$

Distinct oligomer peaks appear in the GPC chromatogram and are consistent with earlier findings. SQUID results show a paramagnetic species with a large number of spins generated but little communication between those spins.

The most successful, yet most misunderstood, reaction remains the irradiated treatment of a polymer solution with iodine (Figure 28). Envisioned as a method to photogenerate an increased number of radicals, UV irradiation successfully generates magnetically active spin centers.

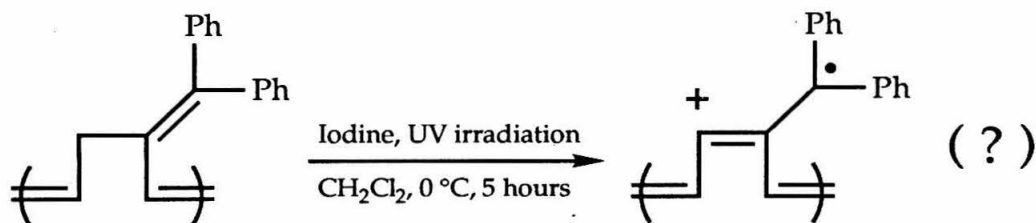


Figure 28: Radical generation by UV irradiation.

Treatment of the polymer with iodine gives a distinctly forest green, paramagnetic, granular solid in quantitative yield. GPC analysis of the polymer shows extensive chain degradation as a consequence of this photolysis. For example, a sample of molecular weight 420,000, PDI 1.6 is reduced to a material with molecular weight 21,000, PDI 2.56 after iminium salt and photolysis treatment.

MMR-III-076 (Iodine + hv)

$$S = 2.17$$

$$\# = 7.05 \times 10^{20} \text{ spins/mole monomer}$$

MMR-III-082 (Iodine + hv)

$$S = 1.84$$

$$\# = 1.22 \times 10^{21} \text{ spins/mole monomer}$$

MMR-III-086 (Iodine + hv)

$$S = 2.38$$

$$\# = 4.84 \times 10^{20} \text{ spins/mole monomer}$$

The photolyzed polymer shows substantial degradation as a result of irradiation, though rephotolysis does not cause a (expected) drop in either the number of spins generated or spin value. Magnetic results do not fluctuate more than 10 % in their paramagnetic behavior after days under ambient conditions.

More spins are generated and magnetically aligned upon unfiltered UV photolysis of treated polymer solutions. The S value again indicate the presence of some level of ferromagnetic coupling in the solid. SQUID Curie plots show an antiferromagnetic transition between 60 - 80 K, while remaining ferromagnetic at 1.8 K. Curie plot data confirm ferromagnetic coupling in the material. The mechanism of this doping is not known, though it must include hydrogen atom abstraction and partial oxidation of the polymer chain (Figures 29, 30, and 31). Additionally, there is no indication of hysteresis in any of the doped polymer samples.

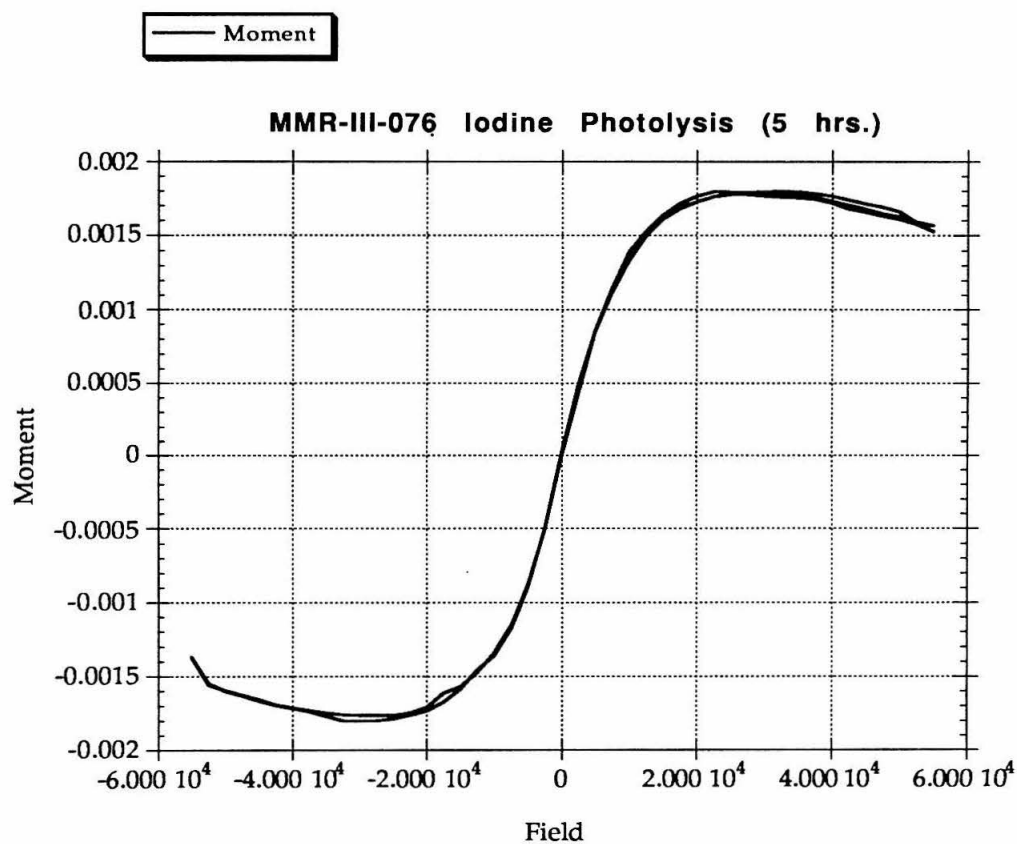


Figure 29: SQUID measurements for a photolyzed polymer sample.

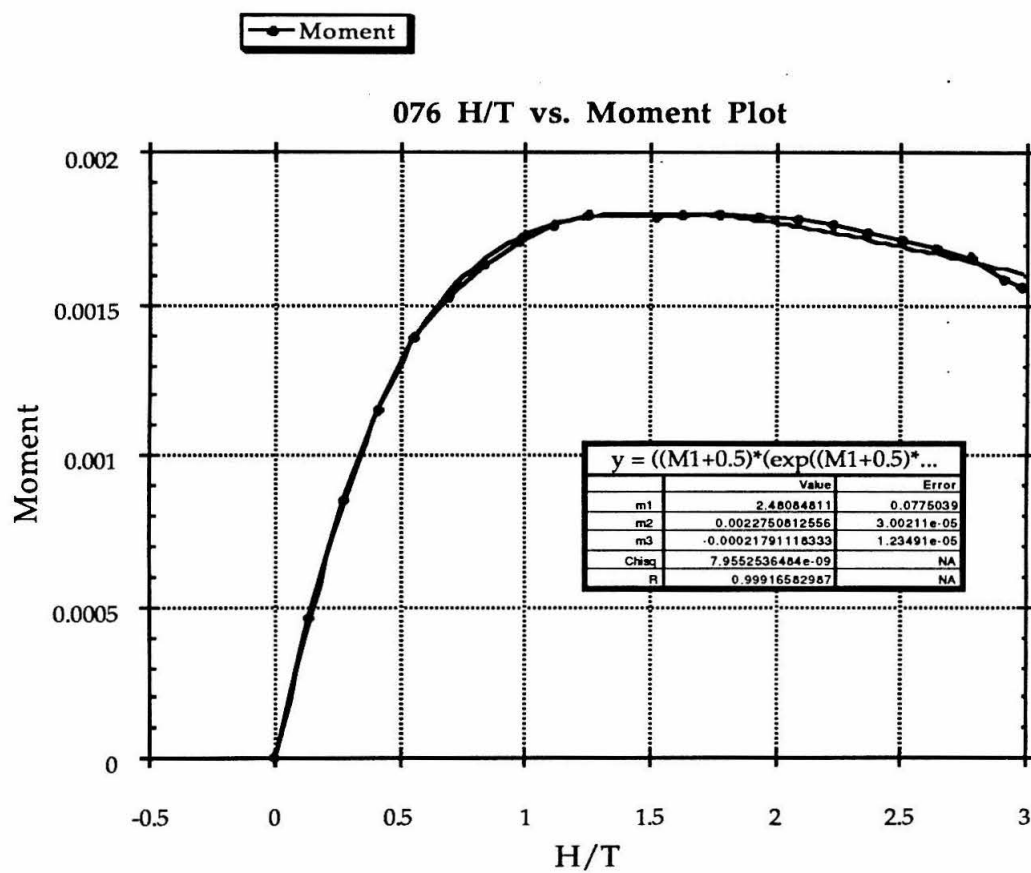


Figure 30: Raw data fit to magnetic data of iodine doped polymer.

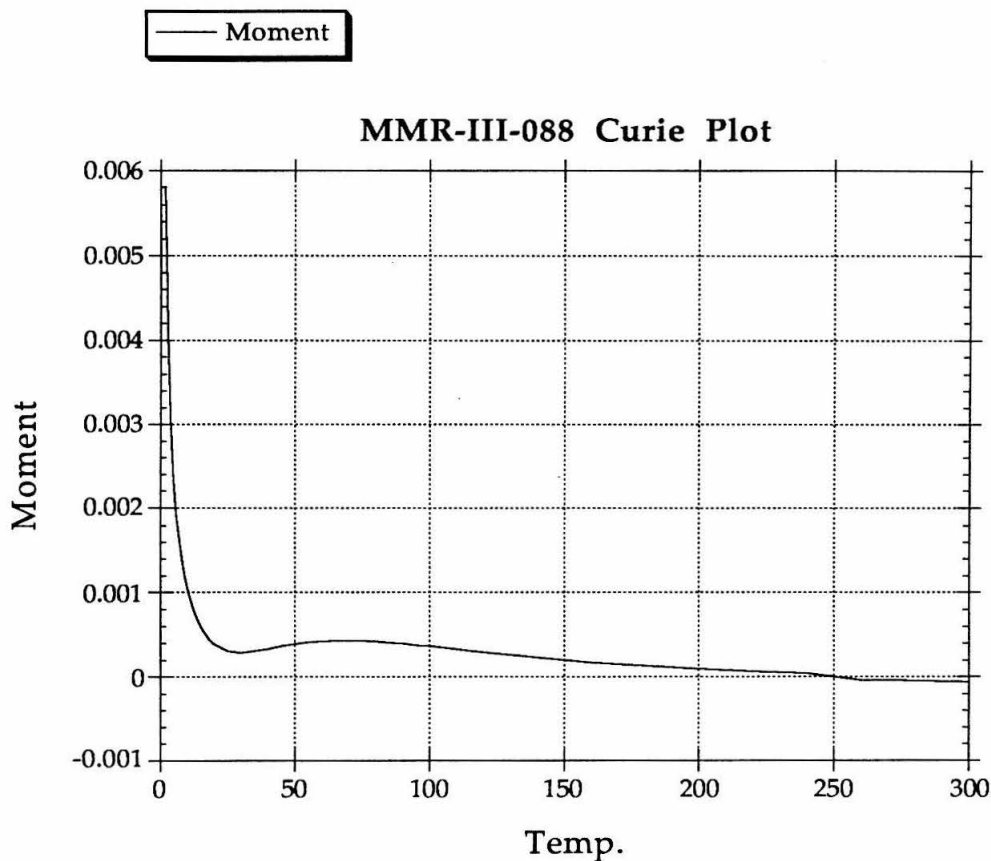


Figure 31: Curie plot of doped iodine sample.

Electrochemical oxidation of the 3-diphenylmethylene cyclobutene polymer at 1.3 V (vs. Ag/Ag⁺) indicates formation of a separated radical cation. According to preliminary experiments, the methylenes are not activated without removal of a proton or hydrogen atom (Figure 32).

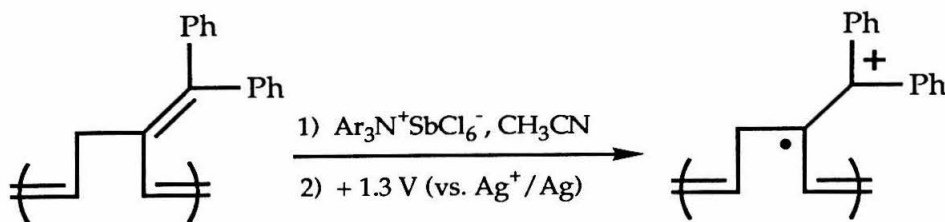


Figure 32: Electrochemical attempts at radical generation.

Instead, a radical cation is formed at the pendant methylene and a white to green electrochromism observed. Additional cyclic voltammetry experiments do not shed any light upon the success or failure of our doping approach because polymer films crumble at the electrodes and dopants/electrolytes can not diffuse into polymer films.

Conclusions and Future Prospects

These preliminary results hold promise for the development of organic magnetic materials. We have successfully generated and aligned (in an external magnetic field) unpaired spins in a previously diamagnetic organic solid. Treatment of poly(3-diphenylmethylene)cyclobutene with various dopants under different conditions have yielded soluble, highly colored solids with magnetic properties. Magnetic results indicate the presence of ferromagnetic coupling, albeit slight, in these doped organic polymers.

The synthesis and polymerization of 3-diphenylmethylene)cyclobutene has been conquered. Ring-opening metathesis polymerization via a "one pot" route allows multigram preparation of a diamagnetic organic polymer. The focus must now turn toward a quantitative understanding of the doping process. To date, the mechanism of doping in these materials is unknown. While the nature of the charge carriers in these doped polymers has been postulated, we have no proof. Rational attempts at doping have delivered mixed results, while the photolysis (with iodine) approach has consistently generated reproducible magnetic results.

Ferromagnet Experimentals:

General Considerations

All manipulations of air and/or moisture sensitive compounds were carried out using standard Schlenk or vacuum line techniques with argon as the flush gas. The argon was purified by passage through columns of activated BASF RS-11 (Chemlog) oxygen scavenger and Linde 4Å molecular sieves. Manipulation of air sensitive solids was performed in a Vacuum Atmospheres dry box equipped with a MO-40-1 purification train, a DK-3E Dri-Kool conditioner, and a Dri-Cold freezer. The catalyst dry train contained activated RidoxTM oxygen scavenger and Linde 11Å molecular sieves. In most cases involving the synthesis of these materials, glassware was dried in a 140 °C oven and subjected to vacuum while still hot.

¹H and ¹³C NMR were recorded on either a Jeol 400 GX (399.65 MHz ¹H), General Electric QE-300 Plus (300.199 MHz ¹H, 75.49 MHz ¹³C), or Bruker WM-500 (500.14 MHz ¹H) spectrometer. Chemical shifts were referenced to the solvent or to the residual protons of the solvent. Infrared spectra were acquired on both a Shimadzu IR-435 and Perkin-Elmer Series 1600 spectrometer. Infrared samples were either thin films or KBr pellets. Elemental analyses were performed by the California Institute of Technology Analytical Facility. Conductivity measurements were made with a home built probe or a commercially available Sigmatone sheet resistivity probe. Current was supplied to these probes by a Power Designs 605 precision power source and measured with a Keithley 160B digital multimeter. The voltage was monitored using a Fluke 895A differential

voltmeter. Thermal analyses were performed on a Perkin Elmer DSC-7 differential scanning calorimeter, TGA-7 thermogravimetric analyzer, and dual Tac 3/7 data stations. The thermal equipment is driven by an IBM PS/2 computer driven with Perkin Elmer computer software. Scanning rates for these analyses varied.

Polymer samples were run on a Millipore-Waters 150 C Gel Permeation Chromatography Spectrometer equipped with differential refractometer and a Waters 820 chromatographic data station. A home-built GPC station was also used and utilized Waters Ultrastyrigel columns connected to a Knauer differential refractometer. Polymer solutions of various ($\sim 0.5\%$ w/v) concentrations were prepared using either spectral grade 1,2 dichlorobenzene, methylene chloride, or tetrahydrofuran. These solutions were filtered using 0.2 and 0.45 μm UnifloTM filters to protect the Ultrastyrigel columns while sample injections of 0.2 ml and 1.0 ml/min flow rates were commonly used.

Solvents for all polymerizations were kept free of oxygen and moisture. Benzene was dried and deoxygenated with sodium benzophenone ketyl. Pentane was dried and deoxygenated after treatment with sulfuric acid for days. The tungsten alkylidene catalysts were provided by departing group members, but were initially prepared from the published procedures (catalyst references) and recrystallized from pentane. The large volume of hexane, pentane, and methanol used for precipitation of the polymer was degassed with an argon bleed for thirty minutes.

Preparation of 1-carboxy-3-chlorocyclobutane.

The 1,1-Cyclobutanedicarboxylic acid (125 g, 0.867 mol) was dissolved in benzene and placed in a one liter, three-necked flask equipped with a reflux condenser and dropping funnel. The solution was heated to reflux and 120 mls of benzene/water azeotrope removed by distillation. The sulfonyl chloride (75 mls, 126 g, 0.934 mol) was added via the addition funnel over the course of one hour. Benzoyl peroxide (3.0 g, 0.0124 mol) was added in portions over this same hour through the condenser and washed into the flask with benzene. The solution was purged with argon for one hour and the condenser was capped with a drying tube. The solution was left to reflux for 22 hours, and upon completion, the benzene was distilled off. The resulting dark brown solution was poured into a 150 ml round bottom flask and the dark brown viscous oil distilled at 15 torr. Three fractions were collected over the temperature range 110 - 125 °C. ¹H NMR (CDCl₃): 4.59 (1H, quin), 4.30 (1H, quin), 3.22 (1H, bm), 3.35 (1H, bm), 2.77 -2.94 (4H, vbm), 2.58 (4H, bm) ppm (2 isomers).

Preparation of 1-methylcarbonate-3-chlorocyclobutane.

The 1-carboxy-3-chlorocyclobutane (52.00 g, 0.387 mol), 2,2-dimethoxypropane (75 ml, 63.5 g, 0.610 moles), methanol (11 mls), and methanesulfonic acid (0.506 g) were added together in a 250 ml round bottom flask equipped with a reflux condenser and flushed with argon for one hour. The solution was then heated to 65 °C under argon for 18 hours. Upon completion, the volatiles were removed by rotary evaporation at 30 °C and the residue dissolved in ether. This solution was then washed with saturated sodium bicarbonate (NaHCO₃), water, and

brine solutions. The ether layer was dried over magnesium sulfate and rotovapped to dryness. The resulting red oil was distilled at 45 torr in several fractions from 96 - 110 °C to give the colorless liquid product in 60 % yield.

^1H NMR (CDCl_3): 4.58 (1H, m), 4.28 (1H, m), 3.69 (6H, d), 3.22 (2H, vbm), 2.8 (4H, vbm), 2.54 (4H, vbm) ppm (2 isomers).

Preparation of 1-diphenylmethylene-3-chlorocyclobutane.

The 1-carboxy-3-chlorocyclobutane (3.50 g, 23.6 mmol) was dissolved in 25 ml of anhydrous ether in a dry 100 ml round bottom flask under argon. The 2 equivalents of phenylgrignard were added dropwise, via cannula, over the course of one hour to the flask, now placed in an ice bath. Once the addition was complete, the reaction was stirred for 30 minutes at 0 °C then allowed to warm to room temperature (25 °C) and stirred an additional 2 hours.

25 mls of a saturated ammonium chloride solution was added dropwise to the reaction mixture and the pH adjusted to ~1 using aliquots of concentrated HCl and 1 N HCl. The solution was then extracted several times with ether, dried and the organic layers combined. Dropwise addition of 40 mls of concentrated sulfuric acid to the organic layer (dehydration) causes vigorous bubbling and is allowed to continue stirring for one hour. A second extraction of the ether layer with water, the volatiles were evaporated using rotary evaporation and pumped dry under dynamic vacuum to yield a brownish solid. Column chromatography using a 10 % ether/hexane solvent system moves the product off as a brown solid, which recrystallizes from ether/hexane to

give the product as white or yellow needles. Yield upon recrystallization drops to 55 %.

^1H NMR (CDCl_3): 7.32 (4H, m), 7.22 (2H, m), 7.13 (4H, m), 4.48 (1H, m), 3.45 (2H, m), 3.23 (2H, m) ppm. ^{13}C NMR (CDCl_3): 139.95, 135.35, 131.09, 128.71, 128.21, 126.80, 48.35, 44.64 ppm. Elemental Analysis: C: 80.15 (80.15) H: 5.97 (5.93).

The same double grignard reaction has been run with a variety of grignard reagents to give equally outstanding results:

p-tolylmagnesium bromide: yellow plates ^1H NMR (CDCl_3): 7.09 (4H, d), 7.01 (4H, d), 4.47 (1H, m), 3.43 (2H, m), 3.19 (2H, m), 2.32 (6H, s) ppm. ^{13}C NMR (CDCl_3): 137.20, 136.39, 134.98, 129.73, 128.85, 128.59, 48.43, 44.60, 21.15 ppm. Elemental Analysis: C: 80.57 (80.69) H: 6.82 (6.77).

4-chlorophenylmagnesium bromide: ^1H NMR (CDCl_3): 7.27 (4H, m), 7.03 (4H, m), 4.47 (1H, m), 3.41 (2H, m), 3.17 (2H, m) ppm. ^{13}C NMR (CDCl_3): 137.88, 133.24, 132.86, 132.53, 129.94, 128.54, 47.98, 44.47 ppm. Elemental Analysis: C: 63.51 (63.09) H: 4.24 (4.05).

4-fluorophenylmagnesium bromide: ^1H NMR (CDCl_3): 7.07 (4H, m), 6.98 (4H, m), 4.47 (1H, m), 3.40 (2H, m), 3.17 (2H, m) ppm. ^{13}C NMR (CDCl_3): 158.41, 155.33, 132.40, 132.36, 130.18, 128.13, 127.25, 127.15, 113.18, 112.91, 49.71, 46.26 ppm. C: 70.04 (70.23) H: 4.57 (4.51).

p-thioanisolemagnesium bromide: white needles ^1H NMR (CD_2Cl_2): 7.20 (4H, m), 7.06 (4H, m), 4.53 (1H, m), 3.45 (2H, m), 3.20 (2H, m) ppm. ^{13}C NMR (CD_2Cl_2): 137.52, 136.96, 134.42, 131.31, 129.48, 126.35, 48.83, 44.92, 15.74 ppm. Elemental Analysis: C: 65.42 (65.78) H: 5.55 (5.52).

dimethylaniline/thioanisole: pale yellow solid ^1H NMR (CD_2Cl_2): 7.30 (2H, m), 7.18 (2H, m), 6.98 (2H, m), 6.67 (2H, m), 4.51 (1H, m), 3.49 (1H, m), 3.41 (1H, m), 3.22 (1H, m), 3.16 (1H, m), 2.94 (6H, m), 2.48 (3H, m) ppm. ^{13}C NMR (CDCl_3): 149.82, 137.87, 137.09, 134.92, 129.72, 128.50, 128.23, 126.40, 112.27, 49.09, 45.06, 44.90, 40.59, 15.85 ppm. Elemental Analysis: C: 69.82 (69.85) H: 6.41 (6.45) N: 4.30 (4.07).

Preparation of 3-chloro-1-cyclobutaneacetyl chloride.

The 1-carboxy-3-chlorocyclobutane is added to a 100 ml Schlenk flask fitted with a dropping funnel and the system purged with argon for 30 minutes. Thionyl chloride was then added dropwise to the flask. Upon addition, the flask was heated to 35 °C upon which the vigorous evolution of gases began and continued for 2 hours. The flask was heated slowly to reflux and the reflux was maintained for 30 minutes after the evolution of gases had ceased. The thionyl chloride was removed by distillation at 75 - 78 °C and the system left to cool. Further distillation at 30 torr allowed collection of three fractions, the product distilling at 70 ° at 18 torr as a clear liquid in 89 % yield.

^1H NMR (CDCl_3): 4.38 (1H, m), 4.19 (2H, m), 3.68 (1H, m), 3.19 (2H, m), 2.83 (4H, m), 2.54 (4H, m) ppm (2 isomers).

Preparation of (2-chlorocyclobutane)phenyl ketone.

The manganese reagent (manganese iodide and phenylmagnesium bromide) was cooled to -12 °C and the 3-chloro-1-cyclobutaneacetyl chloride added dropwise by syringe. The mixture was allowed to warm to room temperature and stirred for 90 minutes. Extraction of the reaction

mixture with 1 N HCl and ether was followed with sodium bicarbonate and brine washes. The ether layer was dried, decolorized with carbon, and rotovapped to give a pale yellow oil. Chromatography on silica gel (10 % ether/pentane) purifies the product (25 % yield).

^1H NMR (CDCl_3): 7.85 (1H, m), 7.55 (1H, m), 7.48 (1H, m), 7.27 (2H, m), 4.46 (1H, m), 3.69 (1H, m), 2.85, 2.67 ppm (2 isomers).

General Polymerization Techniques.

Extreme care was exercised to keep the system air and moisture free during polymerization. All glassware was pumped into the drybox hot and both monomer and catalyst were loaded into separate Schlenk tubes inside the drybox. Polymerizations were monitored by thin layer chromatography since the monomer decomposes with R_f 0 - 0.25 and the polymer sits at the origin. Aliquots of the polymerization solution were taken with a capillary tube under a heavy purge of argon and polymerization was terminated when no monomer streaking was observed. The polymer was precipitated from deoxygenated hexane after dilution of the polymerization solution with small amounts of methylene chloride.

All polymerizations are monitored for monomer consumption by thin layer chromatography and terminated upon completion. Monomer to catalyst ratios of typically 50 - 100 : 1 employed. Catalyst ratios as high as 250 : 1 have been attempted, but the higher ratios have resulted in polymer precipitations of "stickier" quality polymer and poorer reaction yields. Polymerizations run with monomer to catalyst ratios of 100 : 1 or

75 : 1 consistently give materials with high molecular weights and better material properties.

Polymerization of 3-diphenylmethylenecyclobutene.

The 1-diphenylmethylene-3-chlorocyclobutane is dissolved in dry THF along with 0.98 equivalents of hexamethyldisilazide base to give a cloudy white solution. The chloride elimination is left to stir for 30 minutes at room temperature before an appropriate amount of alkylidene catalyst is added to this reaction mixture. Addition of the catalyst immediately turns the polymerization mixture a cloudy orange color that will not dissipate during the length of polymerization. The length of polymerization varies from 3 - 24 hours, depending upon the inorganic base used, but is closely monitored by TLC for monomer depletion.

Upon completion, the pale orange and cloudy polymerization solution is precipitated gently in swirling methanol to give a slightly discolored, yellow solid. If desired, the polymer is easily redissolved and blown through a column of silica gel before precipitation into methanol. This purification step yields a pristine white polymer solid upon precipitation.

^1H NMR (CDCl_3): 6.71 - 7.11 (10H, bm), 5.66 (1H, d), 5.01 (1H, m), 2.16 (2H, bm) ppm. ^{13}C NMR (CDCl_3): 143.27, 142.62, 140.88, 134.54, 130.2, 129.6, 127.8, 126.4, 34.5 ppm. IR spectroscopy: 3050, 3020, 2970, 1600, 1490, 1440, 760, 695 cm^{-1} . Elemental analysis: C :91.08 (93.60), H: 6.44 (6.50).

It is also possible to isolate the 3-diphenylmethylenecyclobutene as a clear and colorless oil (after the first step) with filtration and chromatography of the reaction mixture.

^1H NMR (CDCl_3): 7.20 - 7.32 (10H, bm), 6.73 (1H, s), 6.47 (1H, s), 3.18 (1H, s) ppm.

Iodine Photolysis doping.

The poly(diphenylmethylene cyclobutene) was dissolved up in dry benzene under argon to give a cloudy, off-white polymer solution and transferred into a modified EPR tube. Solid iodine (~1.5 equivalents) was added to this solution, turning it a striking, dark, but clear, burgundy wine color. The solution is then freeze-pump-thaw-degassed at least three times to insure occlusion of water and oxygen from the system. Upon completion of these preliminaries, the solution is cooled to 0 °C, loaded into an optical dewar at 0° C and photolyzed for 8 hours with unfiltered UV radiation.

Upon completion of the photolysis, the solution, still a dark burgundy, is precipitated into swirling pentane, collected, washed repeatedly with fresh pentane, and dried. The markedly green granular solid remains soluble and subject to SQUID, GPC and NMR analysis.

This procedure was also used with benzoquinone and DDQ photolyses, benzoquinone treatment produced a dirty brown polymer while DDQ produced a dark green polymeric solid.

Simple solution doping.

Simple solution doping took place at 25 °C and followed the procedure outlined above, except for the freeze-pump precautions and reaction temperature. Homogeneous and heterogeneous doping attempts involved addition of an oxidant to methylene chloride (or benzene) solutions of the poly(diphenylmethylene cyclobutene). Left to react for hours in some cases, the treated polymers were then precipitated into swirling pentane to insure against loss of spin activity. In the case of heterogeneous oxidants like lead dioxide and silver oxide, the polymer solution was simply filtered away from the oxidants and reprecipitated again into pentane.

This procedure was used effectively in the treatment of the polymer samples with iodine, ferricinium salts, DDQ, and the antimony iminium salt.

Rational (Rajca) Doping Efforts.

A sample of poly(diphenylmethylene cyclobutene) was dissolved in dry THF and the solution purged with argon. Lithium diisopropylamide (LDA) was added to the polymer solution which became a dark green, almost black color within 15 minutes. To this green solution was added solid iodine, which immediately turned the polymer solution a dark red. Precipitation of the polymer into degassed pentane yielded an orange-brown solid that darkens considerable upon exposure to air.

Magnetic Measurements (SQUID).

Magnetic measurements were taken on a Quantum Design Magnetic Property Measurement System (MPMS) which itself is a unique and modular integration of a Superconducting Quantum Interference Device (SQUID) detection system. Samples were loaded into cellulose gel caps and suspended with sewing thread inside an ordinary drinking straw. This straw was then dropped into the core of the magnet. Magnetic measurements were typically taken over the range of 0 - 55 kG at a constant temperature (1.8 K) and over the temperature range 1.8 - 300 K at a constant external magnetic field (0 - 10 kG). The data was then fit to the Brillouin function (program courtesy of Dennis Dougherty) and the spin value (S) and number of radical spins generated extracted.

All doped materials were handled with extreme care. Teflon coated spatulas and tweezers were employed to insure against paramagnetic impurities in the treated polymer samples. Gloves and argon flush boxes were also employed to guard against possible polymer oxidation by exposure to ambient conditions. Upon reflection, however, these polymeric materials do not appear to be susceptible to air oxidation.

Ferromagnet References:

- 1) General references for this chapter: Hurd, C. M. *Contemp. Phys.* **1982**, 23, 469. Carlin, R. L. Magnetochemistry. Springer-Verlag. Berlin. 1986. McCaig, M.; Clegg, A. G. Permanent Magnets in Theory and Practice, Second Edition. John Wiley and Sons. New York. 1987. O'Dell, T. H. Ferromagnetodynamics. John Wiley and Sons. New York. 1981. Mabbs, F. E.; Machin, D. J. *Magnetism and Transition Metal Complexes*. Chapman and Hall. London. 1973. Earnshaw, A. *Introduction to Magnetochemistry*. Academic. New York. 1968. Bozworth. Ferromagnetism. 1951.
- 2) Nishide, H.; Yoshioka, N.; Inagaki, K., et al. *Macromolecules*. **1992**, 25, 569. Pei, Y.; Kahn, O.; Nakatani, K. *J. Amer. Chem. Soc.* **1991**, 113, 7994. Andrews, M. P.; Cordes, A. W., et al. *J. Amer. Chem. Soc.* **1991**, 113, 3559. Kollmar, C.; Couty, M.; Kahn, O. *J. Amer. Chem. Soc.* **1991**, 113, 7994. Miller, J. S.; Dougherty, D. A., Editors. *Proceedings of the Symposium on Ferromagnetic and High Spin Molecular Based Materials*, 197th National American Chemical Society Meeting. *Mol. Cryst. Liq. Cryst.* **1989**, 176, 25.
- 3) McConnell, H. M. *J. Chem. Phys.* **1963**, 39, 1910. Mataga, N. *Theor. Chim. Acta.* **1968**, 10, 372. Breslow, R. *Pure and Appl. Chem.* **1987**, 109, 769. Kollmar, C.; Kahn, O. *J. Amer. Chem. Soc.* **1991**, 113, 7987. Miller, J. S. *J. Amer. Chem. Soc.* **1987**, 109, 769.
- 4) Miller, J. S.; Epstein, A. J.; Reiff, W. M. *Chem. Rev.* **1988**, 88, 201. Breslow, R.; Jahn, B.; Kluttz, R. Q.; Xia, C. Z. *Tetrahedron*. **1982**, 38, 863. Thomaides, J.; Maslak, P.; Breslow, R. *J. Amer. Chem. Soc.*

- 1988, 110, 3970. LePage, T. J.; Breslow, R. *J. Amer. Chem. Soc.* **1987**, 109, 6412.
- 5) Heuer, W. B.; Mountford, P.; Green, M. L. H.; Bolt, S. G.; O'Hare, D.; Miller, J. S. *Chem. Mater.* **1990**, 2, 764. Manriques, J. M.; Yee, G. T.; McLean, R. S.; Epstein, A. J.; Miller, J. S. *Science*. **1991**, 252, 1415. Miller, J. S.; Epstein, A. J.; Reiff, W. M. *Chem. Rev.* **1988**, 88, 201.
- 6) Fukutome, H.; Takahashi, A.; Ozaki, M. *Chem. Phys. Lett.* **1987**, 133, 34. Dougherty, D. A. *Accts. Chem. Res.* **1991**, 24, 88. Dougherty, D. A. *Mol. Cryst. Liq. Cryst.* **1989**, 176, 25. Dougherty, D. A.; Grubbs, R. H.; Kaisaki, D. A., et al. *Magnetic Molecular Materials*. **1991**, 105. Novak, J. A.; Jain R. J.; Dougherty, D. A. *J. Amer. Chem. Soc.* **1989**, 111, 7618. Jain, R. J.; Sponsler, M. B.; Coms, F. D.; Dougherty, D. A. *J. Amer. Chem. Soc.* **1988**, 110, 1356. Kaisaki, D. A. California Institute of Technology. Thesis. 1990.
- 7) Braun, D. *Pure Appl. Chem.* **1972**, 30, 41. Braun, D.; Tormala, P.; Wittig, W. *Macrom. Chem.* **1981**, 182, 2217. Saint Paul, M.; Veyret, C. *Phys. Lett. A*. **1973**, 45, 362. Awaga, K.; Maruyama, Y. *Chem. Phys. Lett.* **1989**, 158, 556. Awaga, K.; Sugano, T.; Kinoshita, M. *J. Chem. Phys.* **1986**, 85, 2211. Allemand, P-M.; Srdanov, G.; Wudl, F. *J. Amer. Chem. Soc.* **1990**, 112, 9391.
- 8) Alexander, S. A.; Klein, D. J. *J. Amer. Chem. Soc.* **1988**, 110, 3401. Ovchinikov, A. A. *Theoret. Chim. Acta. (Berl.)* **1978**, 47, 297. Mataga, N. *Theoret. Chim. Acta. (Berl.)* **1968**, 10, 372. Teki, Y.; Takui, T.; Itoh, K.; Iwamura, H.; Kobayashi, K. *J. Amer. Chem. Soc.* **1986**, 108, 2147. Sugawara, T.; Bandow, S.; Kimura, K.; Iwamura, H.; Itoh, K. *J. Amer. Chem. Soc.* **1986**, 108, 368. Lahti, P. M.; Ichimura,

- A. S. *J. Org. Chem.* **1991**, *56*, 5030. Lahti, P. M.; Ichimura, H.; Berson, J. A. *J. Org. Chem.* **1989**, *54*, 958.
- 9) Murata, S.; Iwamura, H. *J. Amer. Chem. Soc.* **1991**, *113*, 5547. Itoh, K. *Chem. Phys. Lett.* **1967**, *1*, 235. Teki, Y.; Takui, T.; Itoh, K.; Iwamura, H.; Kobayashi, K. *J. Amer. Chem. Soc.* **1986**, *108*, 2147. Sugawara, T.; Bandow, S.; Kimura, K.; Iwamura, H.; Itoh, K. *J. Amer. Chem. Soc.* **1986**, *108*, 368. Agawa, K.; Sugano, T.; Kinoshita, M. *J. Chem. Phys.* **1986**, *85*, 2211.
 - 10) Torrance, J. B.; Oostra, S.; Nazzari, A. *Synth. Met.* **1987**, *19*, 709.
 - 11) Lampman, G. M.; Aumiller, J. C. *Org. Syn.* **1971**, *51*, 73.
 - 12) Hall, H. H.; Smith, C. D.; Blanchard, E. P., Jr.; Cherkofsky, S. C.; Sieja, J. B. *J. Amer. Chem. Soc.* **1971**, *93*, 121.
 - 13) Allen, C. F. H.; Converse, S. *Org. Syn. Coll. Vol. 1*, 226. Graham, S. H.; Williams, A. J. S. *J. Chem. Soc.* **1959**, 4066.
 - 14) Jain, R. J. California Institute of Technology. Unpublished results, 1988 - 1989.
 - 15) Miller, J. S.; Epstein, A. J.; Reiff, W. M. *Chem. Rev.* **1988**, *88*, 201. Breslow, R.; Jahn, B.; Kluttz, R. Q.; Xia, C. Z. *Tetrahedron.* **1982**, *38*, 863. Thomaides, J.; Maslak, P.; Breslow, R. *J. Amer. Chem. Soc.* **1988**, *110*, 3970. Miller, J. S.; Epstein, A. J.; Reiff, W. M. *Science.* **1988**, *240*, 40. Alexander, S. A.; Klein, D. J. *J. Amer. Chem. Soc.* **1988**, *110*, 3401. Ovchinikov, A. A. *Theoret. Chim. Acta. (Berl.)* **1978**, *47*, 297. Mataga, N. *Theoret. Chim. Acta. (Berl.)* **1968**, *10*, 372. Magnetochemistry. Springer-Verlag. Berlin. 1986. McCaig, M.; Clegg, A. G. Permanent Magnets in Theory and Practice, Second Edition. John Wiley and Sons. New York. 1987. Rajca, A.;

- Utampanya, S.; Xu, J. *J. Amer. Chem. Soc.* **1991**, *113*, 9235. Dowd, P. *Acc. Chem. Res.* **1972**, *5*, 242.
- 16) Rajca, A.; Utampanya, S.; Xu, J. *J. Amer. Chem. Soc.* **1991**, *113*, 9235. Utampanya, S.; Rajca, A. *J. Amer. Chem. Soc.* **1991**, *113*, 9242. Rajca, A. *J. Amer. Chem. Soc.* **1990**, *112*, 5889. Rajca, A. *J. Amer. Chem. Soc.* **1990**, *112*, 5890.
- 17) Ota, M.; Otani, S.; Igarashi, M. *Chem. Lett.* **1989**, 1183. Tolbert, L. M. *Accts. Chem. Res.* **1986**, *19*, 268.